SI to Mapping the Reaction Landscapes of Molten-Salt Fluxes

Gregory Bassen[1,2,3], Rebecca Y. Han[1,2,3], Thomas J. Whoriskey[1,2,3], Allana Iwanicki[1,2,3], Ragy Ebeid[2], Kathryn Kingsbury[2], Jayson B. Johnson[2], Joshua Hummel[3], Thomas J. Kempa[2], and Tyrel M. McQueen[1,2,3]

[1] Institute for Quantum Matter, William H. Miller III Department of Physics and Astronomy, Johns Hopkins University, 3400 N. Charles Street, Baltimore, MD 21218, United States of America

[2] Department of Chemistry, Johns Hopkins University, 3400 N. Charles Street, Baltimore, MD 21218, United States of America

[3] Department of Materials Science and Engineering, Johns Hopkins University, 3400 N. Charles Street, Baltimore, MD 21218, United States of America

Correspondence: gbassen1@jhu.edu; mcqueen@jhu.edu

March 29, 2026

Table of Contents

Supplemental Text

Fluxes specifically used for oxides generally melt at low-temperature and are used to grow crystals, such as the conventional PbO/PbF_2, Na_2CO_3, K_2CO_3, Bi_2O_3, K_2MoO_4 [1, 2]. However, 'soft alkali halide' fluxes (Br, I) have scarcely been used for the synthesis of oxides [3]. The discovery of high-temperature superconductivity in La_2CuO_4 [4] led to an explosion of synthesis in the oxide phase-space and the subsequent discovery of numerous perovskite-derived structure types [5]. This has since prompted the search for high-temperature superconductivity in structurally and chemically analogous phase spaces to the well-studied cuprate materials. There was a resurgence of interest in the perovskite-derived structure types with the discovery of superconductivity in thin films of the reduced nickelates $LnNiO_2$ (Ln= La, Pr, Nd) [6–10]. Further studies on the Ruddlesden-Popper members of the bulk nickelates led to the discovery of high-temperature superconductivity under pressure [11, 12]. Material scientists have explored molten salt fluxes to synthesize ruddlesden-popper nickelates under ambient oxygen pressure, underscoring the role of oxygen chemical potential in flux reactions. For example, $LaNiO_3$ was first synthesized and discovered using a sodium carbonate flux at 800 °C for 72 hours [13]. Further, KOH flux leads to the formation of $LaNiO_3$, whereas NaOH leads to the formation of La_2NiO_4 under ambient pressures [14]. Synthesizing phase-pure $LaNiO_3$ remains especially challenging: it has been obtained via polycrystalline synthesis at 950°C under 2000bar O_2 [15], and in floating zone growths above 50bar O_2 [16–18].

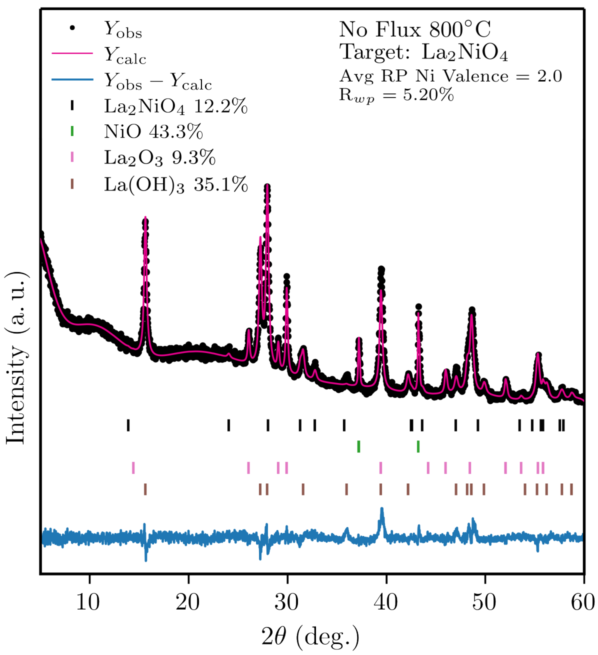

(a) 800°C

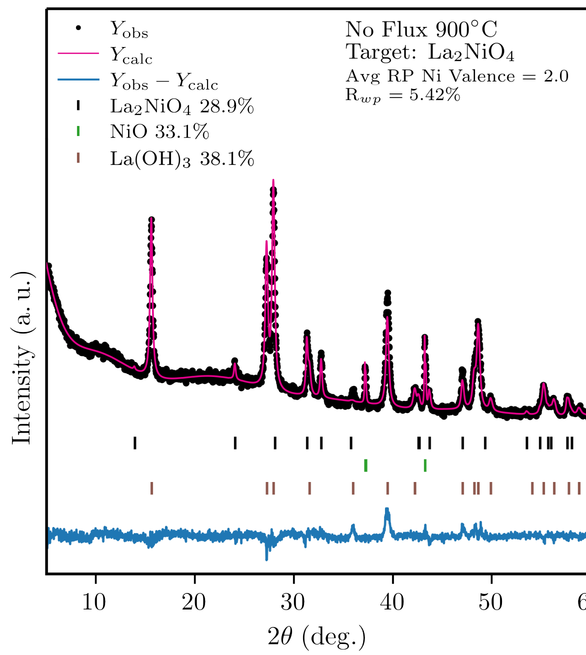

(b) 900°C

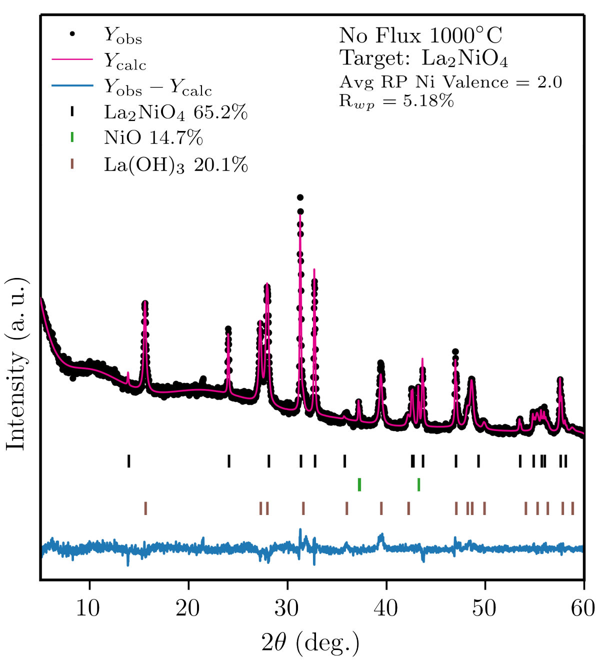

(c) 1000°C

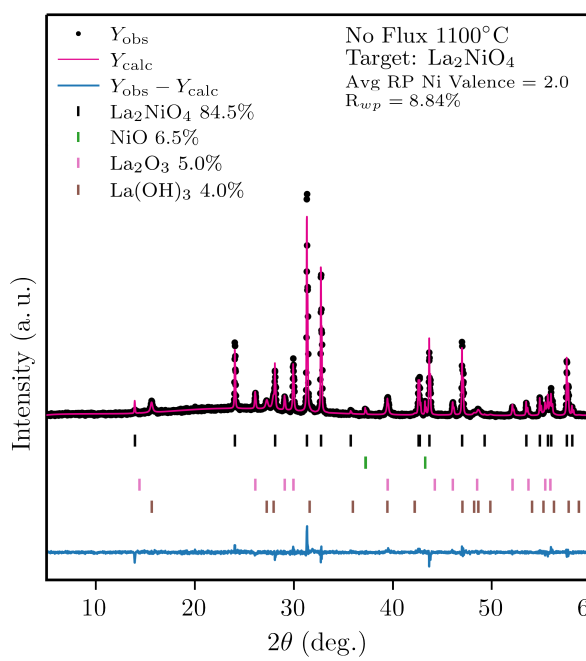

(d) 1100°C

Figure 1: PXRD and Rietveld refinements of targeted La_2NiO_4 where $\frac{Ni}{Ni+La} = 0.33$ without a flux at (a) 800°C, (b) 900°C, (c) 1000°C, and (d) 1100°C.

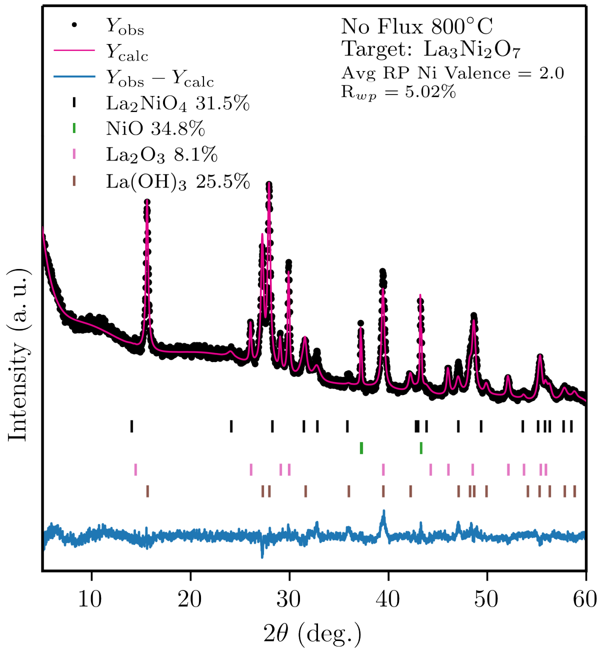

(a) 800°C

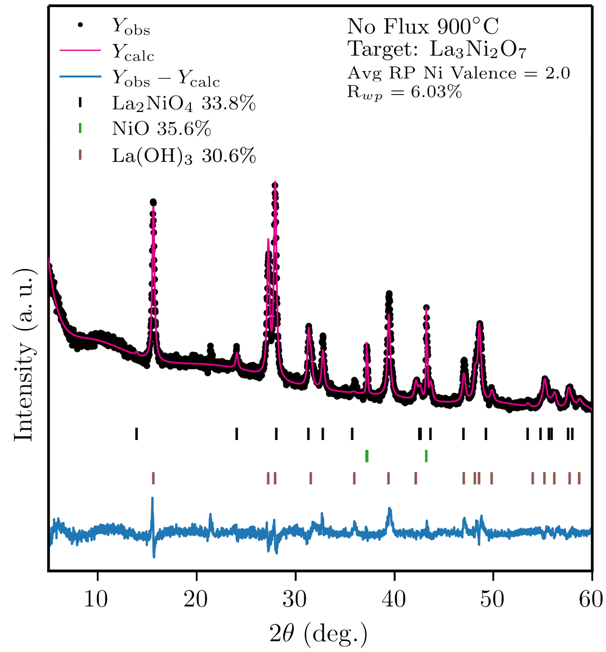

(b) 900°C

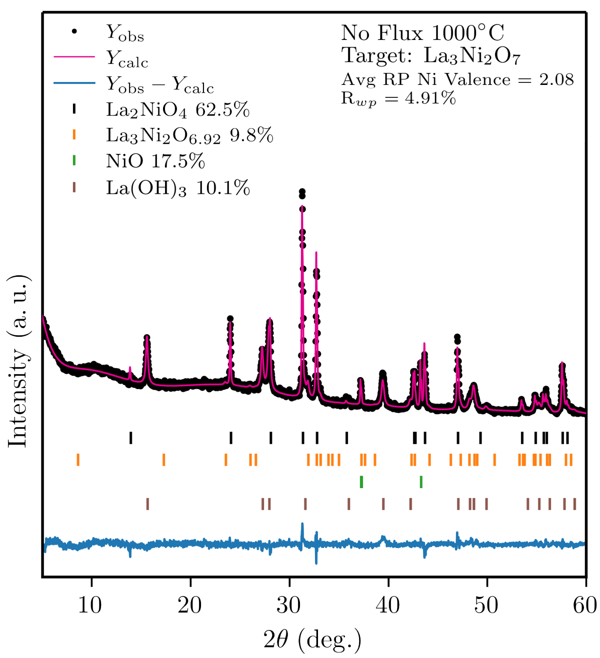

(c) 1000°C

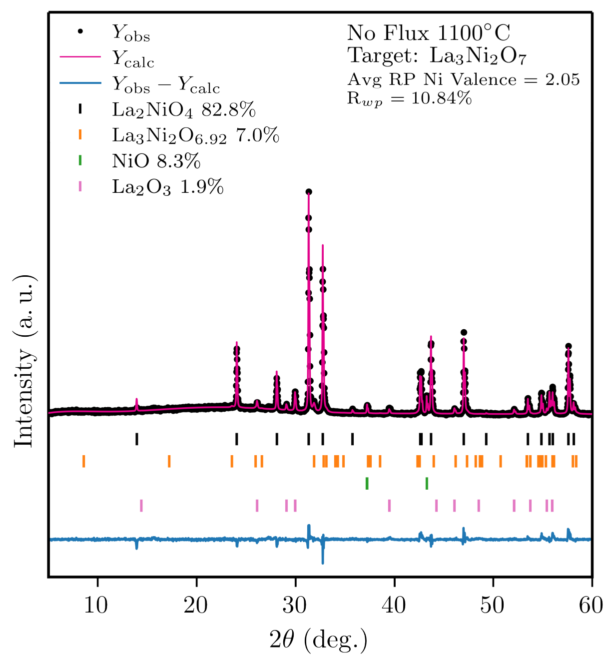

(d) 1100°C

Figure 2: PXRD and Rietveld refinements of targeted $La_3Ni_2O_7$ where $\frac{Ni}{Ni+La} = 0.40$ without a flux at (a) 800°C, (b) 900°C, (c) 1000°C, and (d) 1100°C.

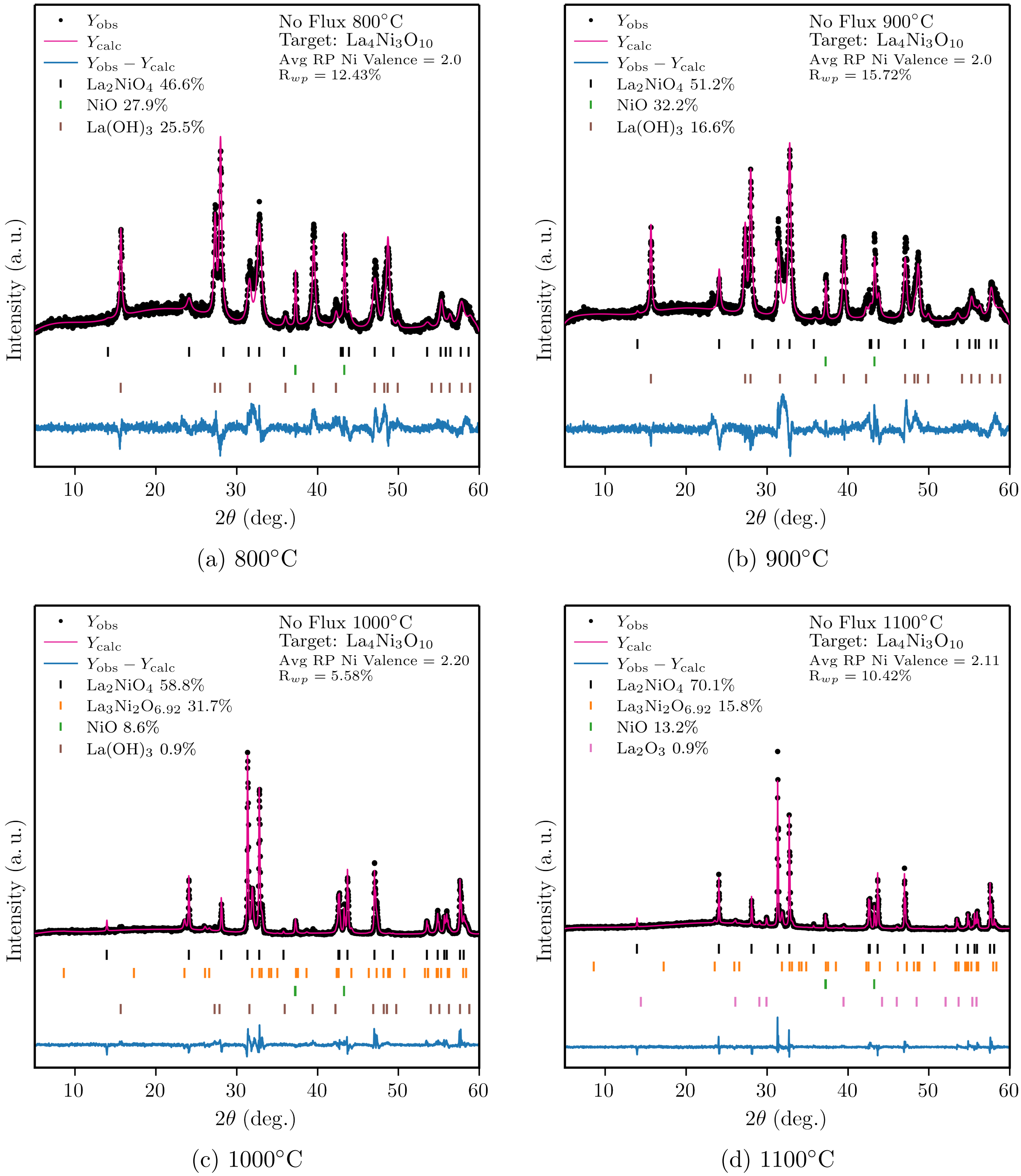

(a) 800°C

(b) 900°C

(c) 1000°C

(d) 1100°C

Figure 3: PXRD and Rietveld refinements of targeted $La_4Ni_3O_{10}$ where $\frac{Ni}{Ni+La} = 0.43$ without a flux at (a) 800°C, (b) 900°C, (c) 1000°C, and (d) 1100°C.

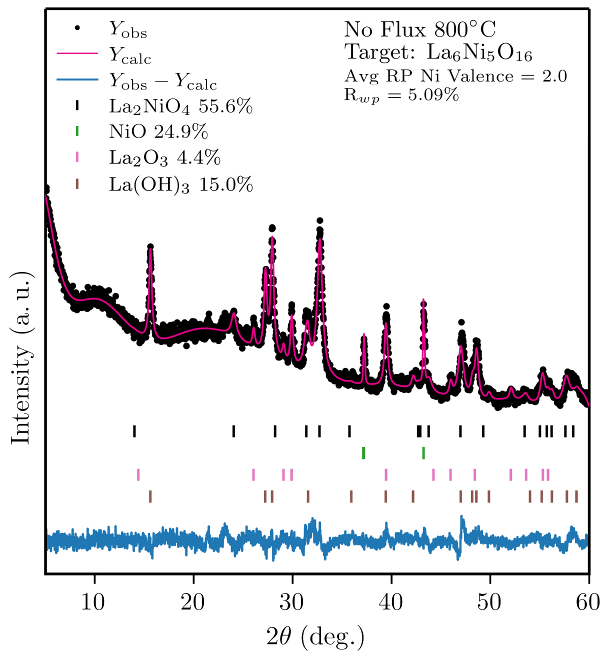

(a) 800°C

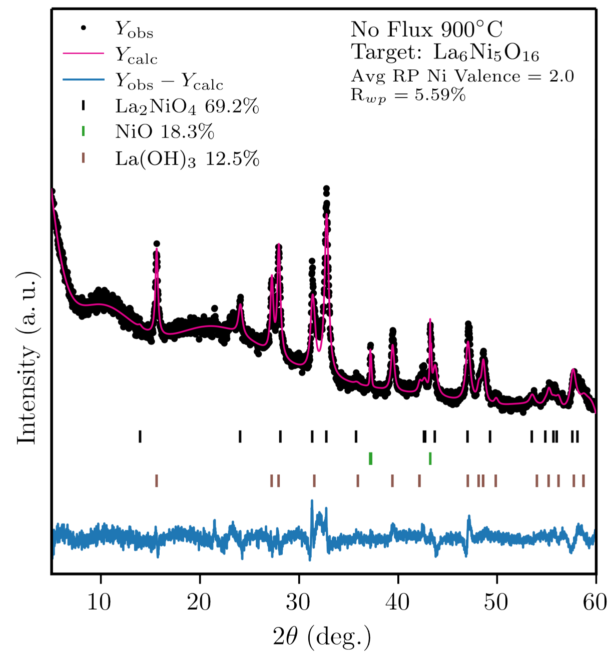

(b) 900°C

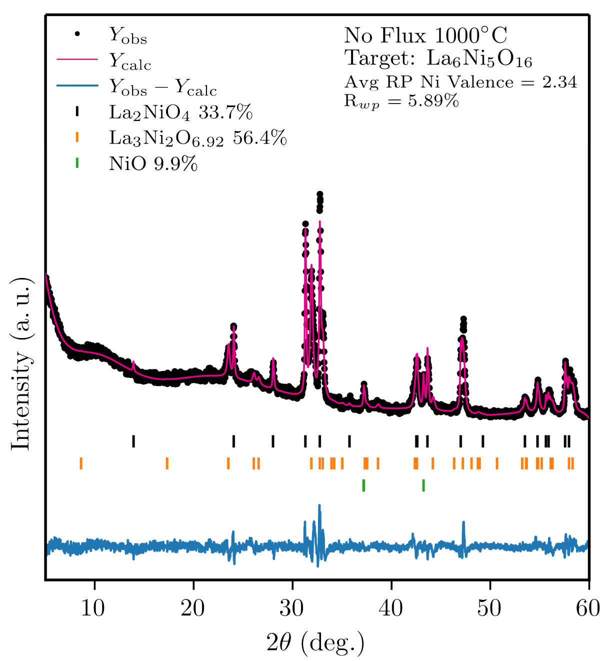

(c) 1000°C

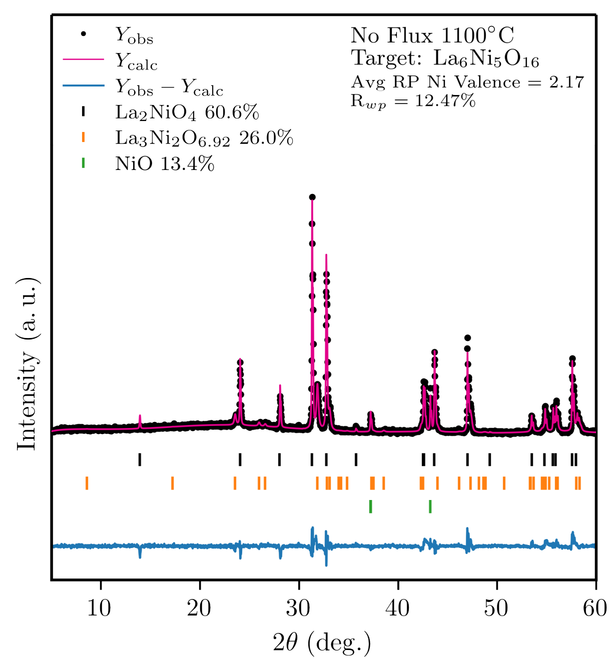

(d) 1100°C

Figure 4: PXRD and Rietveld refinements of targeted $La_6Ni_5O_{16}$ where $\frac{Ni}{Ni+La} = 0.454$ without a flux at (a) 800°C, (b) 900°C, (c) 1000°C, and (d) 1100°C.

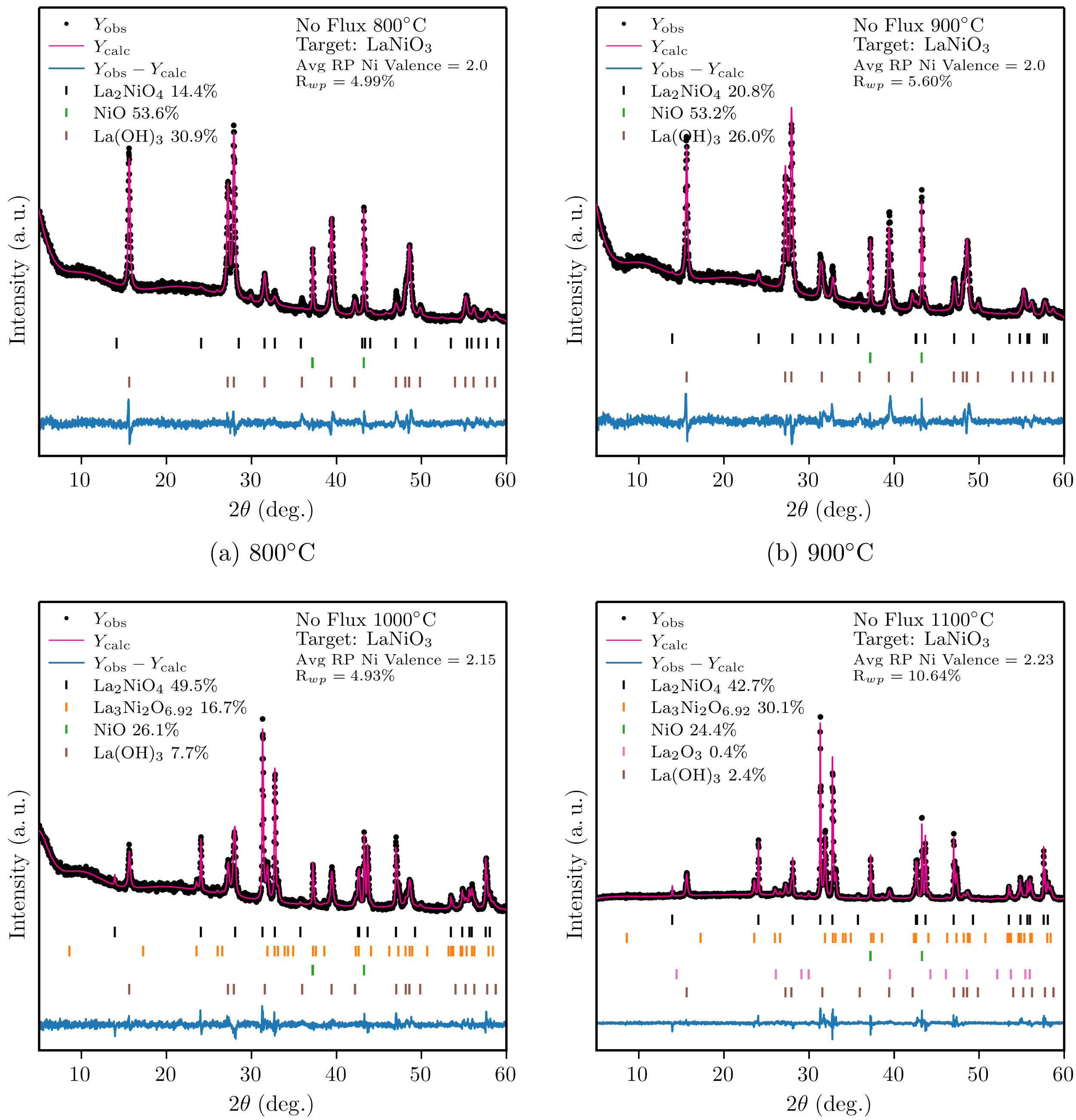

(a) 800°C

(b) 900°C

(c) 1000°C

(d) 1100°C

Figure 5: PXRD and Rietveld refinements of targeted $LaNiO_3$ where $\frac{Ni}{Ni+La} = 0.5$ without a flux at (a) 800°C, (b) 900°C, (c) 1000°C, and (d) 1100°C.

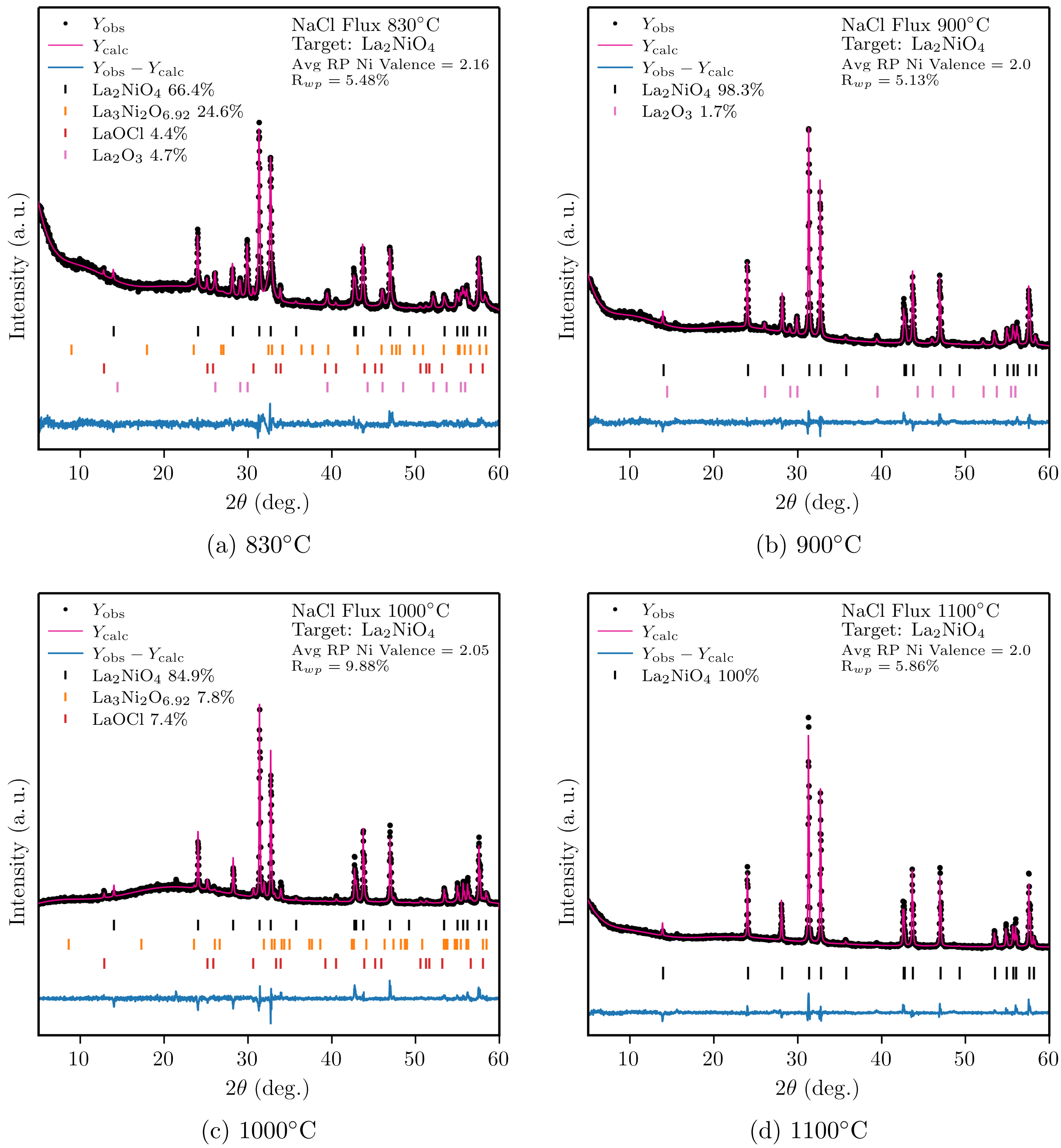

Figure 6: PXRD and Rietveld refinements of targeted La_2NiO_4 where $\frac{Ni}{Ni+La} = 0.33$ in NaCl flux at (a) 830°C, (b) 900°C, (c) 1000°C, and (d) 1100°C.

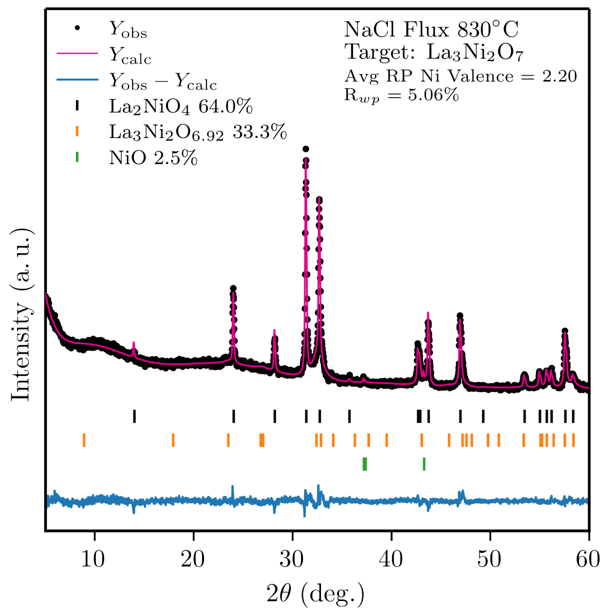

(a) 830°C

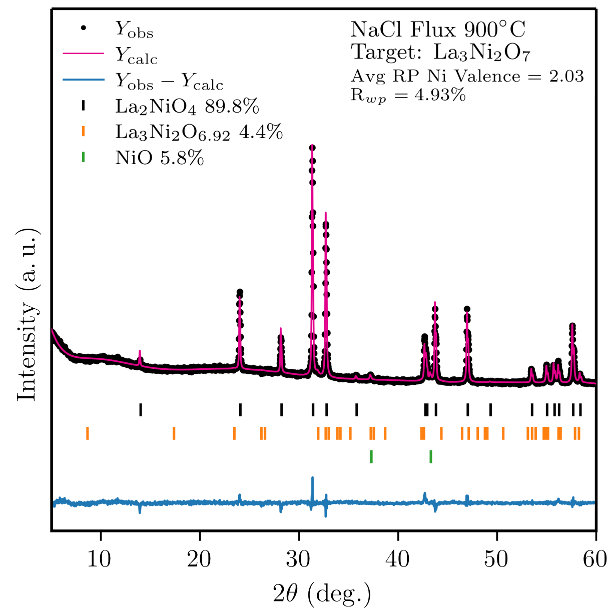

(b) 900°C

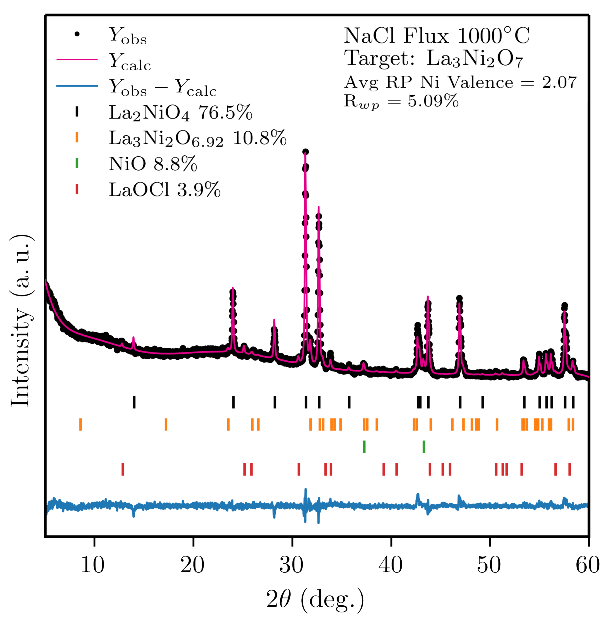

(c) 1000°C

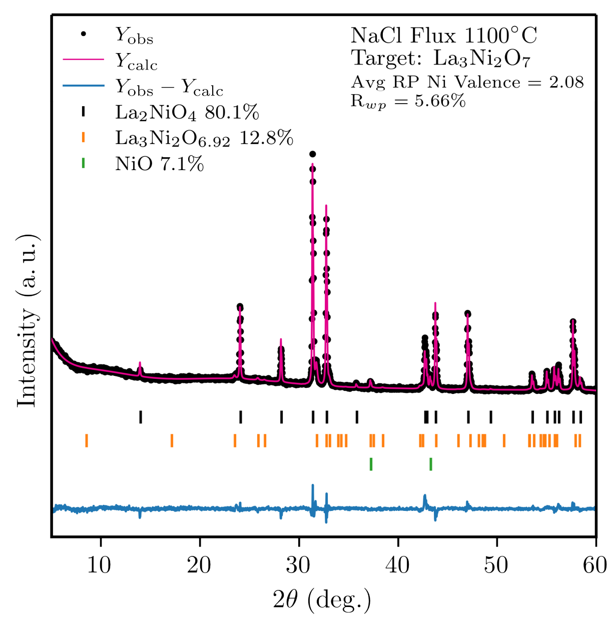

(d) 1100°C

Figure 7: PXRD and Rietveld refinements of targeted $La_3Ni_2O_7$ where $\frac{Ni}{Ni+La} = 0.40$ in NaCl flux at (a) 830°C, (b) 900°C, (c) 1000°C, and (d) 1100°C.

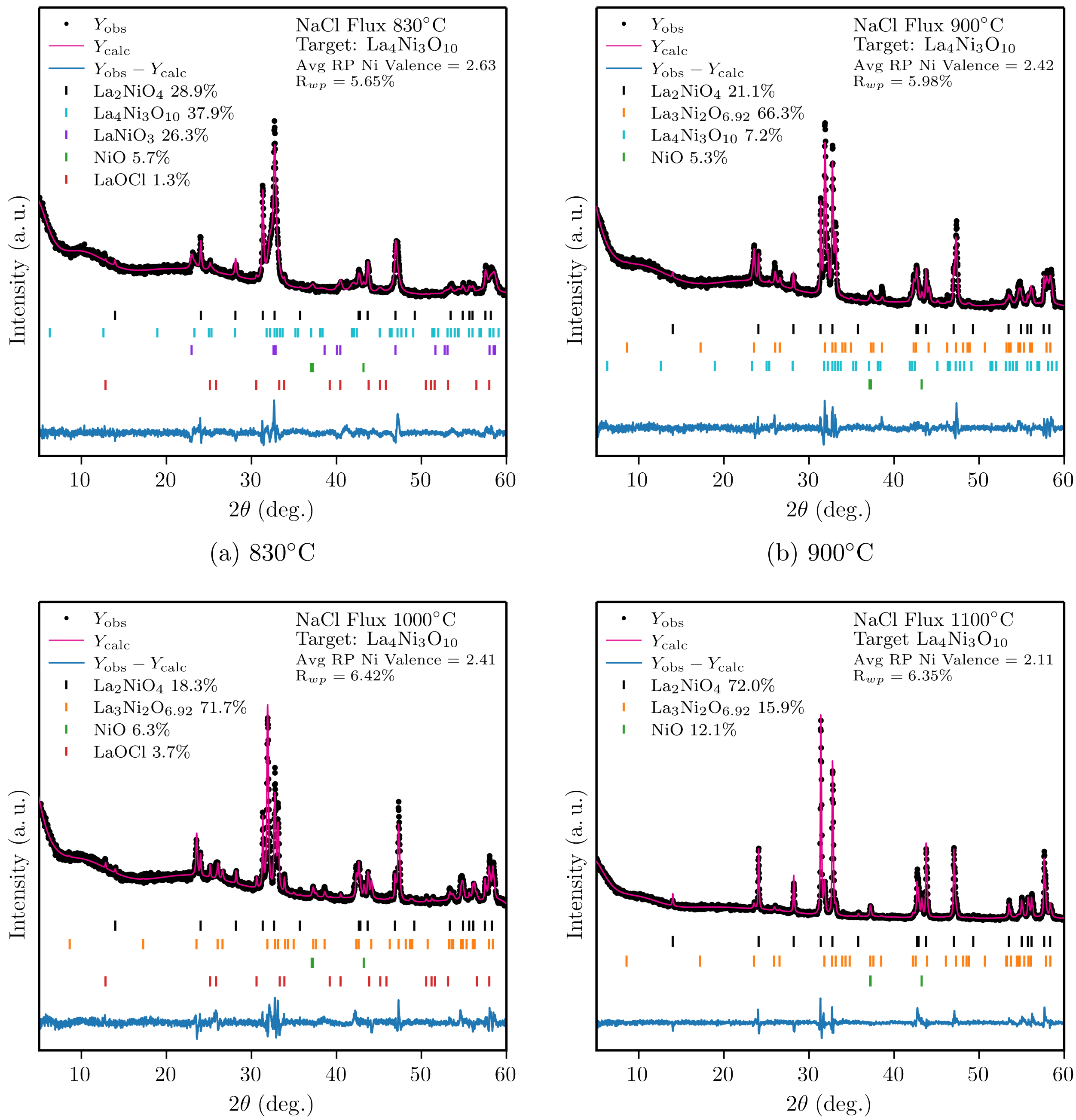

(a) 830°C

(b) 900°C

(c) 1000°C

(d) 1100°C

Figure 8: PXRD and Rietveld refinements of targeted $La_4Ni_3O_{10}$ where $\frac{Ni}{Ni+La} = 0.43$ in NaCl flux at (a) 830°C, (b) 900°C, (c) 1000°C, and (d) 1100°C.

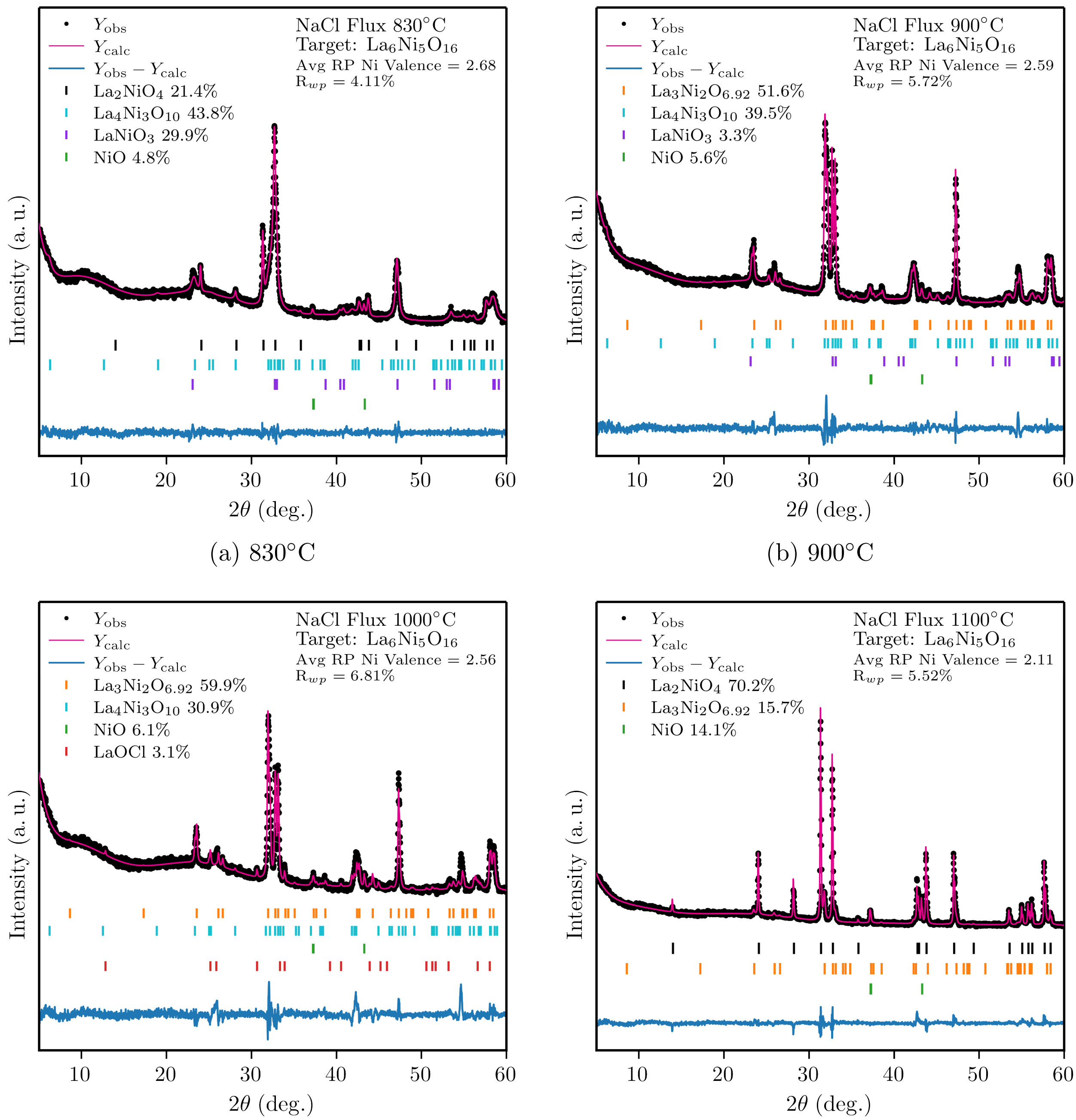

(a) 830°C (b) 900°C

(c) 1000°C (d) 1100°C

Figure 9: PXRD and Rietveld refinements of targeted $La_6Ni_5O_{16}$ where $\frac{Ni}{Ni+La} = 0.454$ in NaCl flux at (a) 830°C, (b) 900°C, (c) 1000°C, and (d) 1100°C.

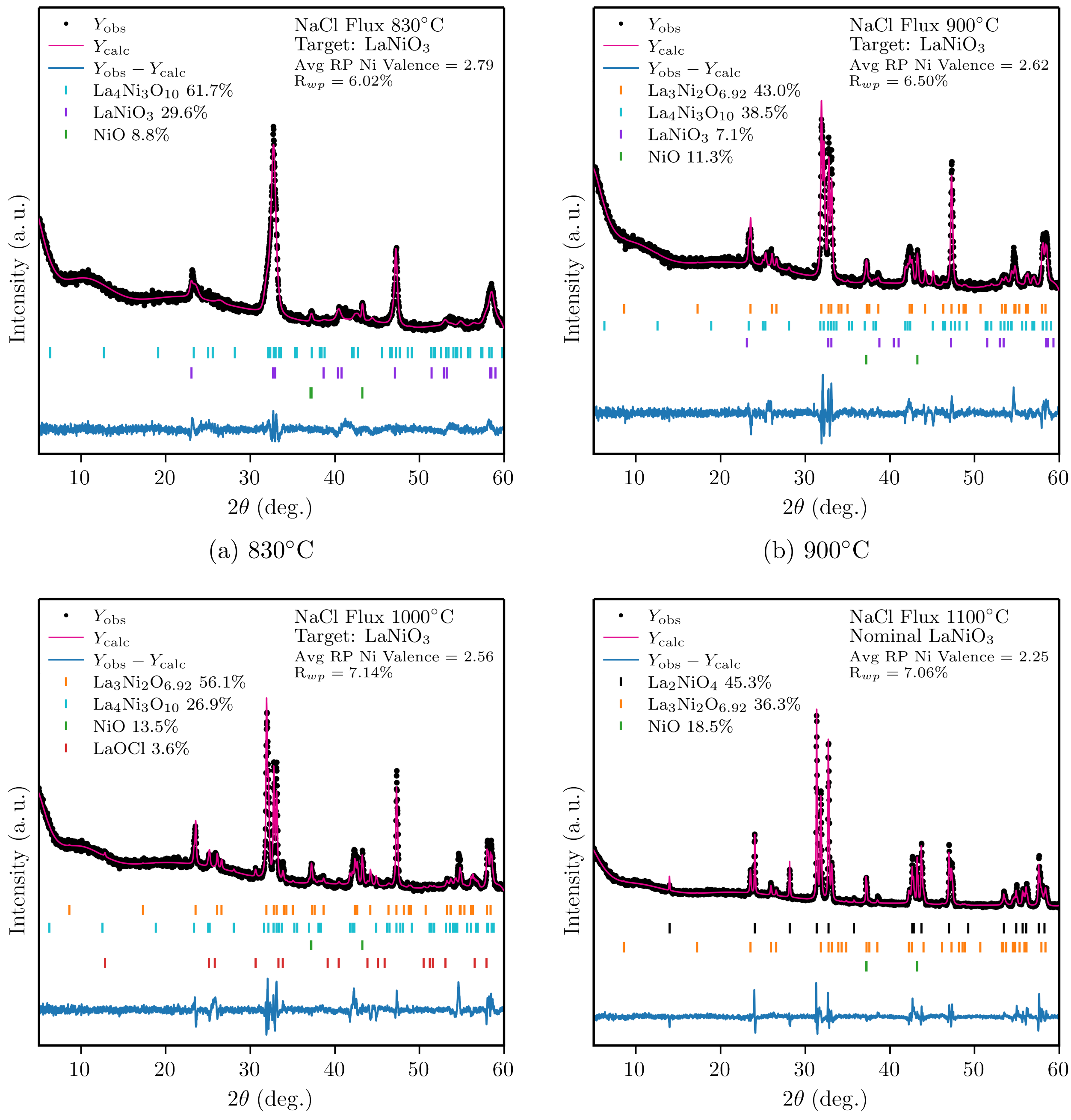

(a) 830°C

(b) 900°C

(c) 1000°C

(d) 1100°C

Figure 10: PXRD and Rietveld refinements of targeted $LaNiO_3$ where $\frac{Ni}{Ni+La} = 0.5$ in NaCl flux at (a) 830°C, (b) 900°C, (c) 1000°C, and (d) 1100°C.

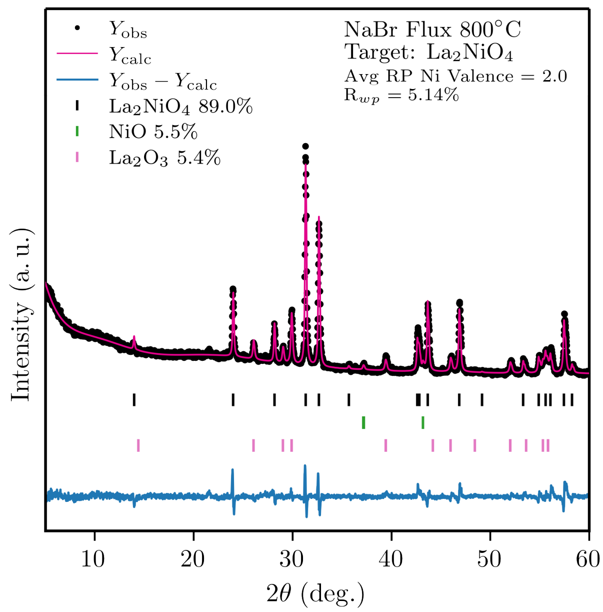

(a) 800°C

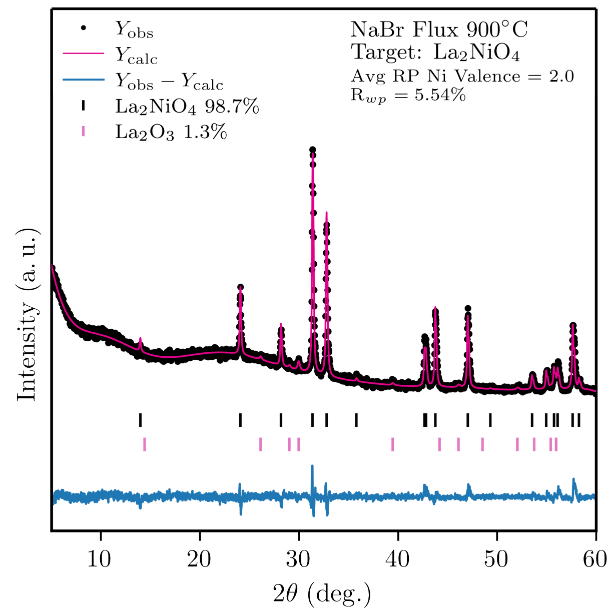

(b) 900°C

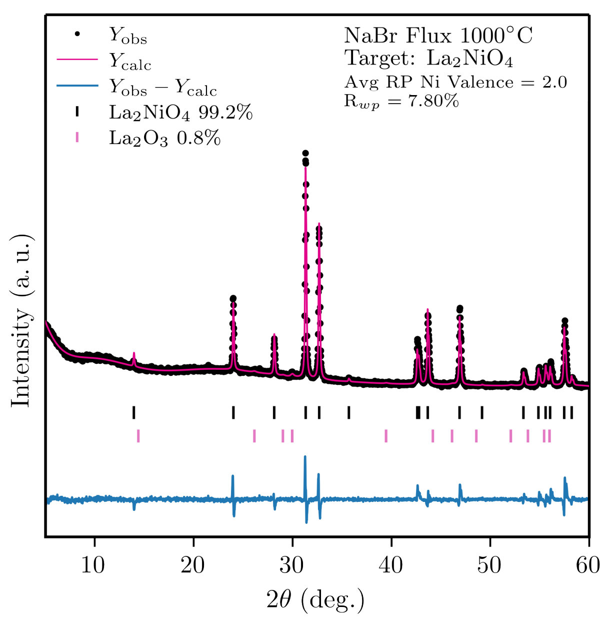

(c) 1000°C

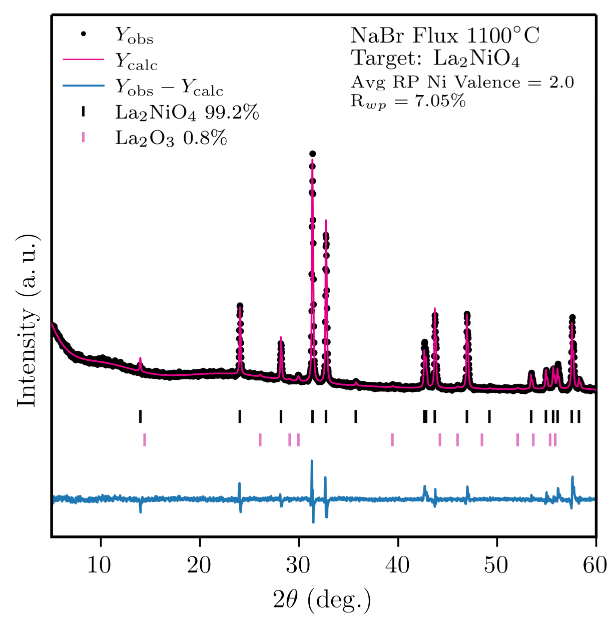

(d) 1100°C

Figure 11: PXRD and Rietveld refinements of targeted La_2NiO_4 where $\frac{\text{Ni}}{\text{Ni+La}} = 0.33$ in NaBr flux at (a) 800°C, (b) 900°C, (c) 1000°C, and (d) 1100°C.

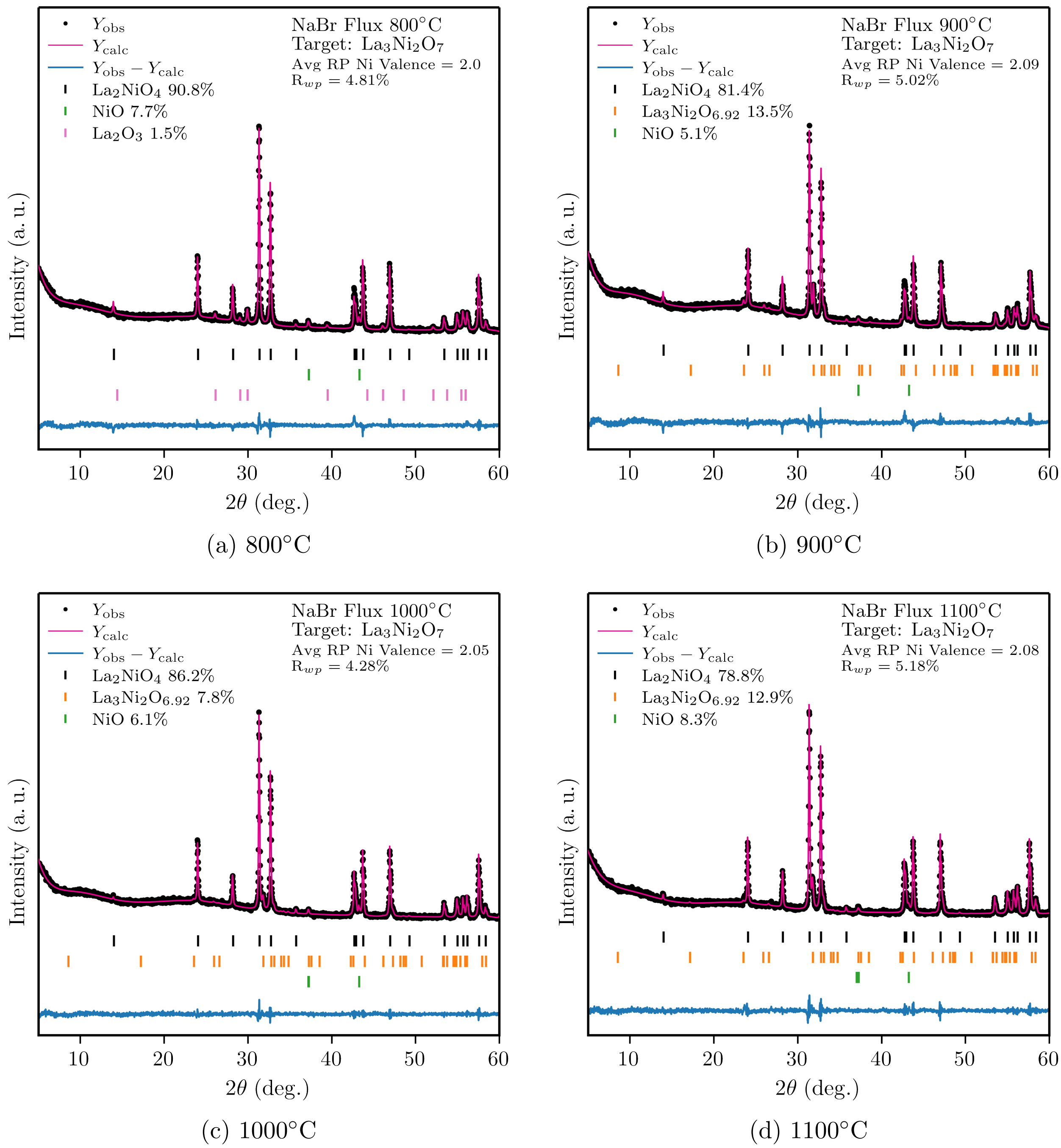

(a) 800°C (b) 900°C (c) 1000°C (d) 1100°C

Figure 12: PXRD and Rietveld refinements of targeted $La_3Ni_2O_7$ where $\frac{Ni}{Ni+La} = 0.40$ in NaBr flux at (a) 800°C, (b) 900°C, (c) 1000°C, and (d) 1100°C.

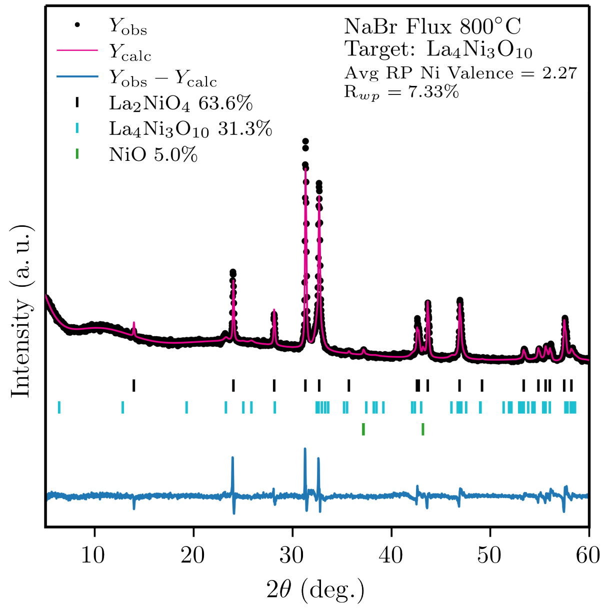

(a) 800°C

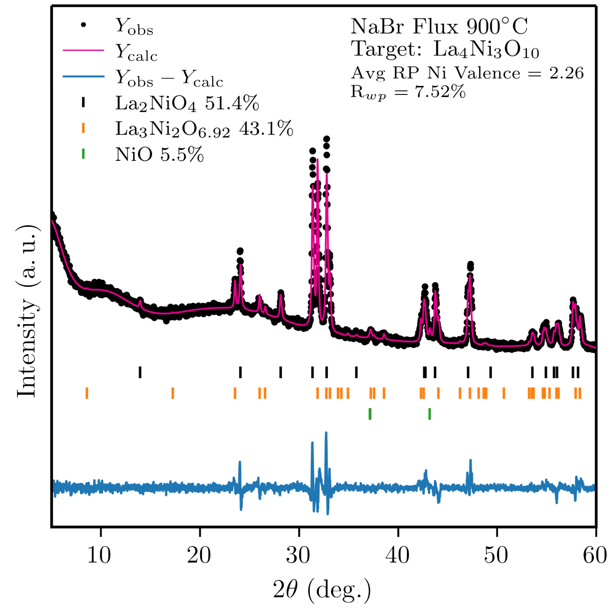

(b) 900°C

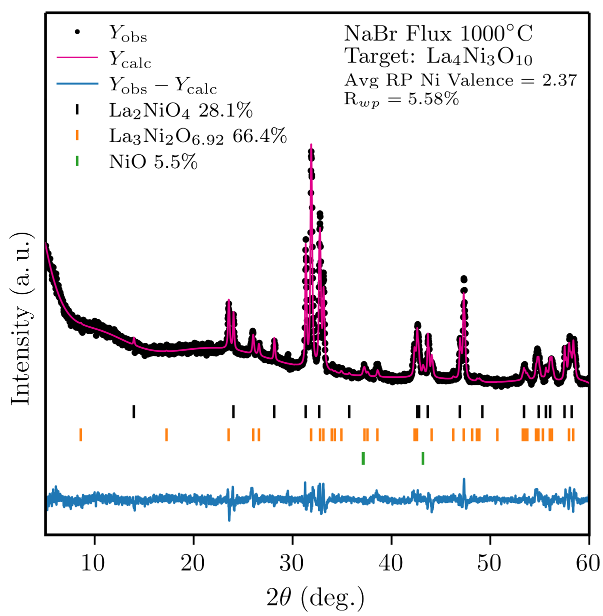

(c) 1000°C

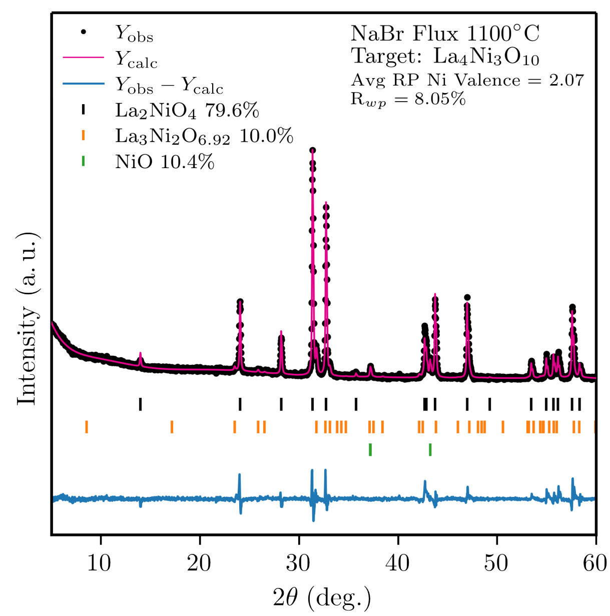

(d) 1100°C

Figure 13: PXRD and Rietveld refinements of targeted $La_4Ni_3O_{10}$ where $\frac{Ni}{Ni+La} = 0.43$ in NaBr flux at (a) 800°C, (b) 900°C, (c) 1000°C, and (d) 1100°C.

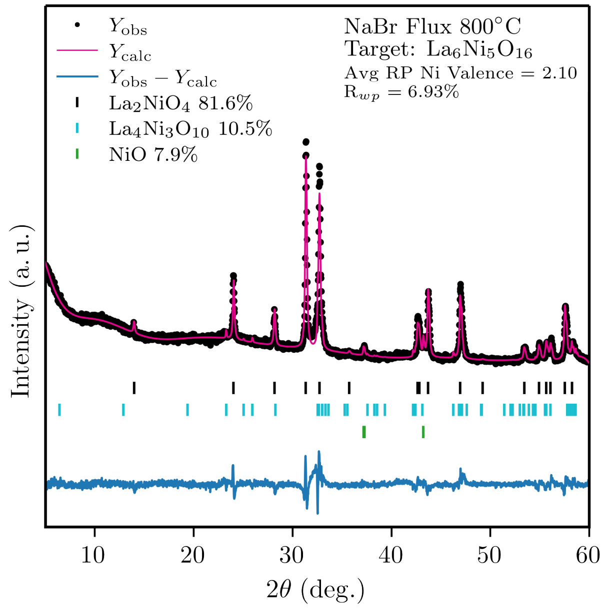

(a) 800°C

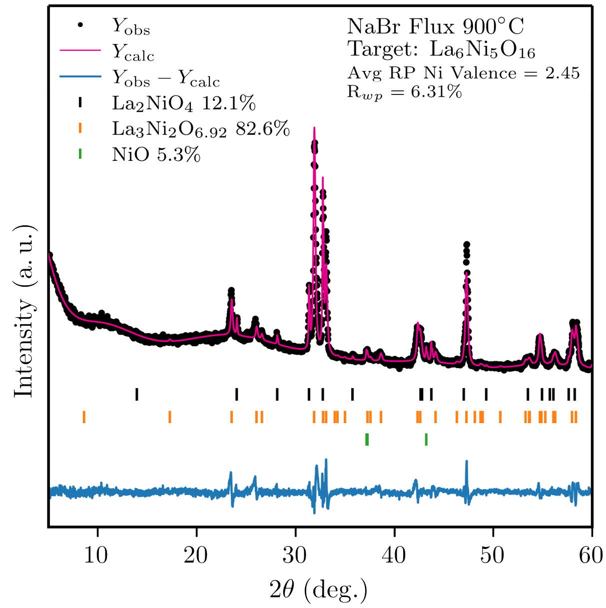

(b) 900°C

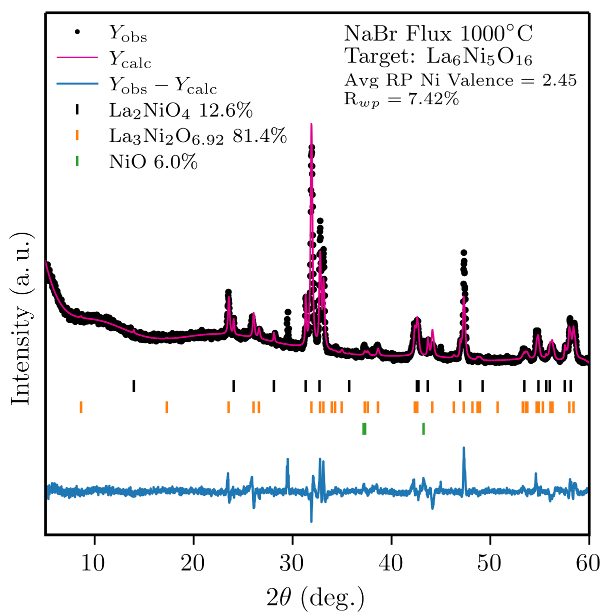

(c) 1000°C

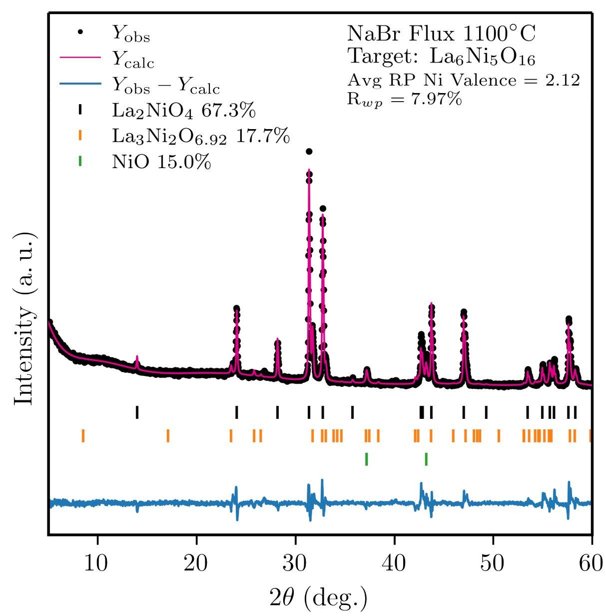

(d) 1100°C

Figure 14: PXRD and Rietveld refinements of targeted $La_6Ni_5O_{16}$ where $\frac{Ni}{Ni+La} = 0.454$ in NaBr flux at (a) 800°C, (b) 900°C, (c) 1000°C, and (d) 1100°C.

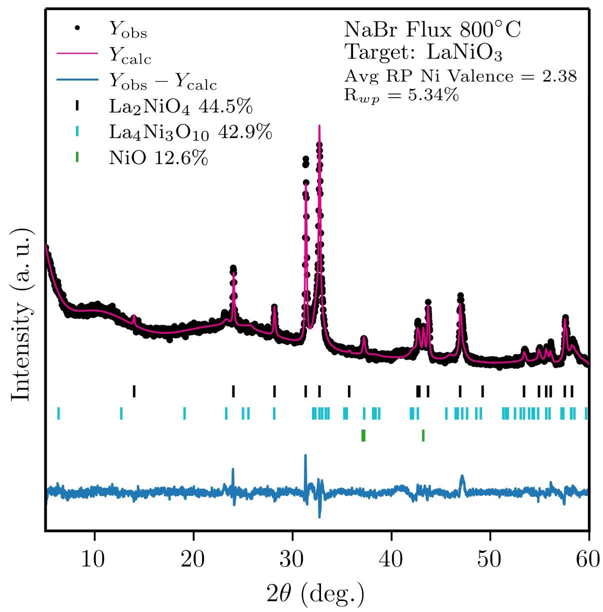

(a) 800°C

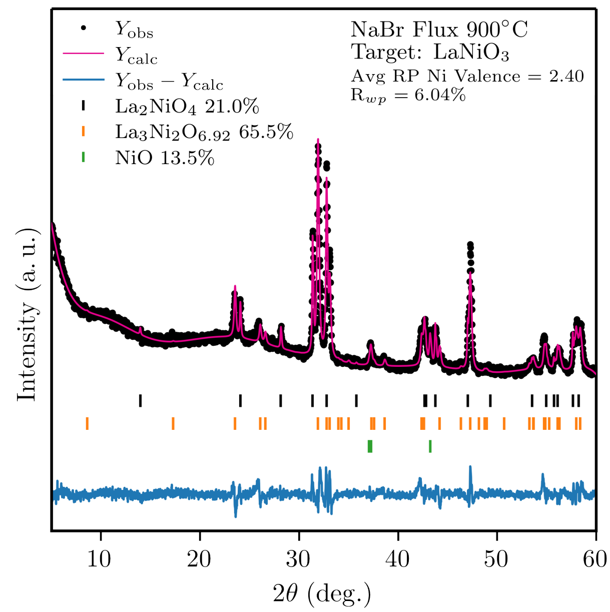

(b) 900°C

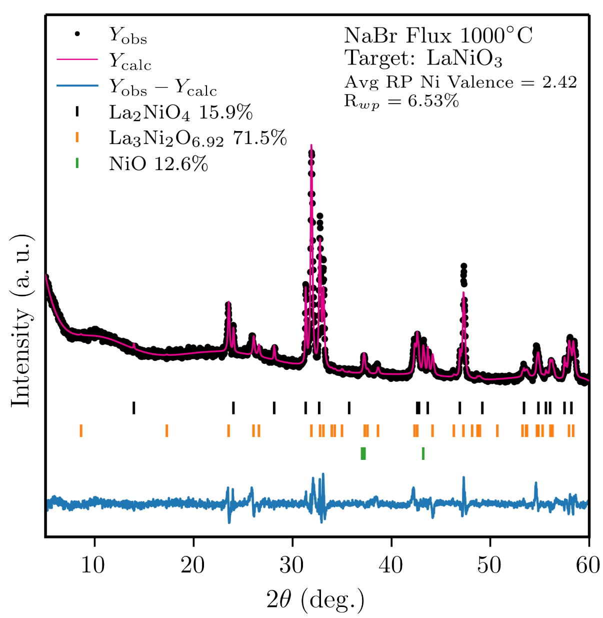

(c) 1000°C

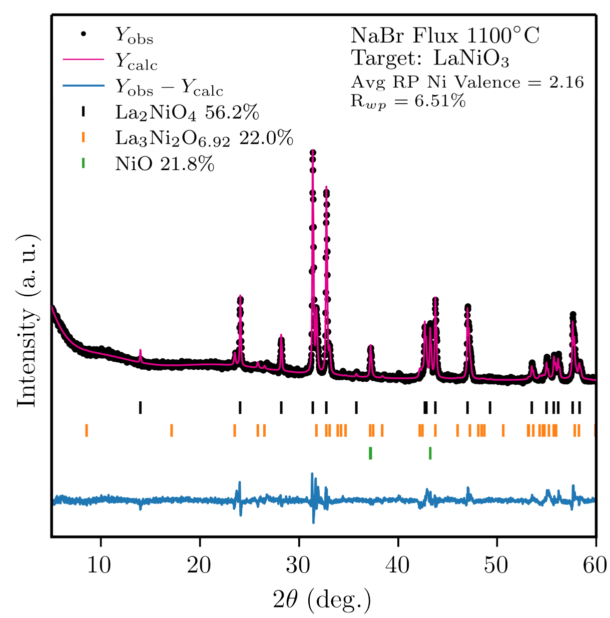

(d) 1100°C

Figure 15: PXRD and Rietveld refinements of targeted $LaNiO_3$ where $\frac{Ni}{Ni+La} = 0.5$ in NaBr flux at (a) 800°C, (b) 900°C, (c) 1000°C, and (d) 1100°C.

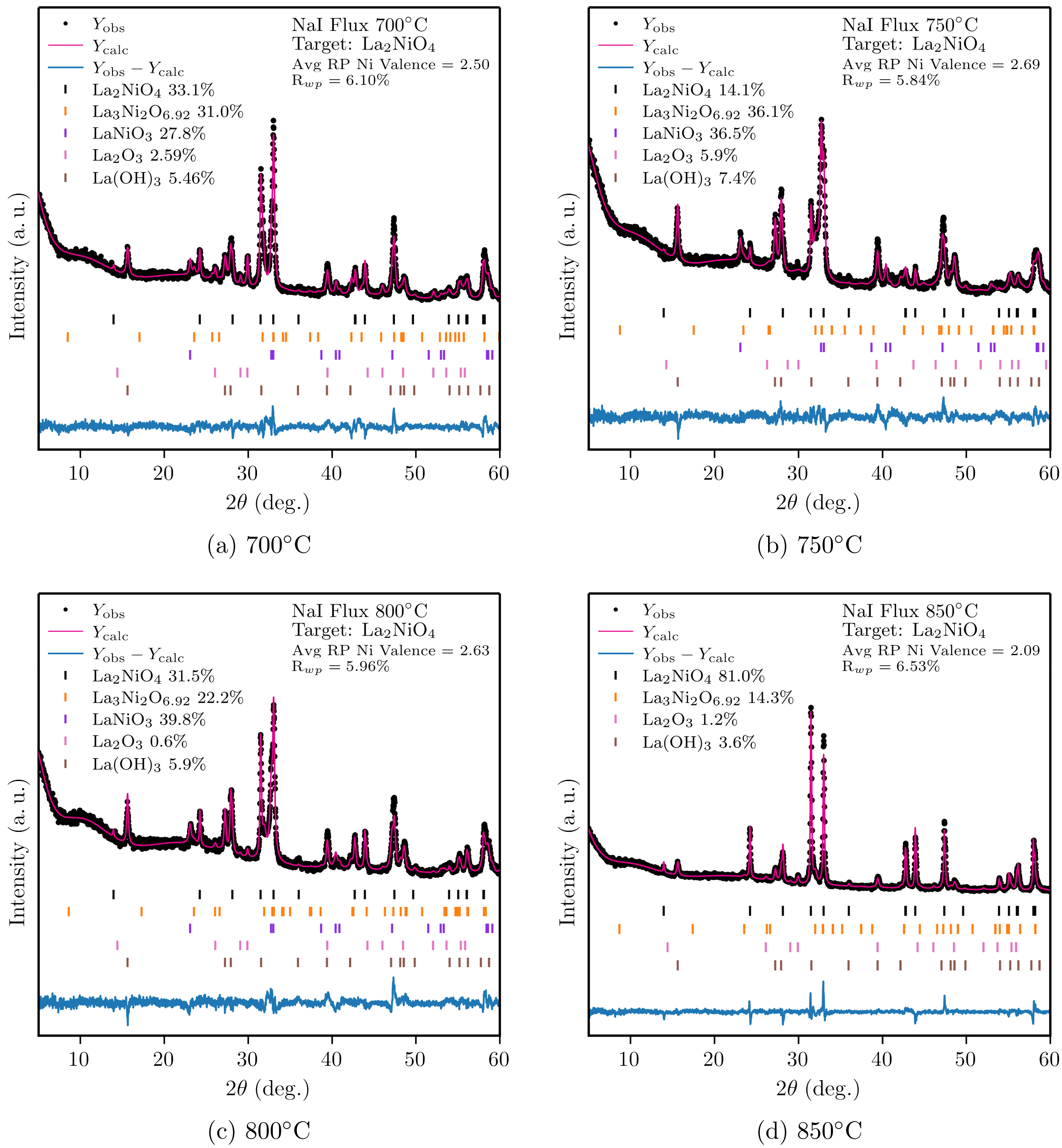

(a) 700°C

(b) 750°C

(c) 800°C

(d) 850°C

Figure 16: PXRD and Rietveld refinements of targeted La_2NiO_4 where $\frac{Ni}{Ni+La} = 0.33$ in NaI flux at (a) 700°C, (b) 750°C, (c) 800°C, and (d) 850°C.

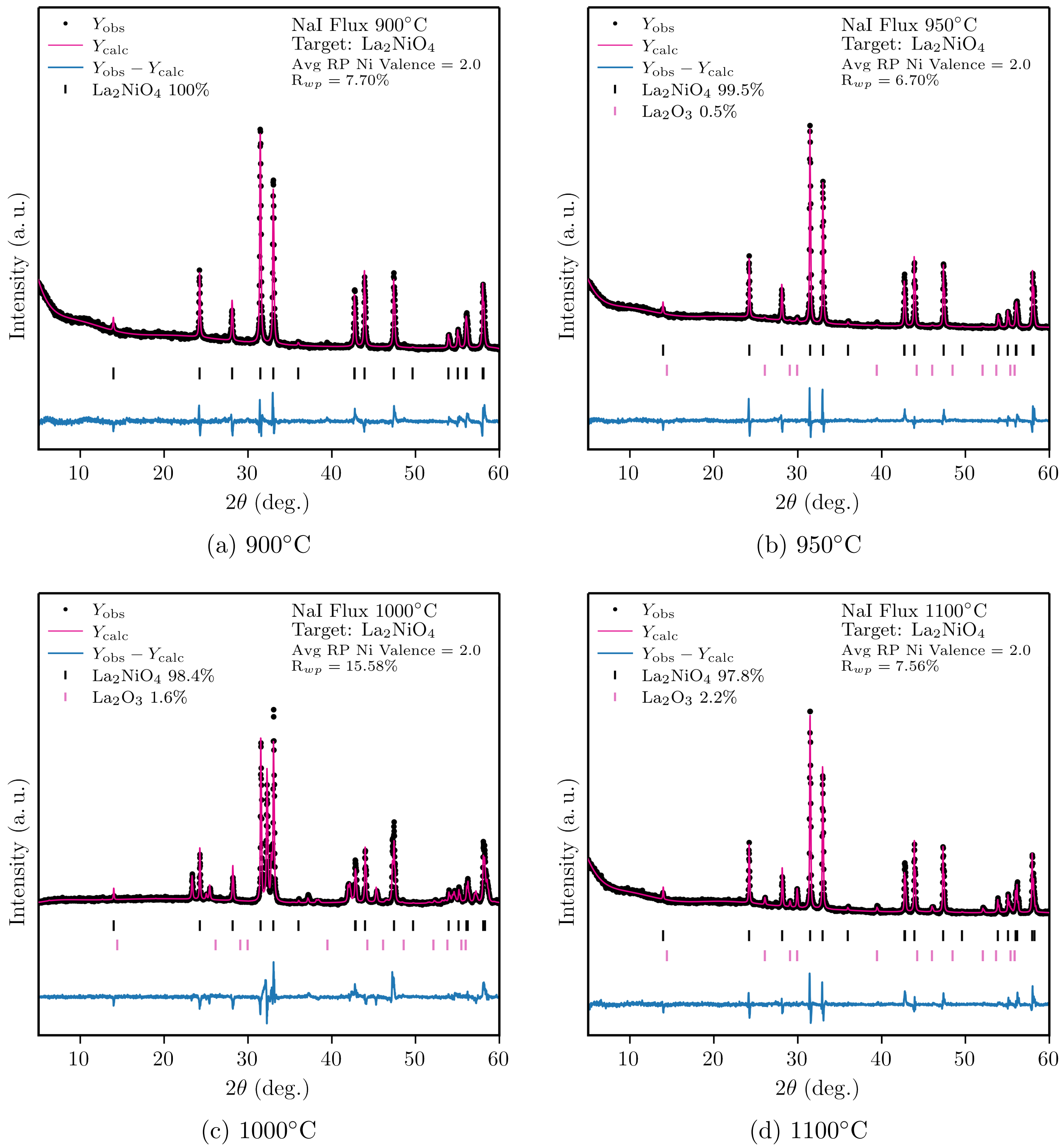

Figure 17: PXRD and Rietveld refinements of targeted La_2NiO_4 where $\frac{\text{Ni}}{\text{Ni+La}} = 0.33$ in NaI flux at (a) 900°C, (b) 950°C, (c) 1000°C, and (d) 1100°C.

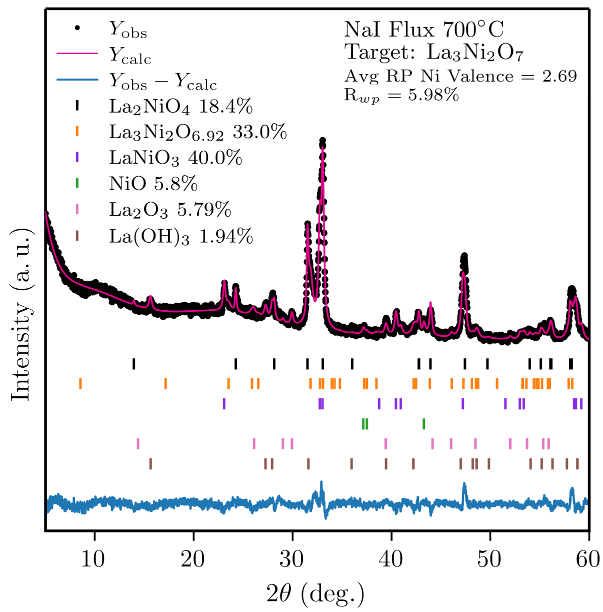

(a) 700°C

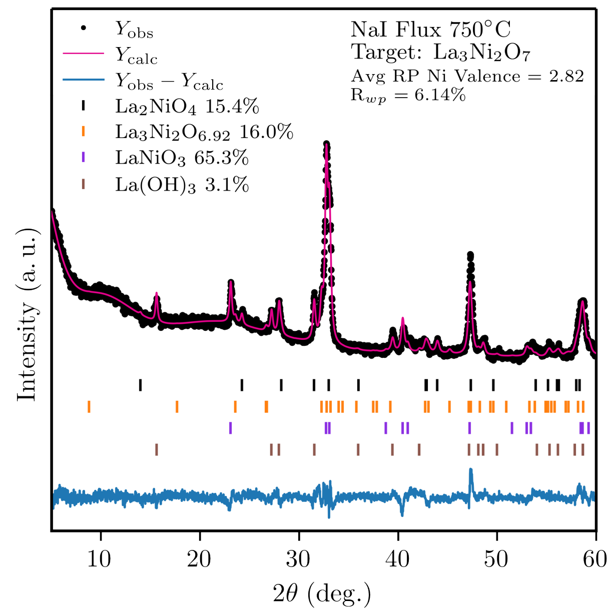

(b) 750°C

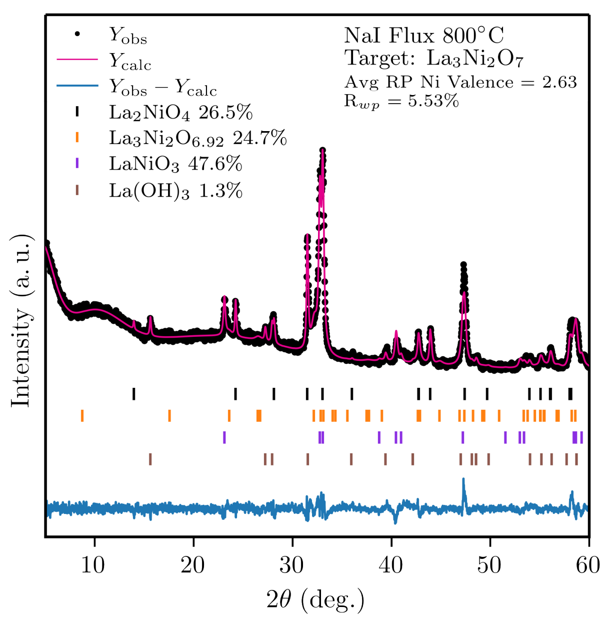

(c) 800°C

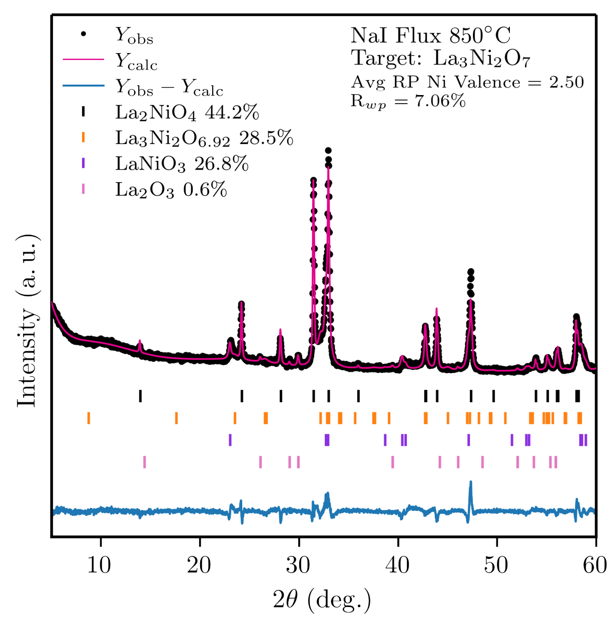

(d) 850°C

Figure 18: PXRD and Rietveld refinements of targeted $La_3Ni_2O_7$ where $\frac{Ni}{Ni+La} = 0.40$ in NaI flux at (a) 700°C, (b) 750°C, (c) 800°C, and (d) 850°C.

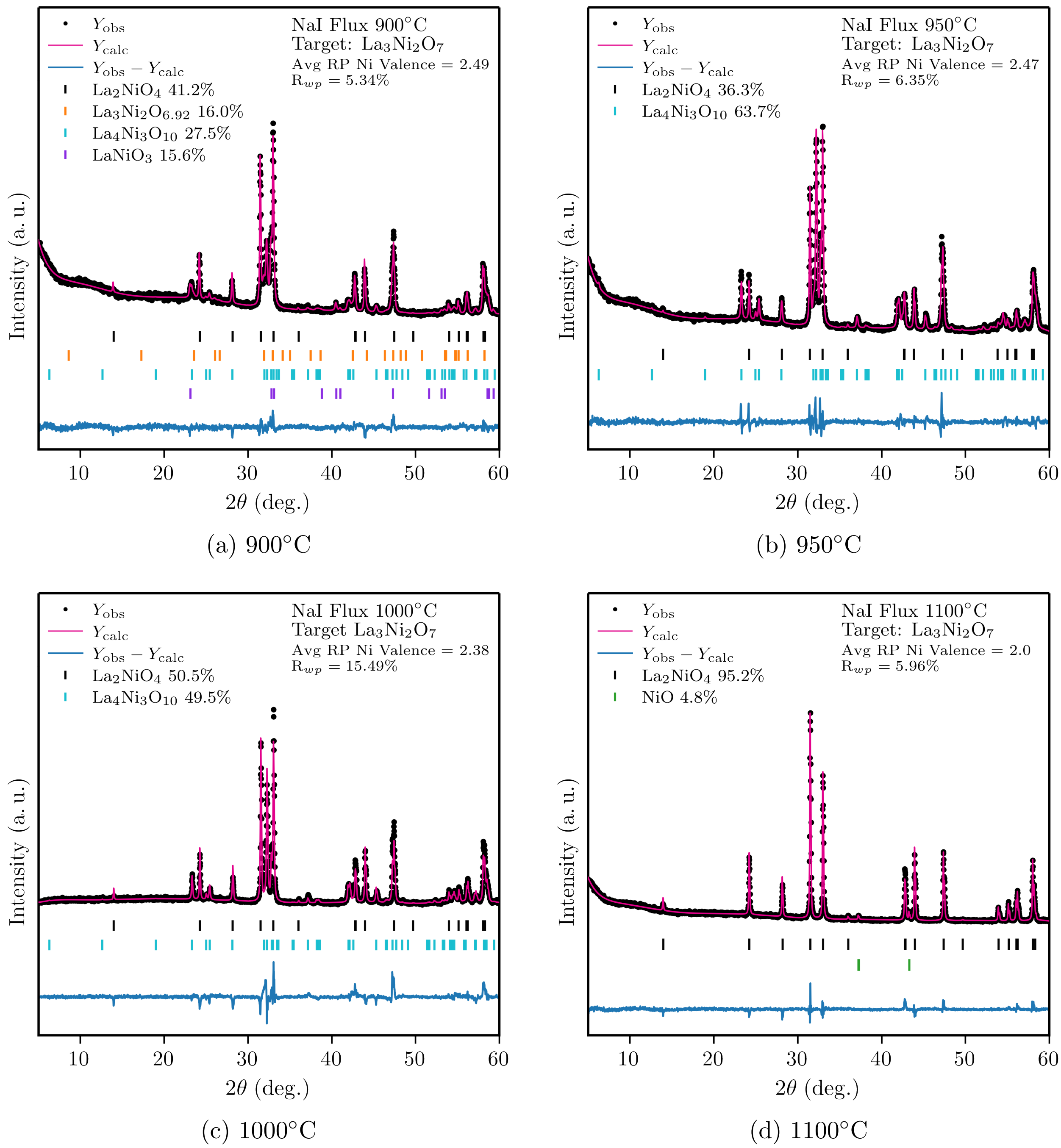

Figure 19: PXRD and Rietveld refinements of targeted $La_3Ni_2O_7$ where $\frac{Ni}{Ni+La} = 0.40$ in NaI flux at (a) 900°C, (b) 950°C, (c) 1000°C, and (d) 1100°C.

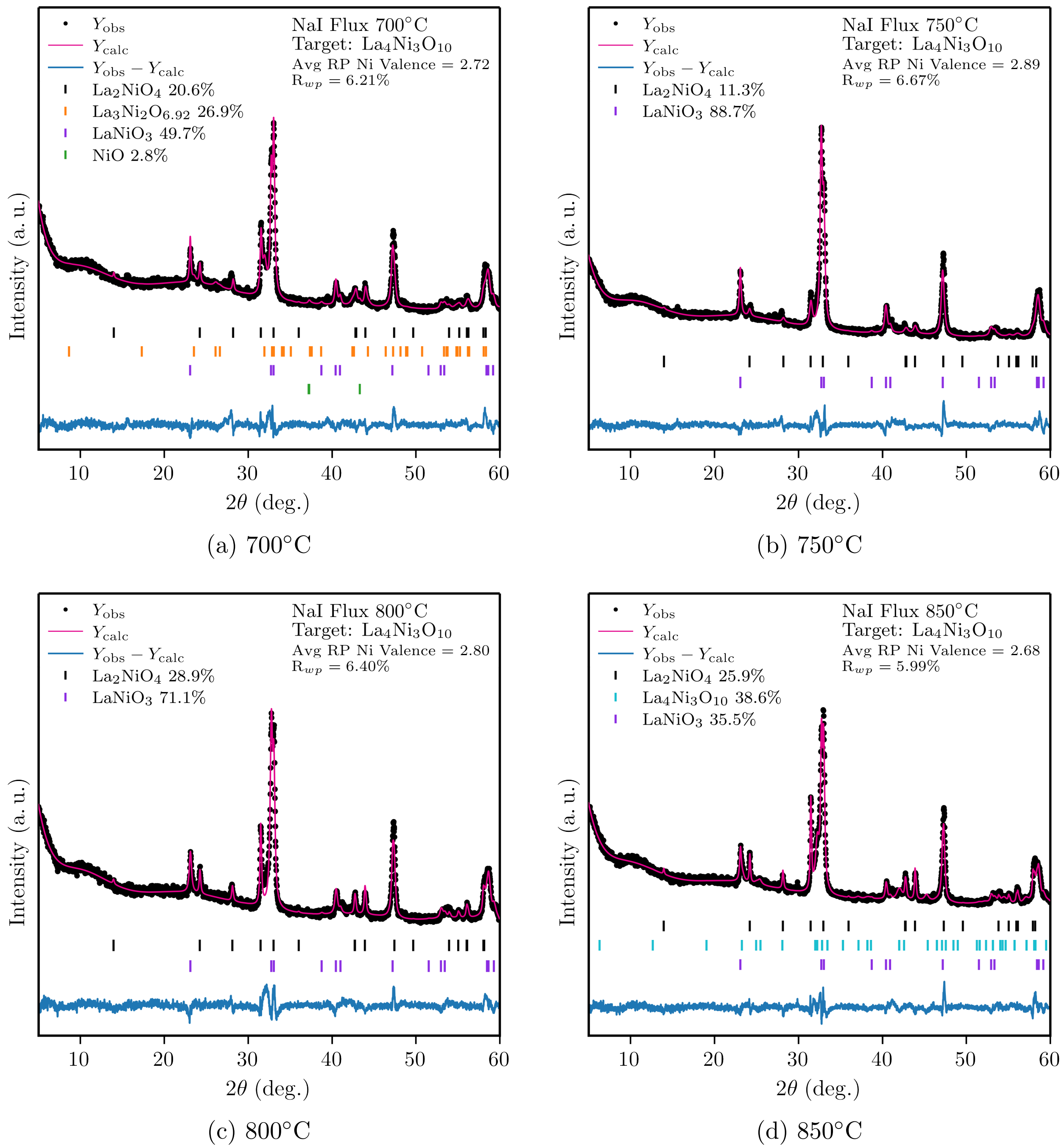

Figure 20: PXRD and Rietveld refinements of targeted $La_4Ni_3O_{10}$ where $\frac{Ni}{Ni+La} = 0.43$ in NaI flux at (a) 700°C, (b) 750°C, (c) 800°C, and (d) 850°C.

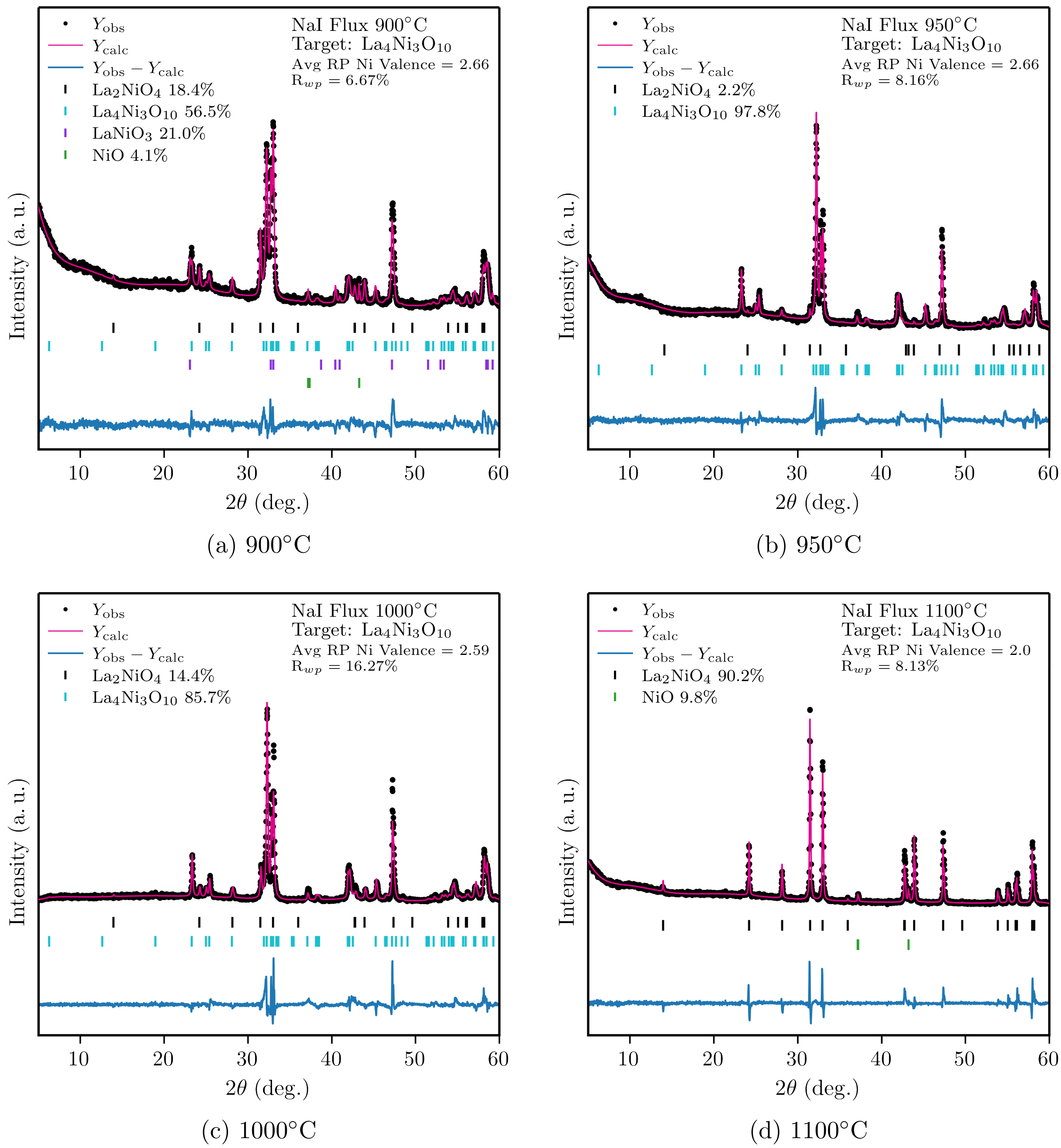

(a) 900°C

(b) 950°C

(c) 1000°C

(d) 1100°C

Figure 21: PXRD and Rietveld refinements of targeted $La_4Ni_3O_{10}$ where $\frac{\text{Ni}}{\text{Ni+La}} = 0.43$ in NaI flux at (a) 900°C, (b) 950°C, (c) 1000°C, and (d) 1100°C.

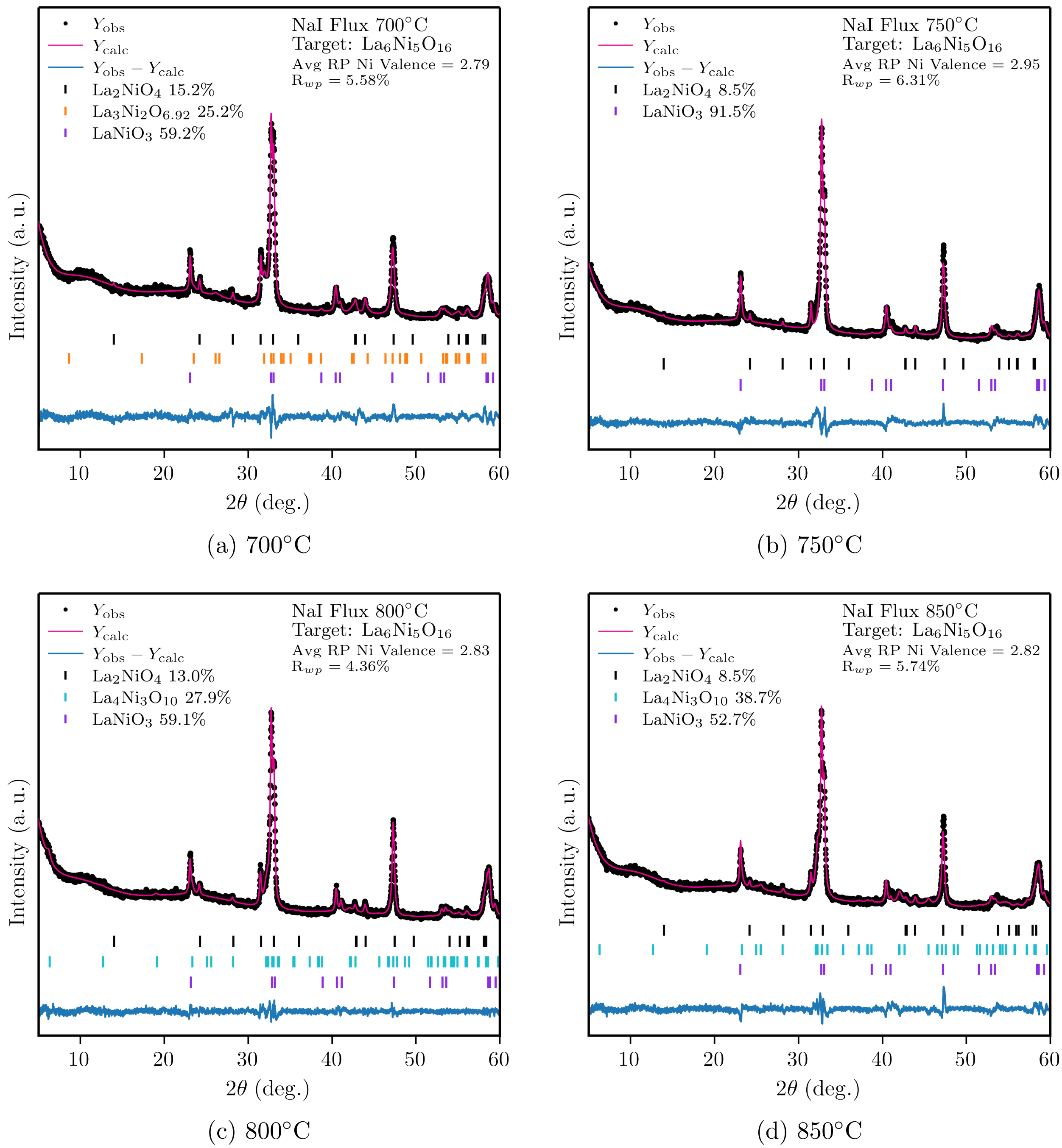

(a) 700°C (b) 750°C

(c) 800°C (d) 850°C

Figure 22: PXRD and Rietveld refinements of targeted $La_6Ni_5O_{16}$ where $\frac{Ni}{Ni+La} = 0.454$ in NaI flux at (a) 700°C, (b) 750°C, (c) 800°C, and (d) 850°C.

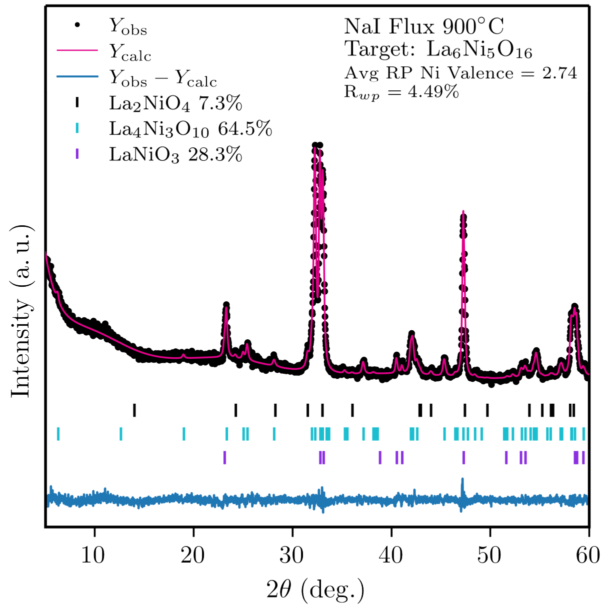

(a) 900°C

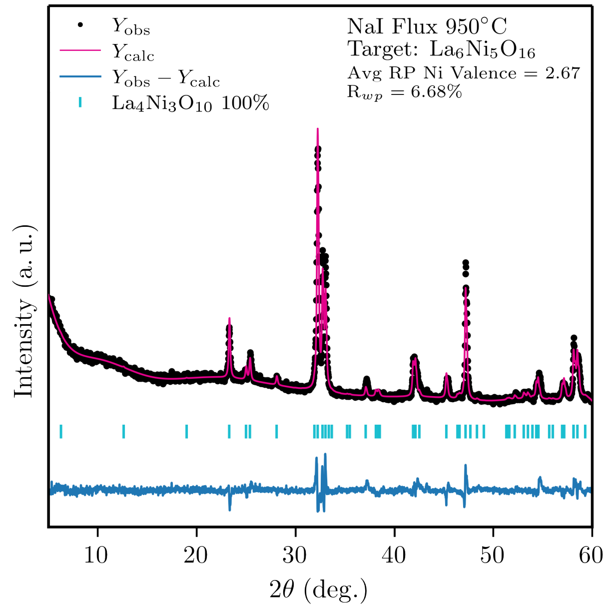

(b) 950°C

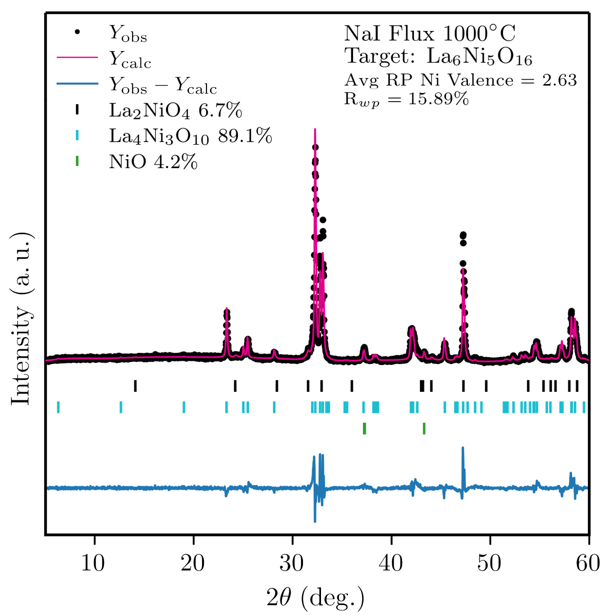

(c) 1000°C

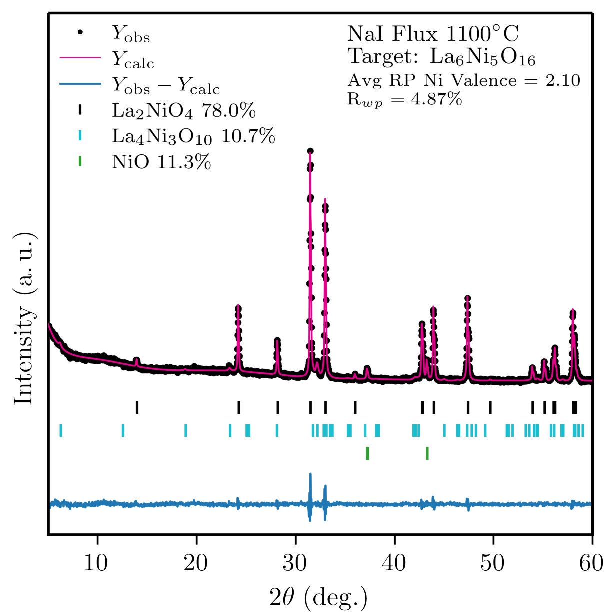

(d) 1100°C

Figure 23: PXRD and Rietveld refinements of targeted $La_6Ni_5O_{16}$ where $\frac{\text{Ni}}{\text{Ni+La}} = 0.454$ in NaI flux at (a) 900°C, (b) 950°C, (c) 1000°C, and (d) 1100°C.

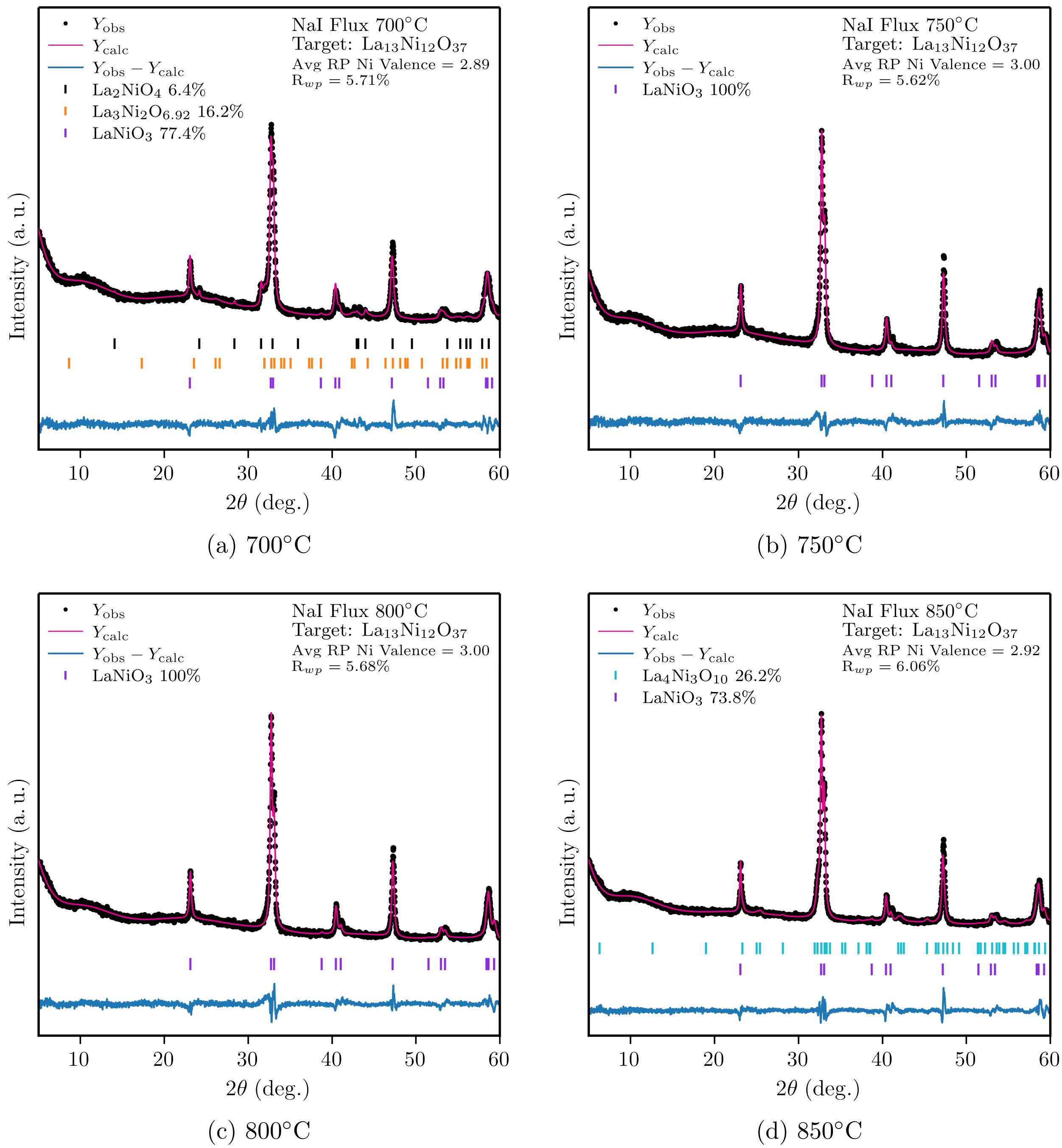

Figure 24: PXRD and Rietveld refinements of targeted $La_{13}Ni_{12}O_{37}$ where $\frac{Ni}{Ni+La} = 0.48$ in NaI flux at (a) 700°C, (b) 750°C, (c) 800°C, and (d) 850°C.

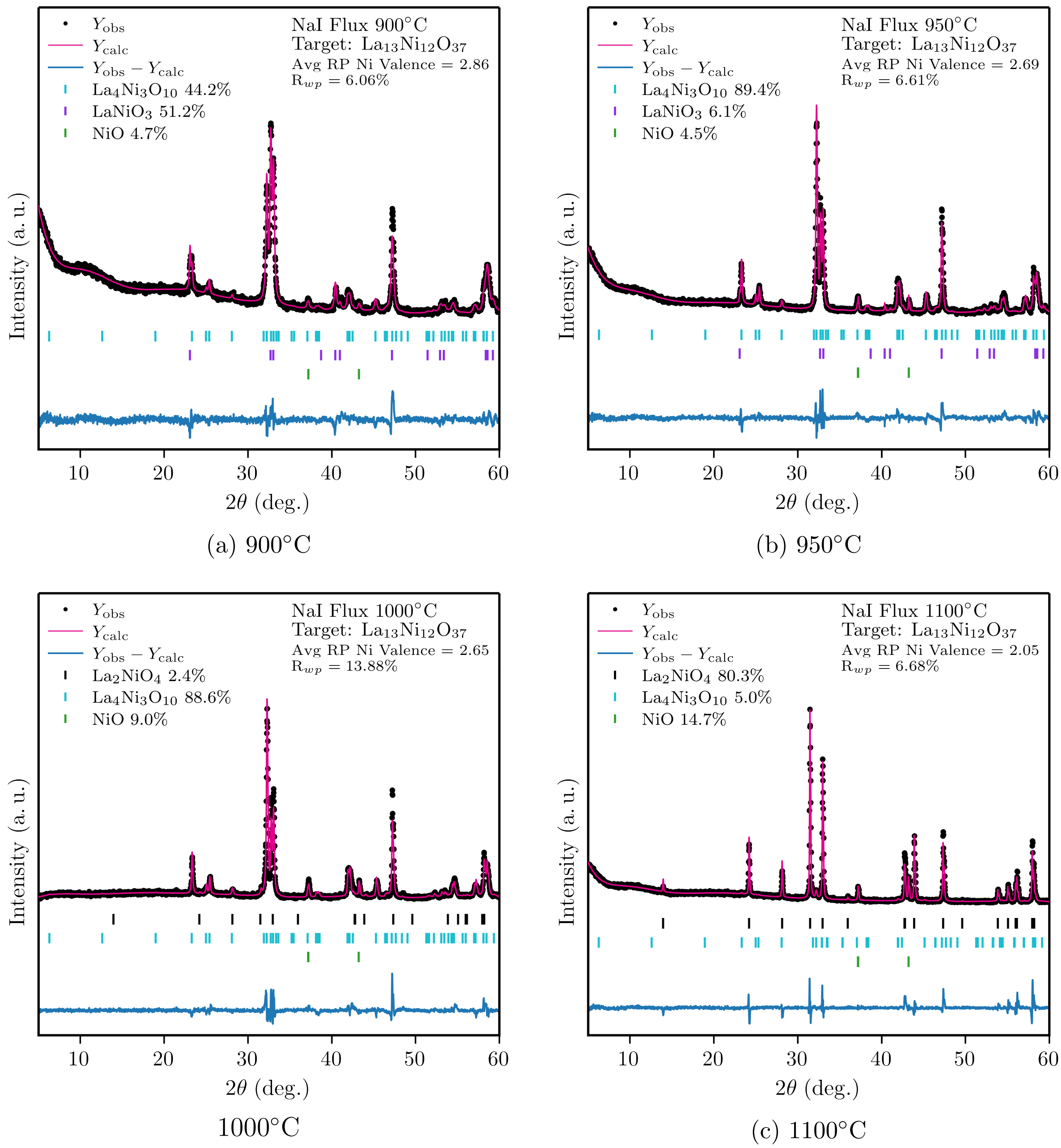

Figure 25: PXRD and Rietveld refinements of targeted $La_{13}Ni_{12}O_{37}$ where $\frac{Ni}{Ni+La} = 0.48$ in NaI flux at (a) 900°C, (b) 950°C, (c) 1000°C, and (d) 1100°C.

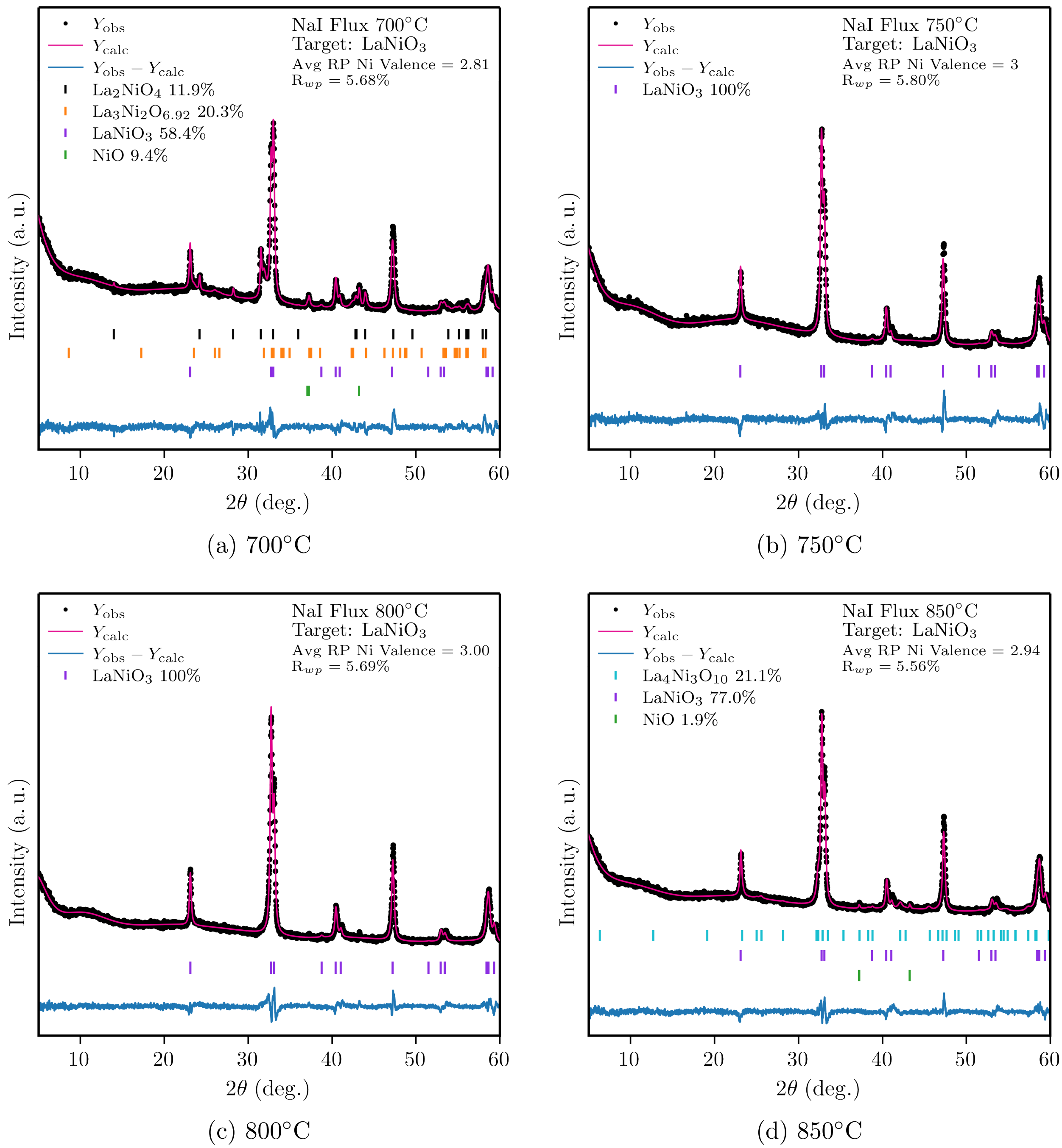

(a) 700°C

(b) 750°C

(c) 800°C

(d) 850°C

Figure 26: PXRD and Rietveld refinements of targeted $LaNiO_3$ where $\frac{Ni}{Ni+La} = 0.5$ in NaI flux at (a) 700°C, (b) 750°C, (c) 800°C, and (d) 850°C.

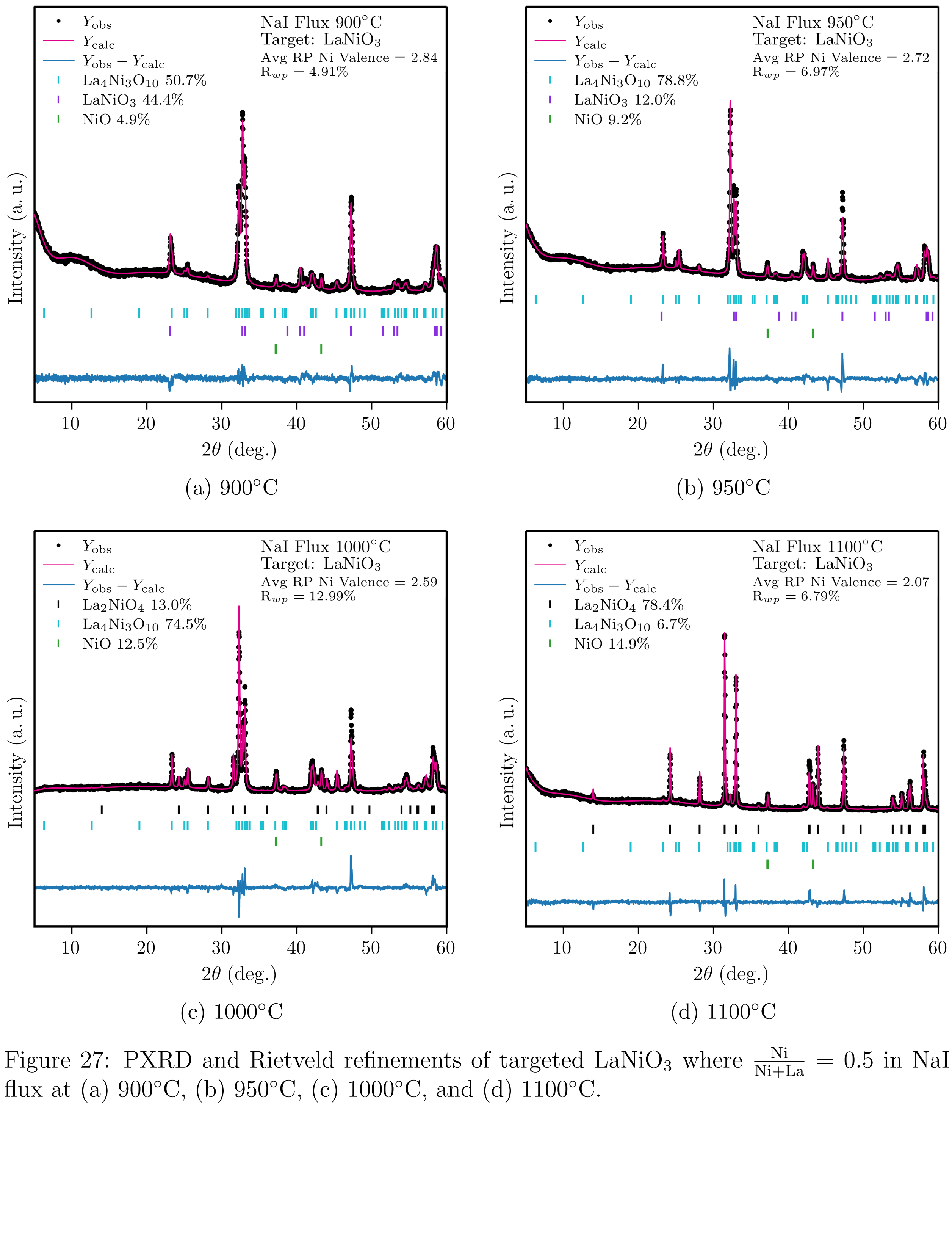

Figure 27: PXRD and Rietveld refinements of targeted $LaNiO_3$ where $\frac{Ni}{Ni+La} = 0.5$ in NaI flux at (a) 900°C, (b) 950°C, (c) 1000°C, and (d) 1100°C.

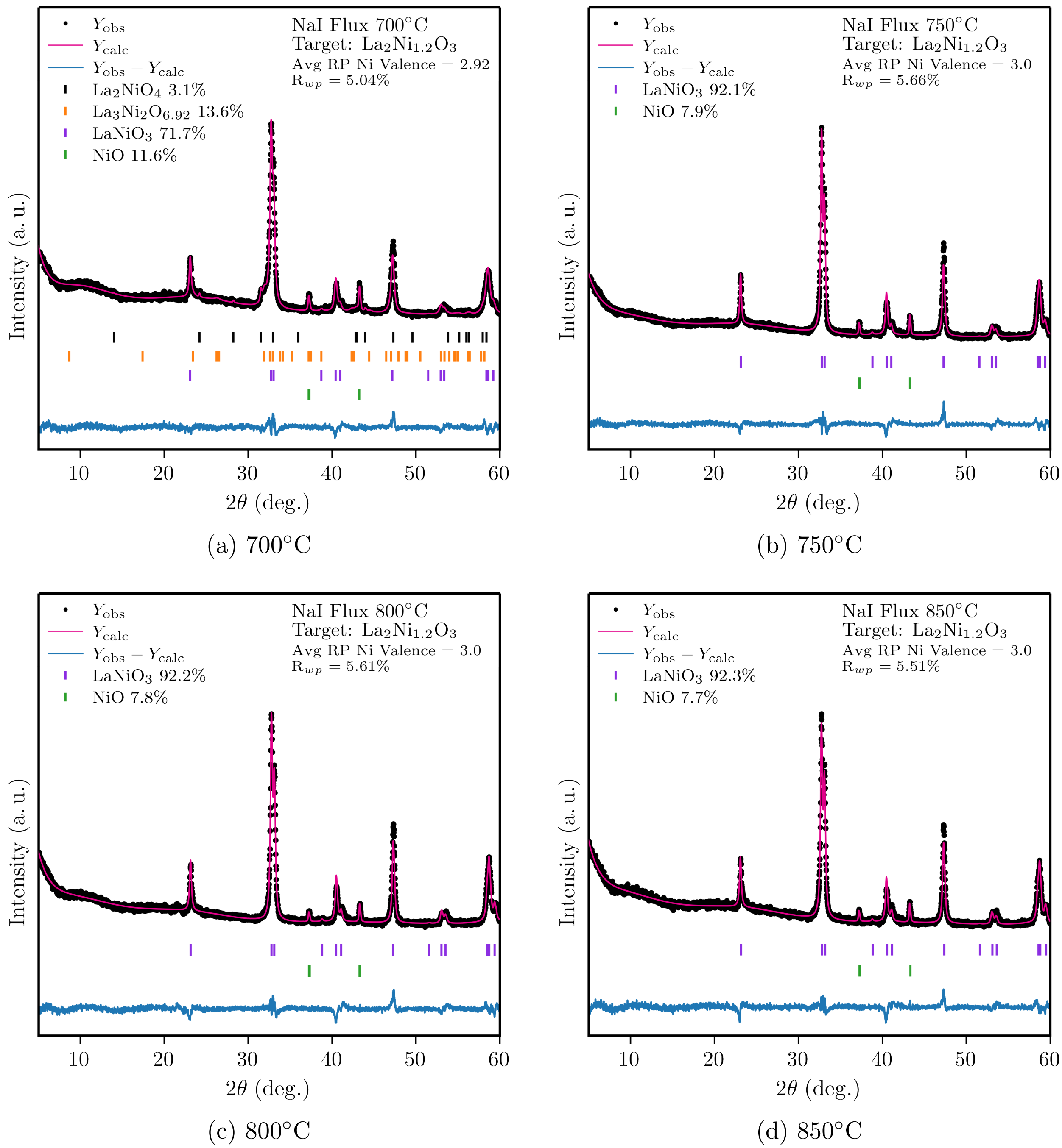

(a) 700°C

(b) 750°C

(c) 800°C

(d) 850°C

Figure 28: PXRD and Rietveld refinements of targeted $LaNi_{1.2}O_3$ where $\frac{Ni}{Ni+La} = 0.6$ in NaI flux at (a) 700°C, (b) 750°C, (c) 800°C, and (d) 850°C.

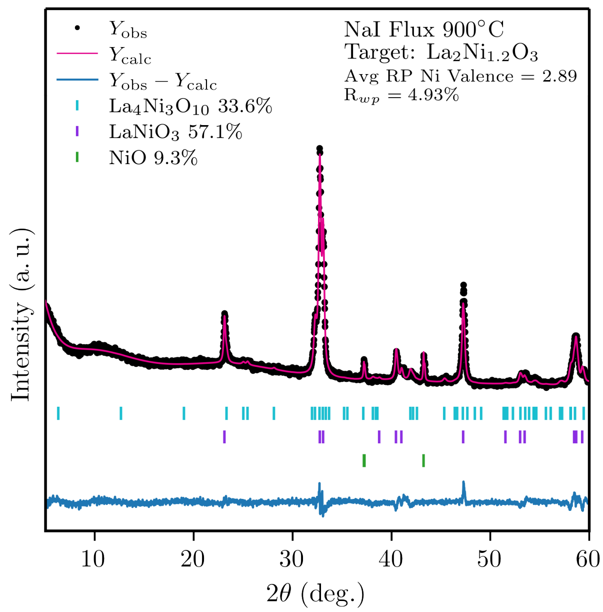

(a) 900°C

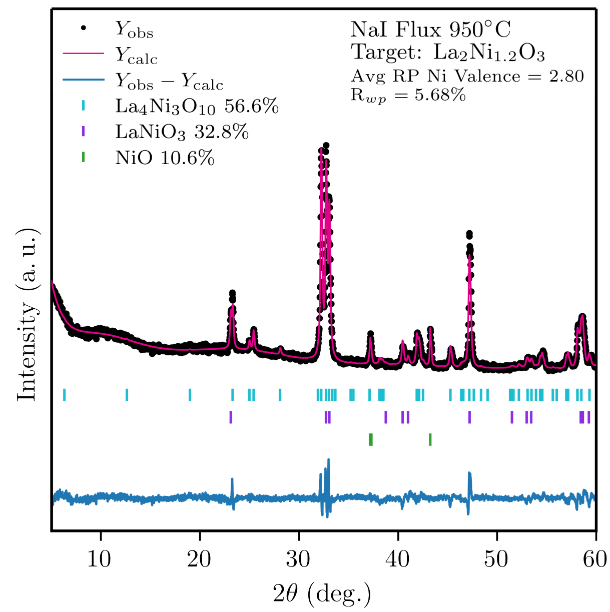

(b) 950°C

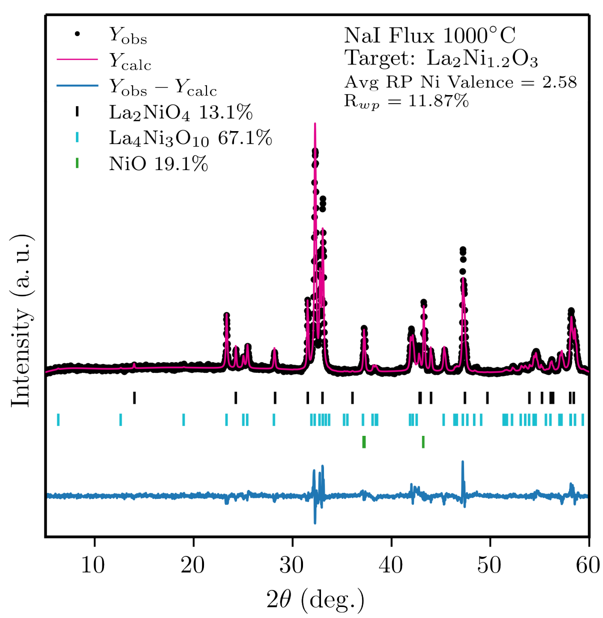

(c) 1000°C

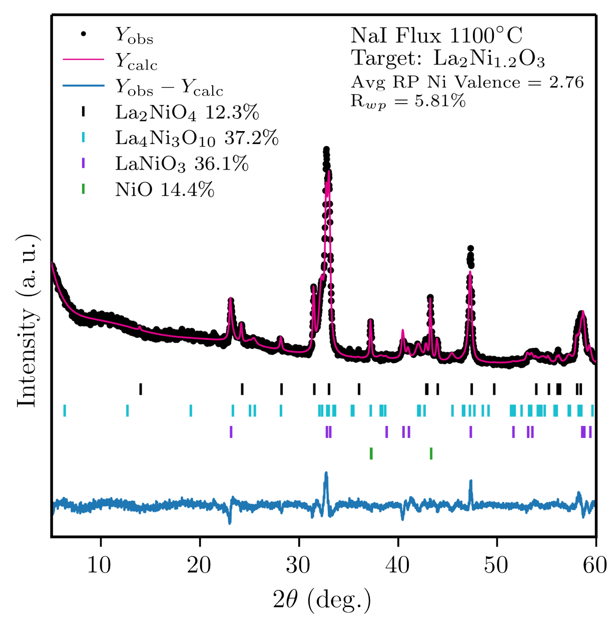

(d) 1100°C

Figure 29: PXRD and Rietveld refinements of targeted $LaNi_{1.2}O_3$ where $\frac{\text{Ni}}{\text{Ni+La}} = 0.6$ in NaI flux at (a) 900°C, (b) 950°C, (c) 1000°C, and (d) 1100°C.

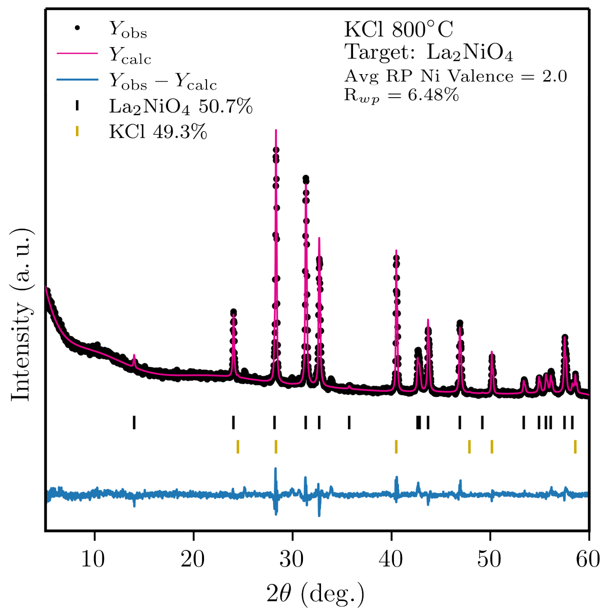

(a) 800°C

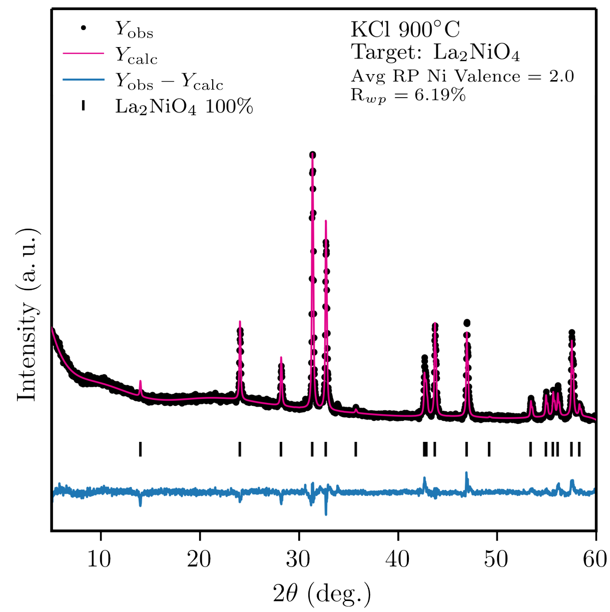

(b) 900°C

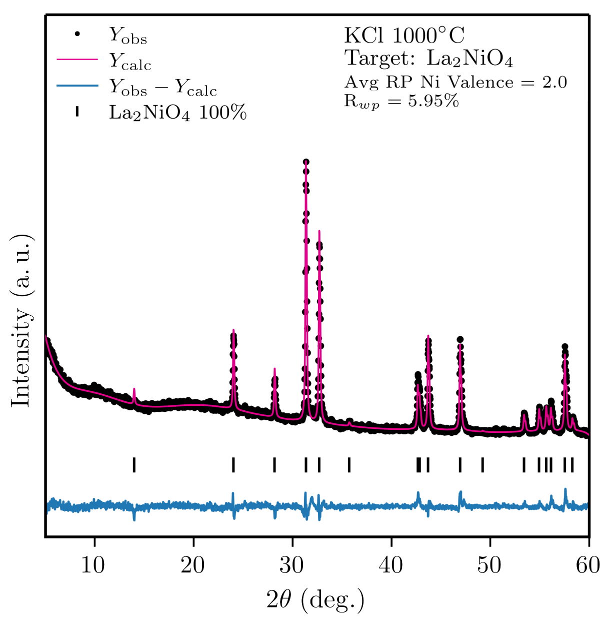

(c) 1000°C

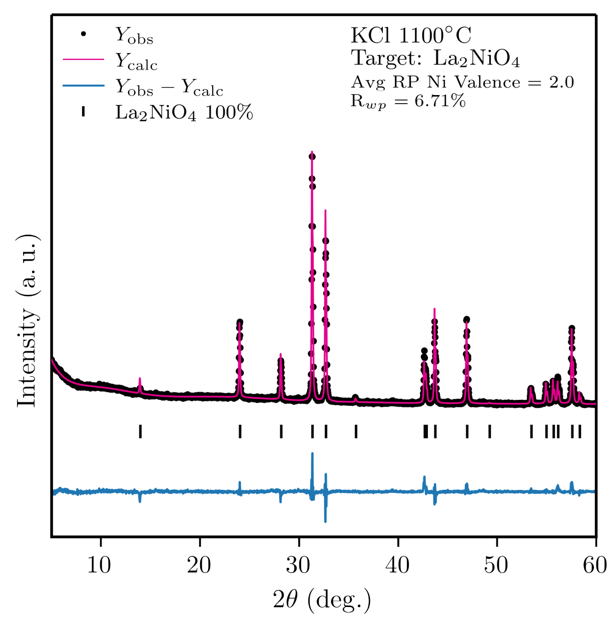

(d) 1100°C

Figure 30: PXRD and Rietveld refinements of targeted La_2NiO_4 where $\frac{Ni}{Ni+La} = 0.33$ in KCl flux at (a) 800°C, (b) 900°C, (c) 1000°C, and (d) 1100°C.

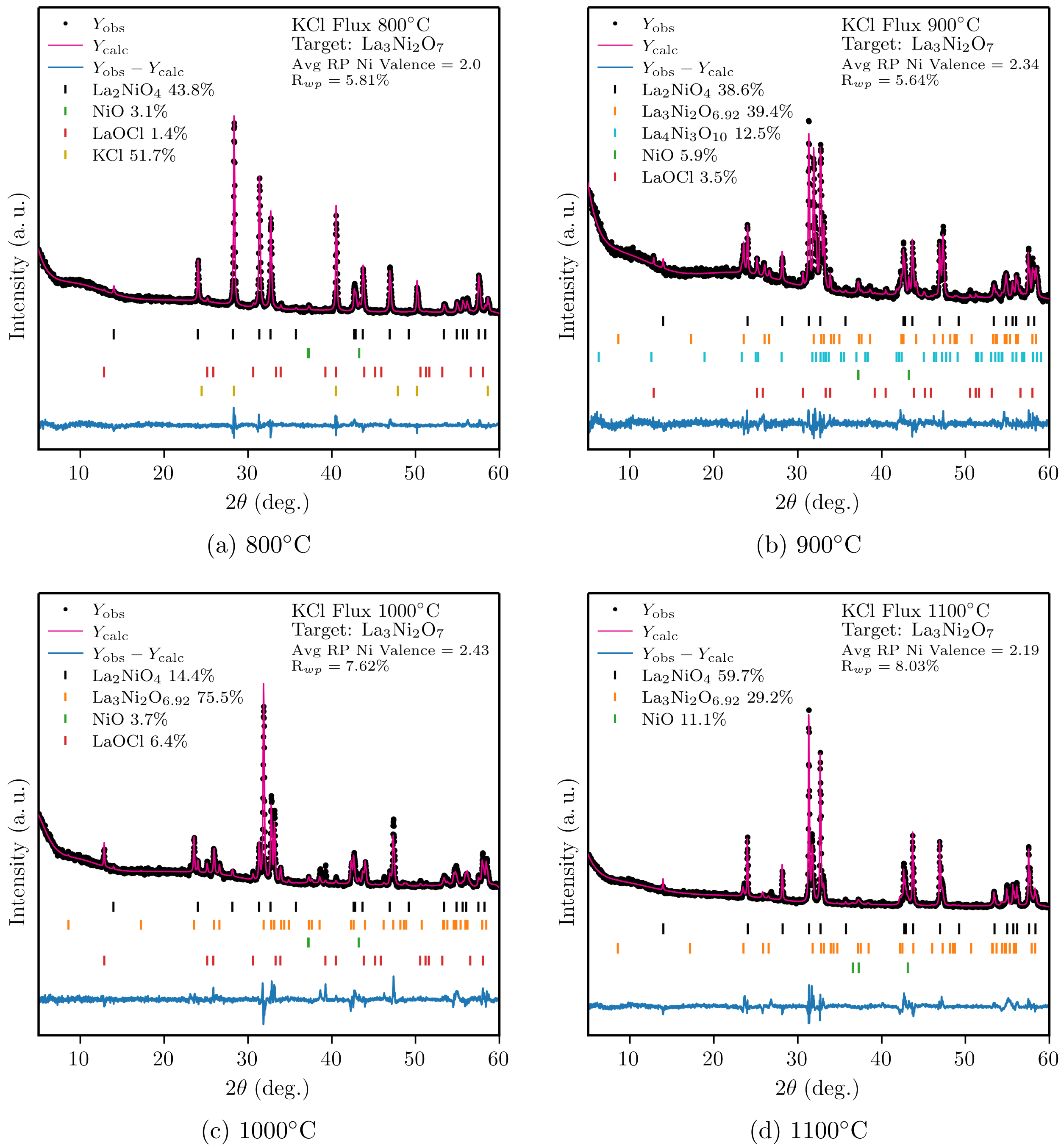

Figure 31: PXRD and Rietveld refinements of targeted $La_3Ni_2O_7$ where $\frac{Ni}{Ni+La} = 0.40$ in KCl flux at (a) 800°C, (b) 900°C, (c) 1000°C, and (d) 1100°C.

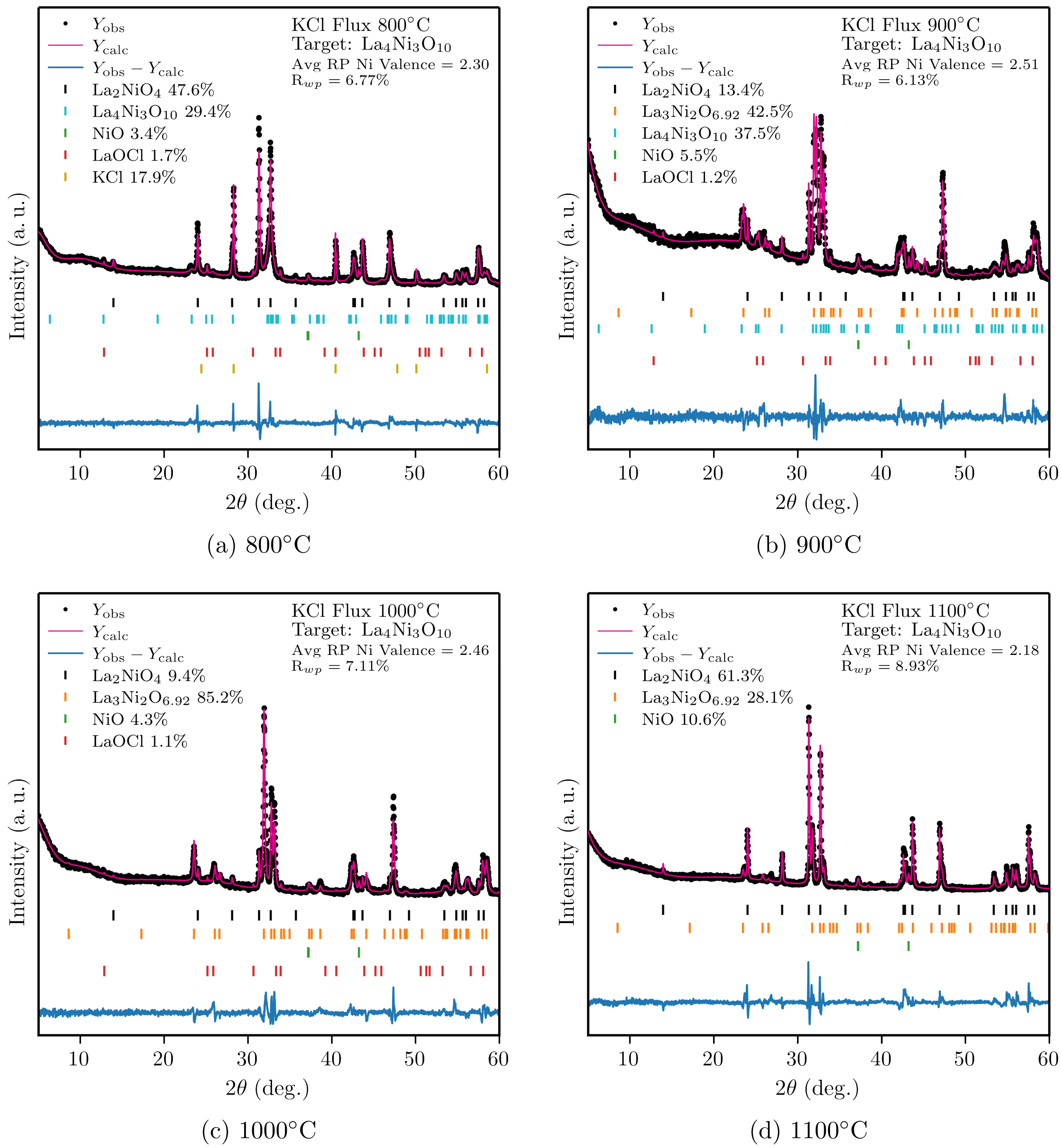

Figure 32: PXRD and Rietveld refinements of targeted $La_4Ni_3O_{10}$ where $\frac{Ni}{Ni+La} = 0.43$ in KCl flux at (a) 800°C, (b) 900°C, (c) 1000°C, and (d) 1100°C.

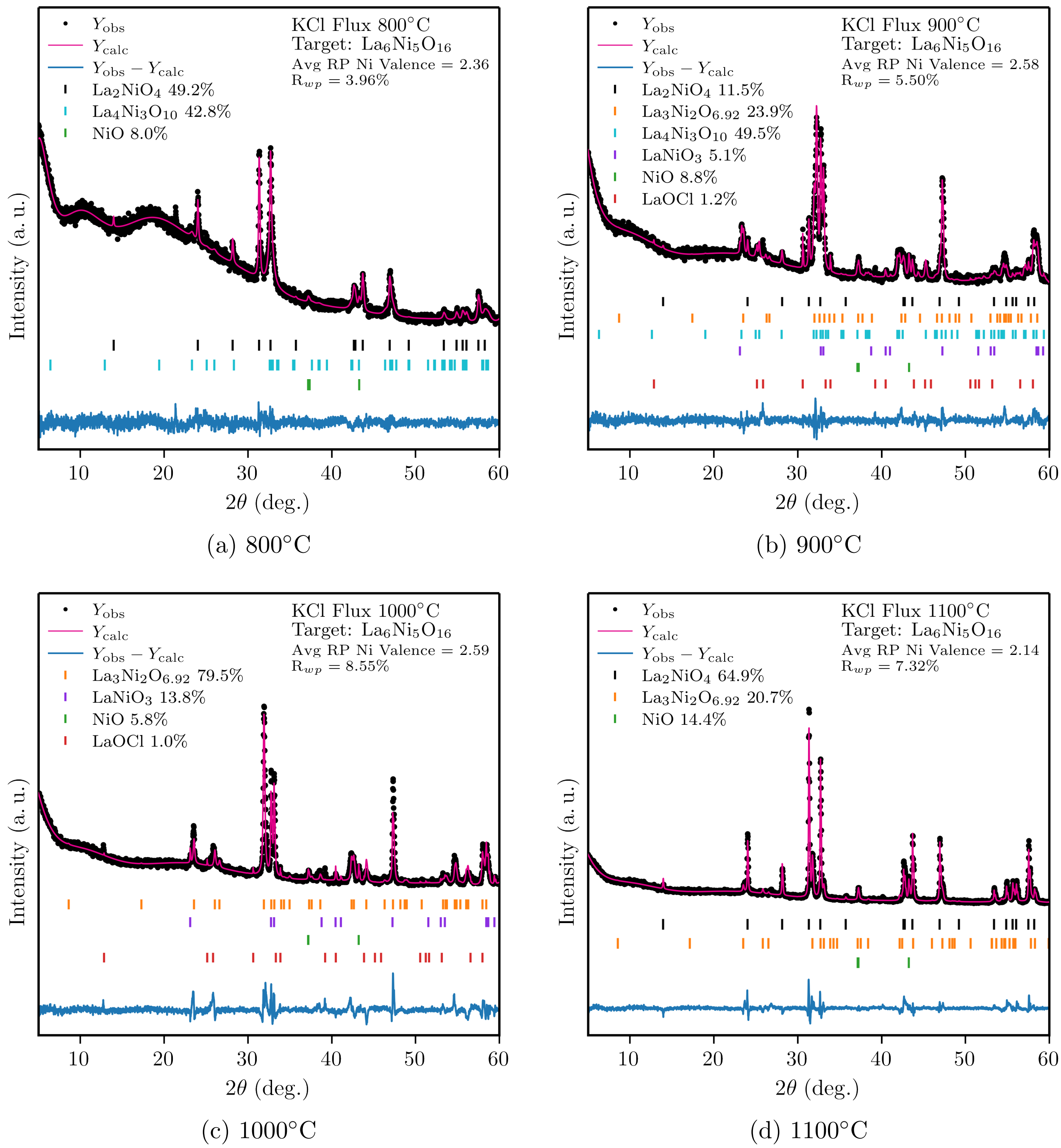

(a) 800°C

(b) 900°C

(c) 1000°C

(d) 1100°C

Figure 33: PXRD and Rietveld refinements of targeted $La_6Ni_5O_{16}$ where $\frac{Ni}{Ni+La} = 0.454$ in KCl flux at (a) 800°C, (b) 900°C, (c) 1000°C, and (d) 1100°C.

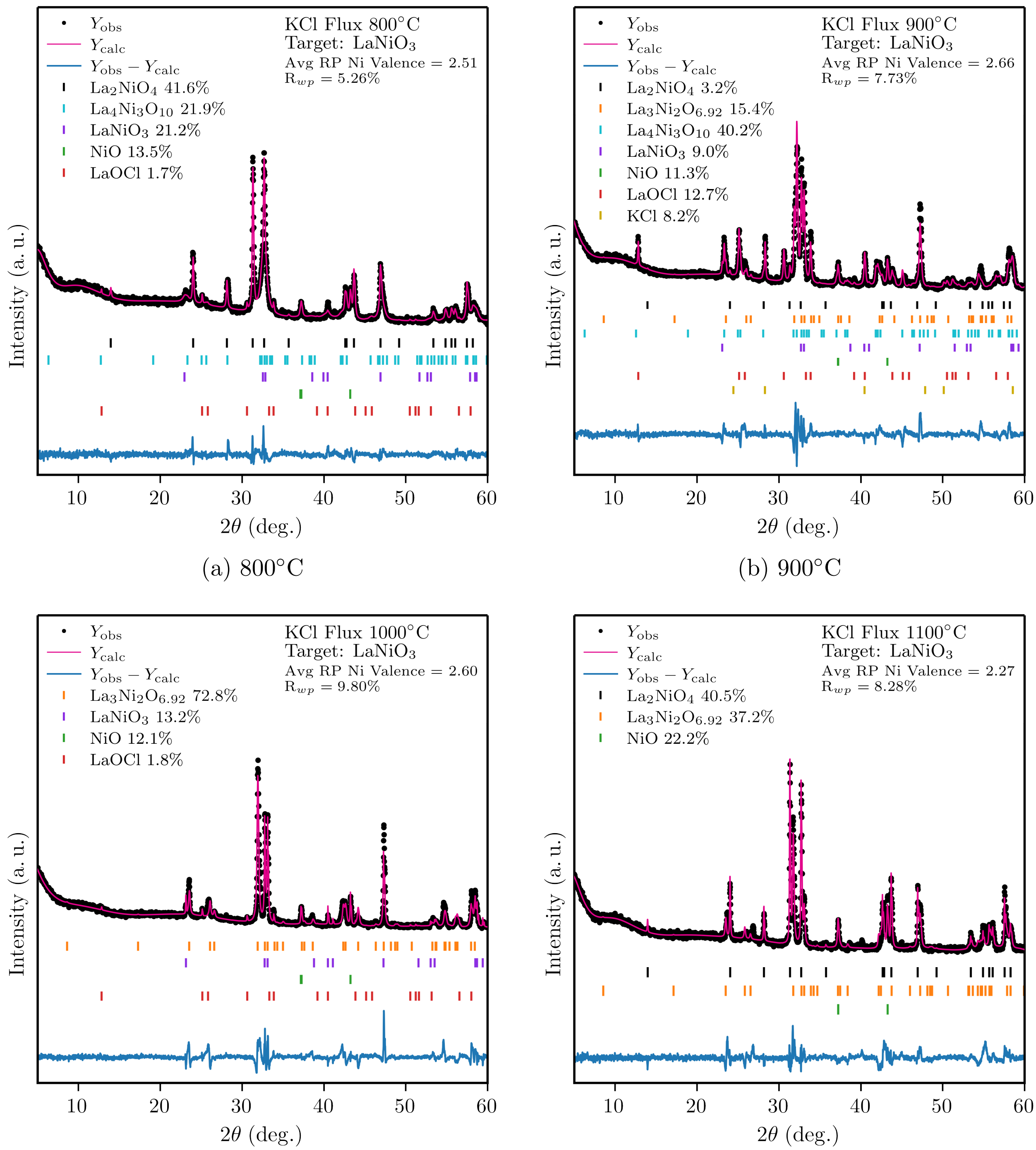

(a) 800°C (b) 900°C

(c) 1000°C (d) 1100°C

Figure 34: PXRD and Rietveld refinements of targeted $LaNiO_3$ where $\frac{Ni}{Ni+La} = 0.5$ in KCl flux at (a) 800°C, (b) 900°C, (c) 1000°C, and (d) 1100°C.

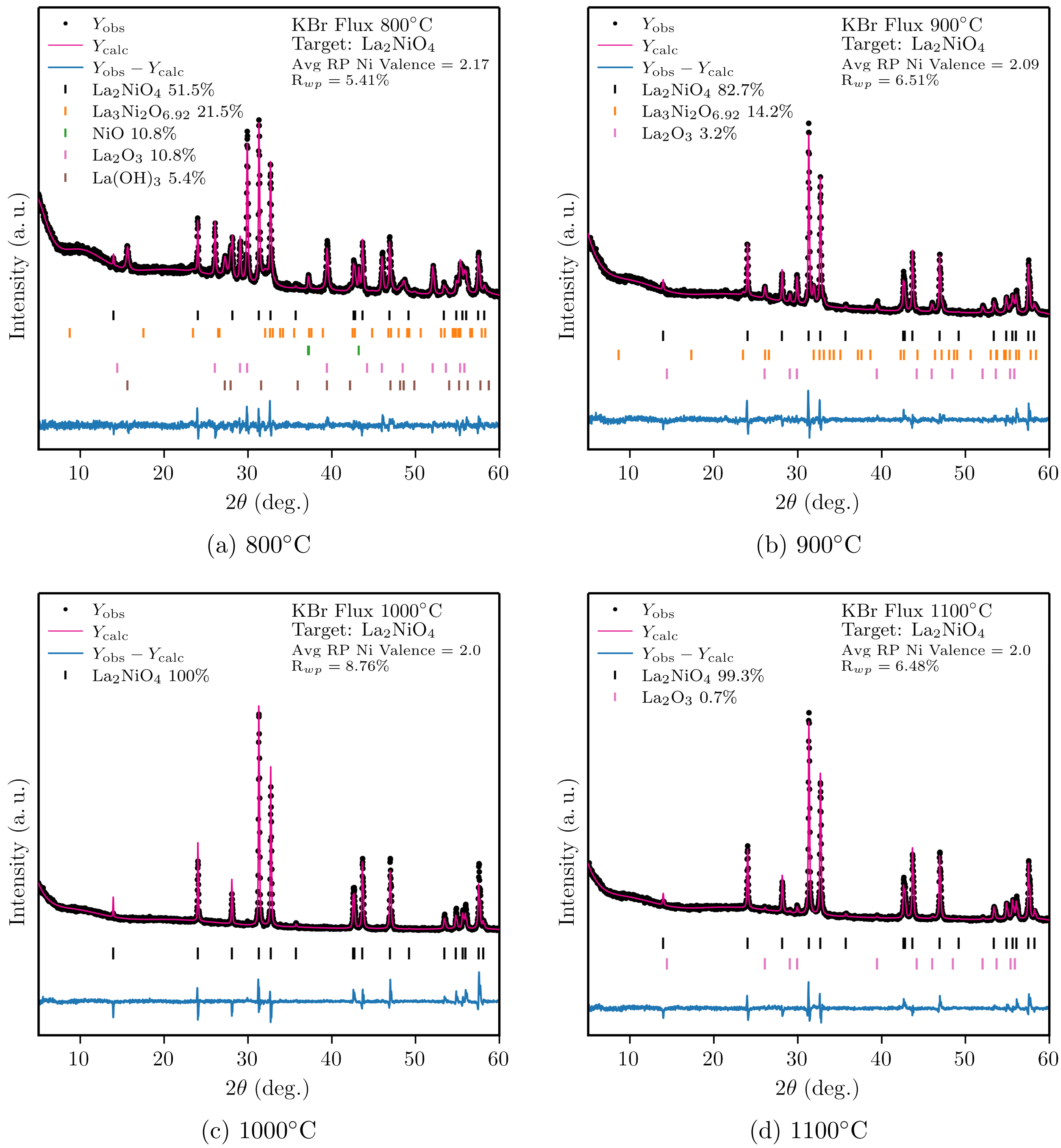

(a) 800°C (b) 900°C (c) 1000°C (d) 1100°C

Figure 35: PXRD and Rietveld refinements of targeted La_2NiO_4 with $\frac{Ni}{Ni+La} = 0.33$ in KBr flux at (a) 800°C, (b) 900°C, (c) 1000°C, and (d) 1100°C.

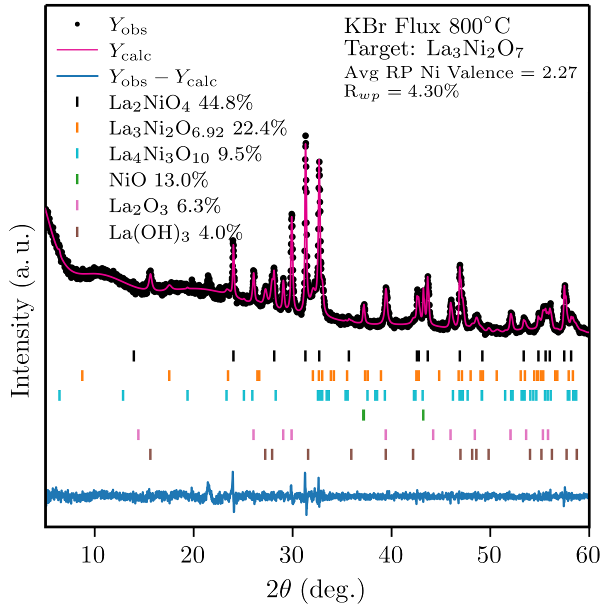

(a) 800°C

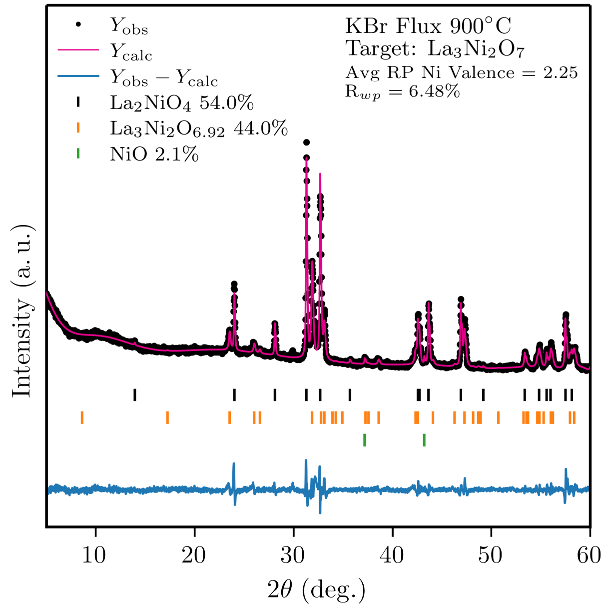

(b) 900°C

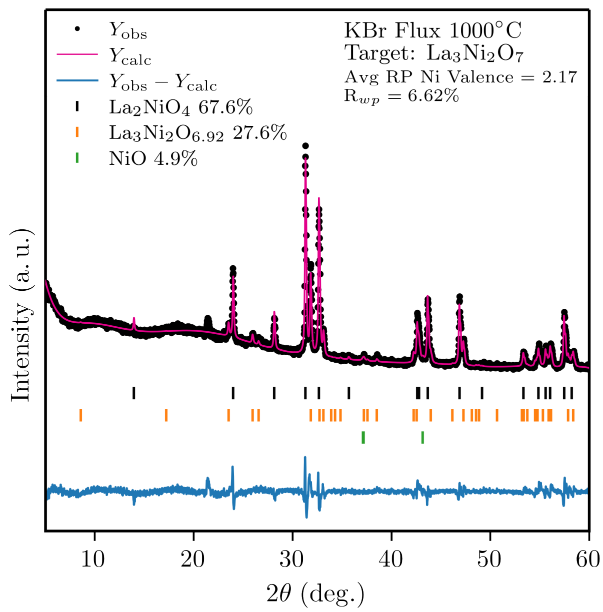

(c) 1000°C

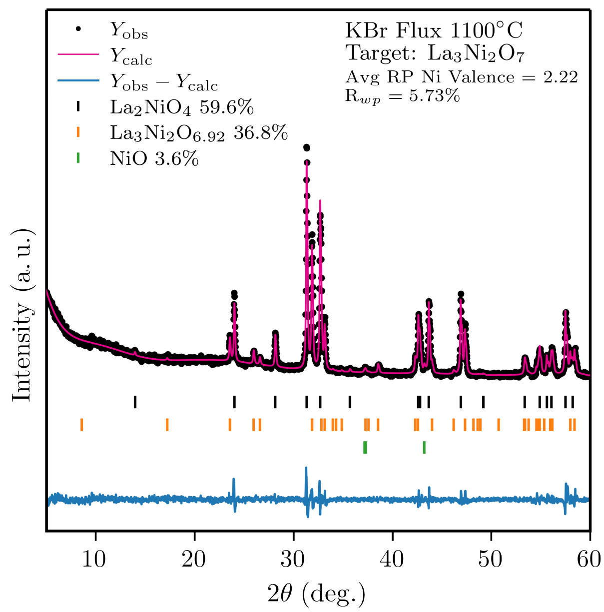

(d) 1100°C

Figure 36: PXRD and Rietveld refinements of targeted $La_3Ni_2O_7$ where $\frac{Ni}{Ni+La} = 0.40$ in KBr flux at (a) 800°C, (b) 900°C, (c) 1000°C, and (d) 1100°C.

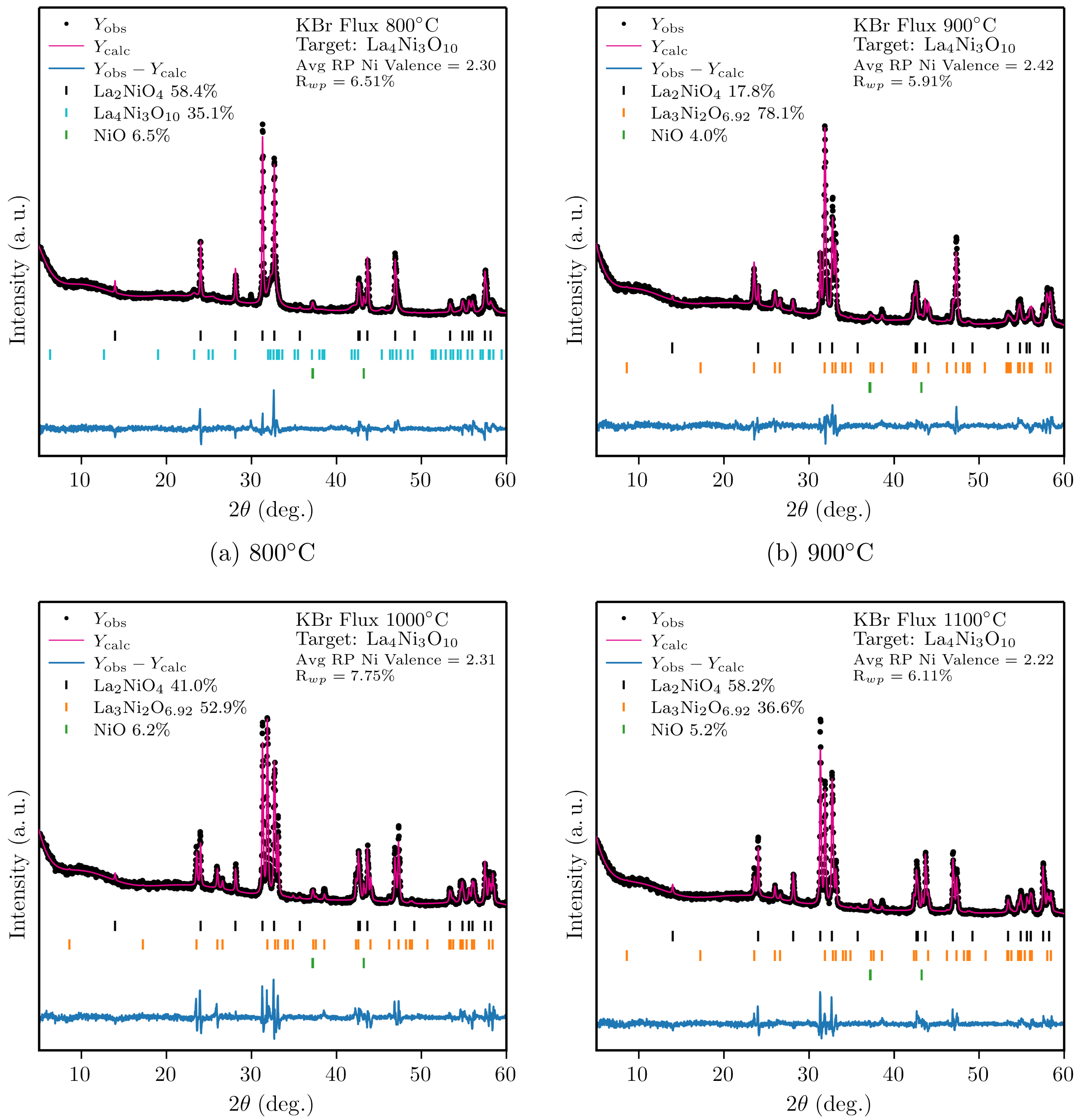

(c) 1000°C

(d) 1100°C

Figure 37: PXRD and Rietveld refinements of targeted $La_4Ni_3O_{10}$ where $\frac{Ni}{Ni+La} = 0.43$ in KBr flux at (a) 800°C, (b) 900°C, (c) 1000°C, and (d) 1100°C.

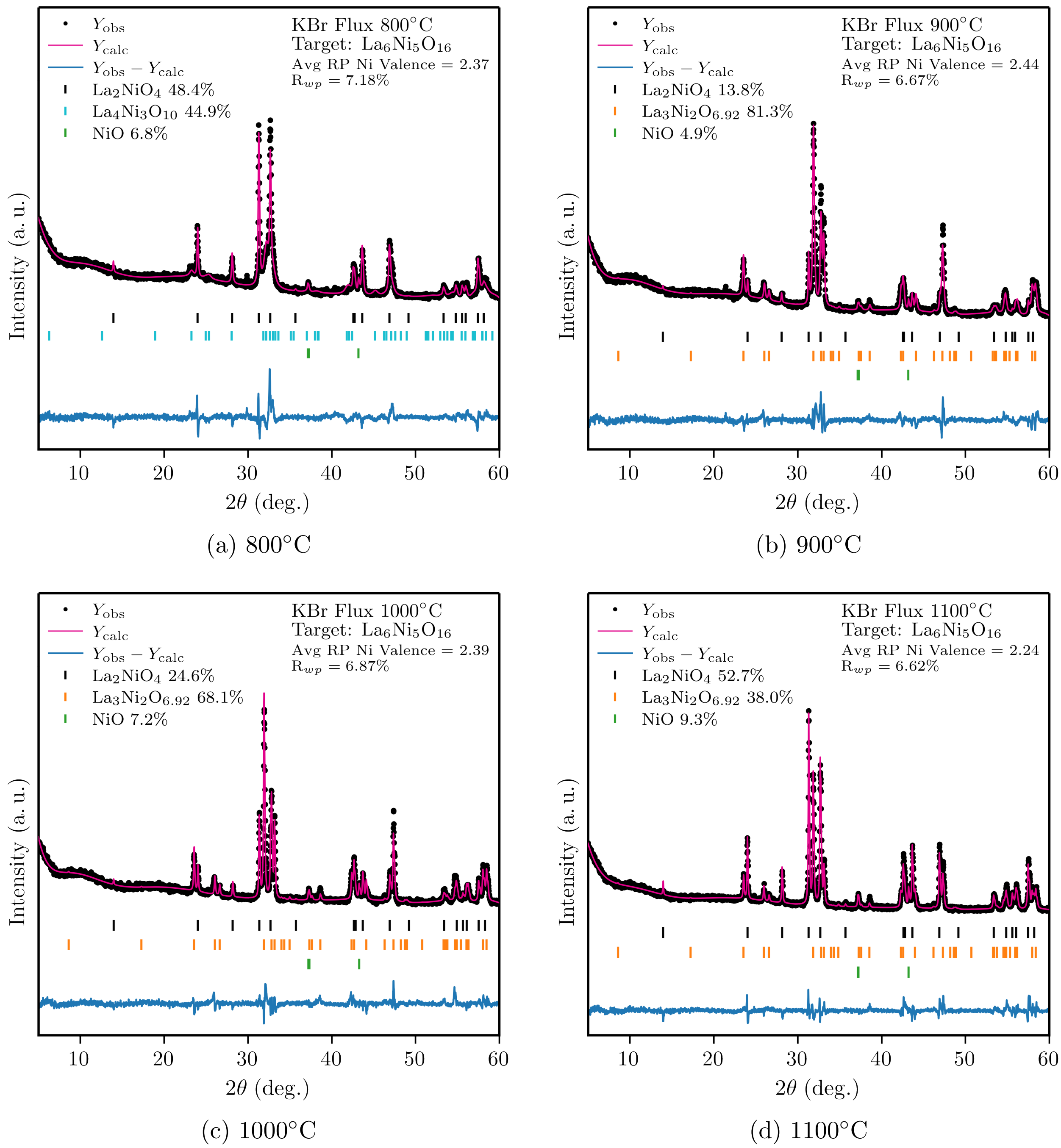

(a) 800°C (b) 900°C

(c) 1000°C (d) 1100°C

Figure 38: PXRD and Rietveld refinements of targeted $La_6Ni_5O_{16}$ where $\frac{Ni}{Ni+La} = 0.454$ in KBr flux at (a) 800°C, (b) 900°C, (c) 1000°C, and (d) 1100°C.

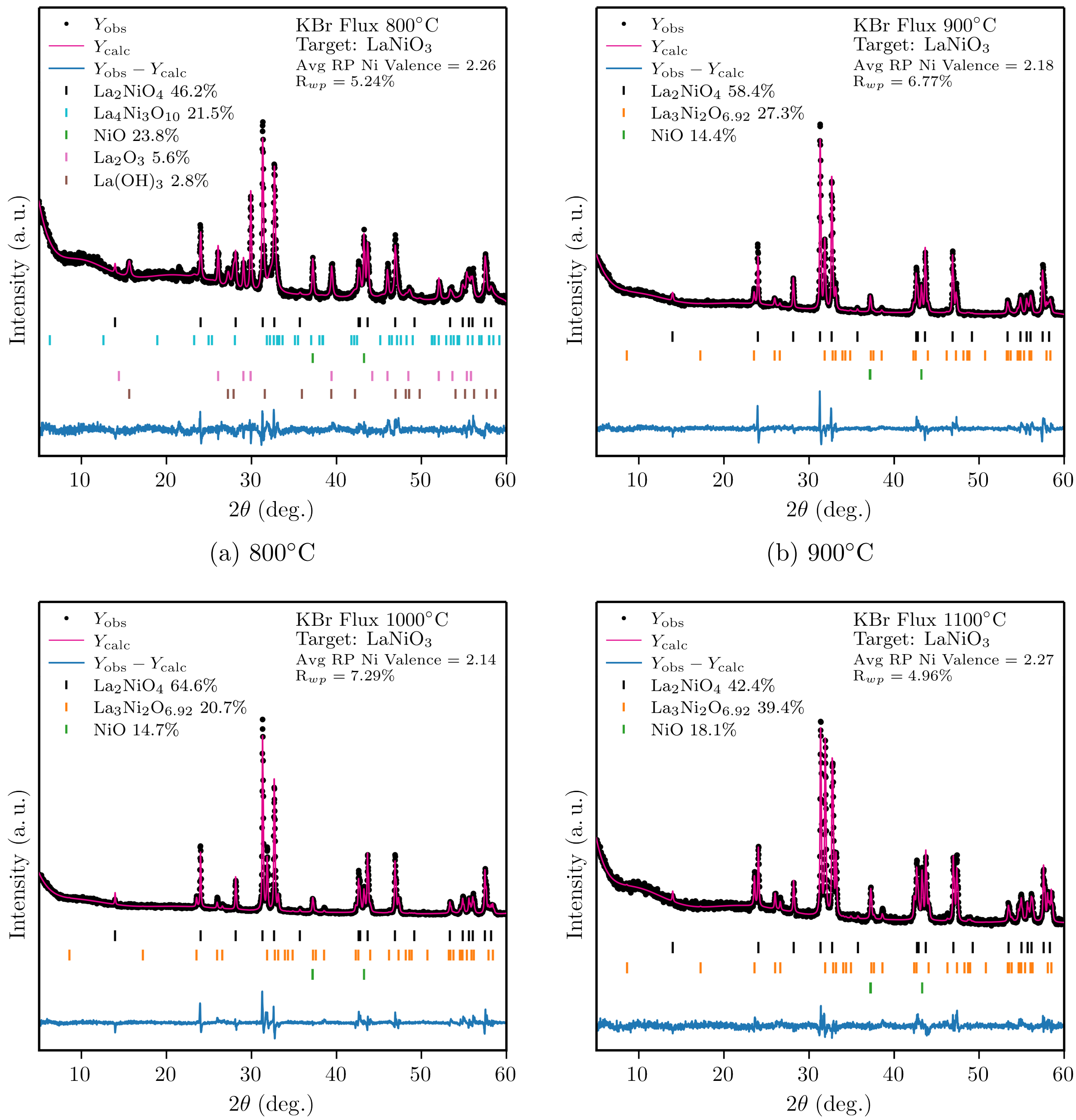

(a) 800°C (b) 900°C (c) 1000°C (d) 1100°C

Figure 39: PXRD and Rietveld refinements of targeted $LaNiO_3$ where $\frac{Ni}{Ni+La} = 0.5$ in KBr flux at (a) 800°C, (b) 900°C, (c) 1000°C, and (d) 1100°C.

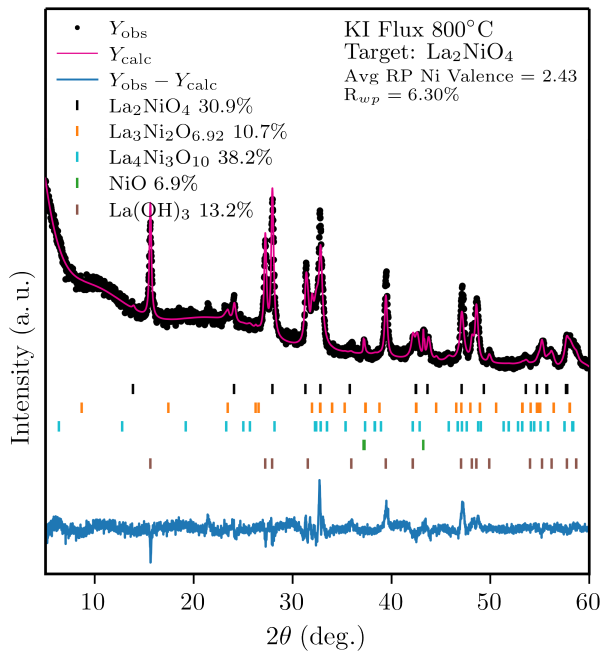

(a) 800°C

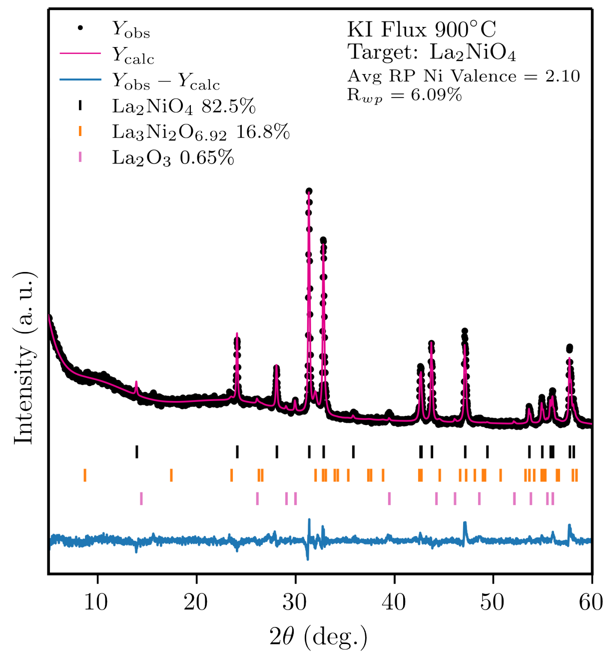

(b) 900°C

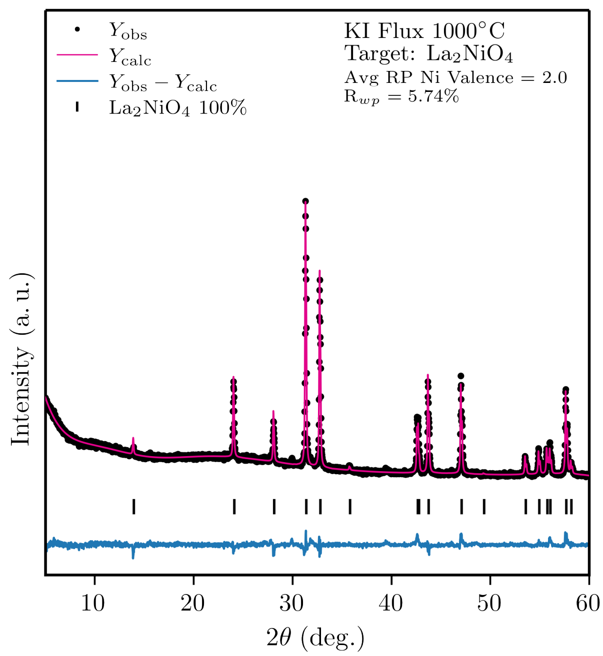

(c) 1000°C

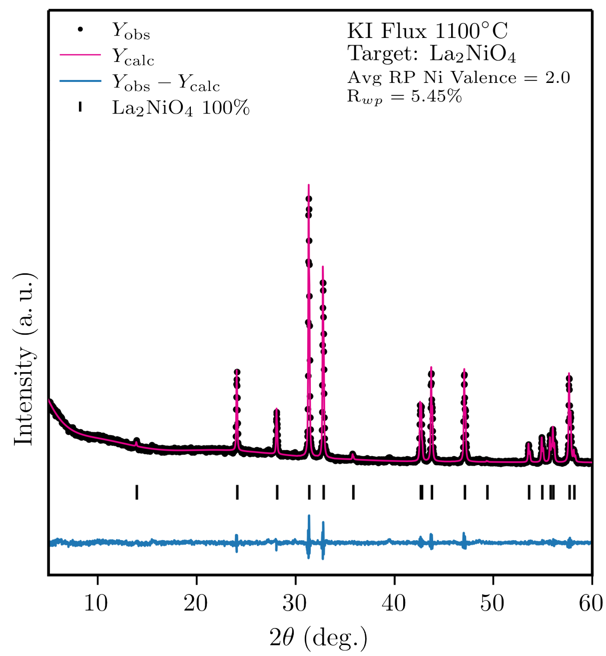

(d) 1100°C

Figure 40: PXRD and Rietveld refinements of targeted La_2NiO_4 where $\frac{Ni}{Ni+La} = 0.33$ in KI flux at (a) 800°C, (b) 900°C, (c) 1000°C, and (d) 1100°C.

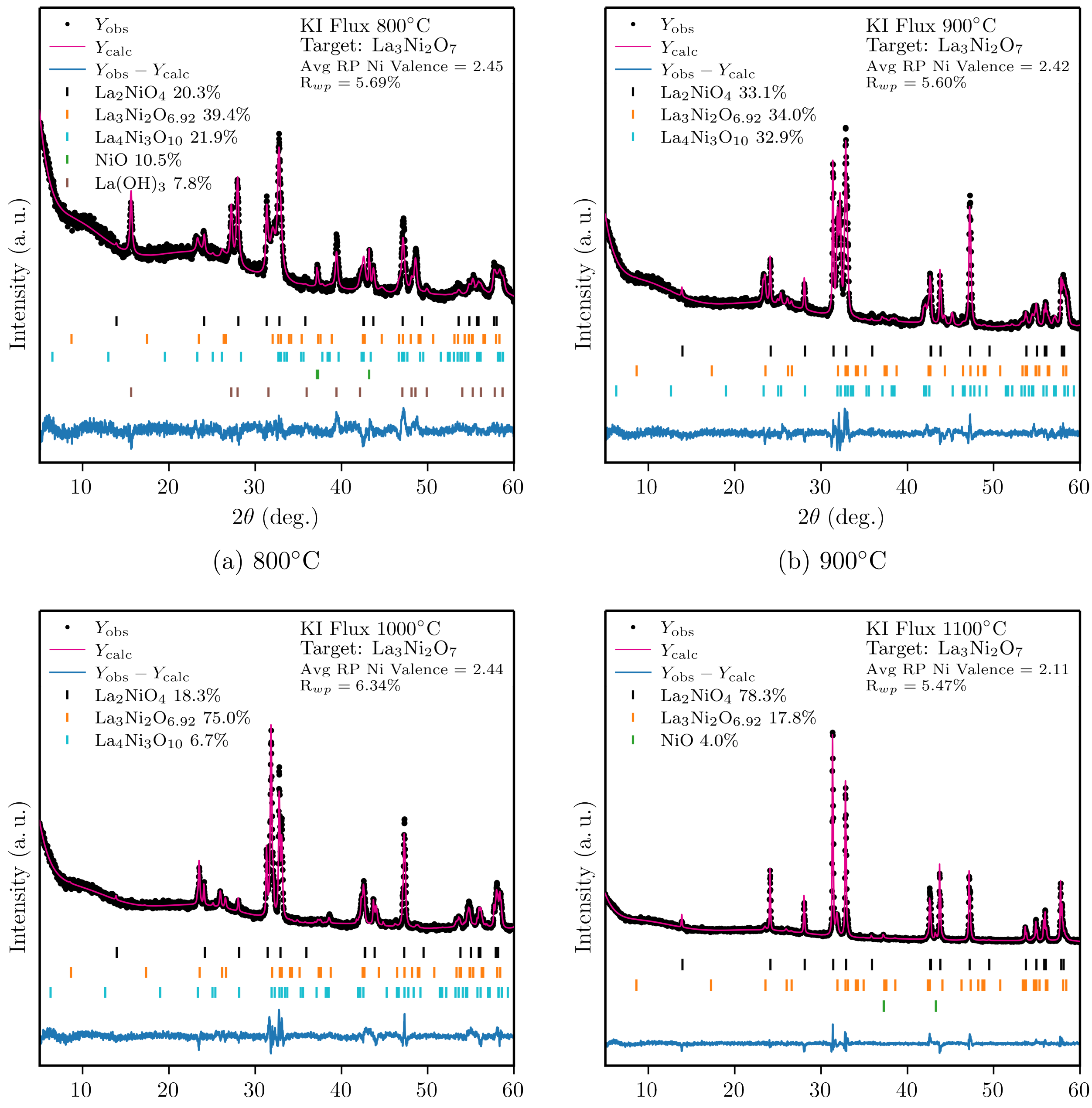

(a) 800°C

(b) 900°C

(c) 1000°C

(d) 1100°C

Figure 41: PXRD and Rietveld refinements of targeted $La_3Ni_2O_7$ where $\frac{\text{Ni}}{\text{Ni+La}} = 0.40$ in KI flux at (a) 800°C, (b) 900°C, (c) 1000°C, and (d) 1100°C.

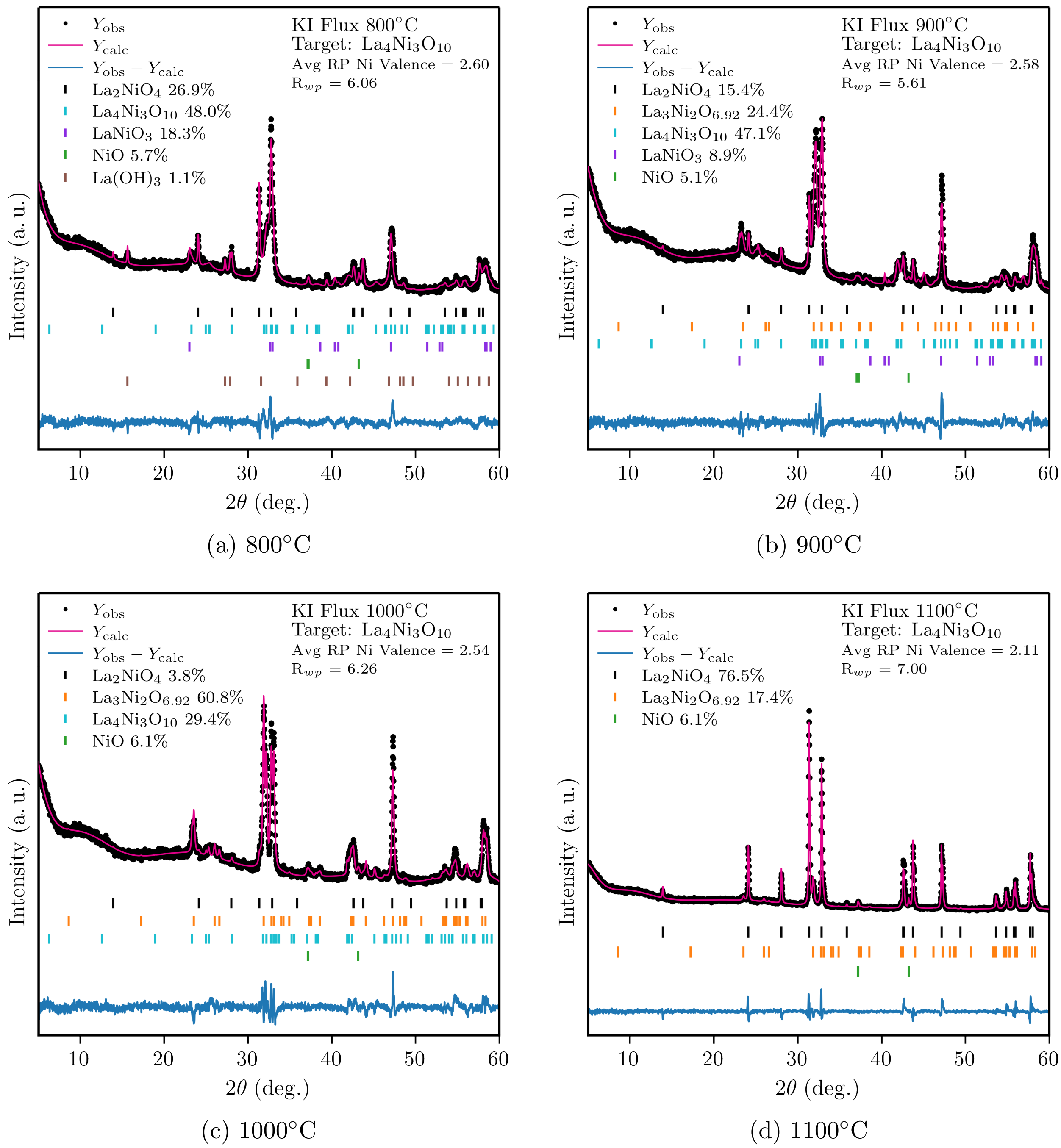

(a) 800°C

(b) 900°C

(c) 1000°C

(d) 1100°C

Figure 42: PXRD and Rietveld refinements of targeted $La_4Ni_3O_{10}$ where $\frac{Ni}{Ni+La} = 0.43$ in KI flux at (a) 800°C, (b) 900°C, (c) 1000°C, and (d) 1100°C.

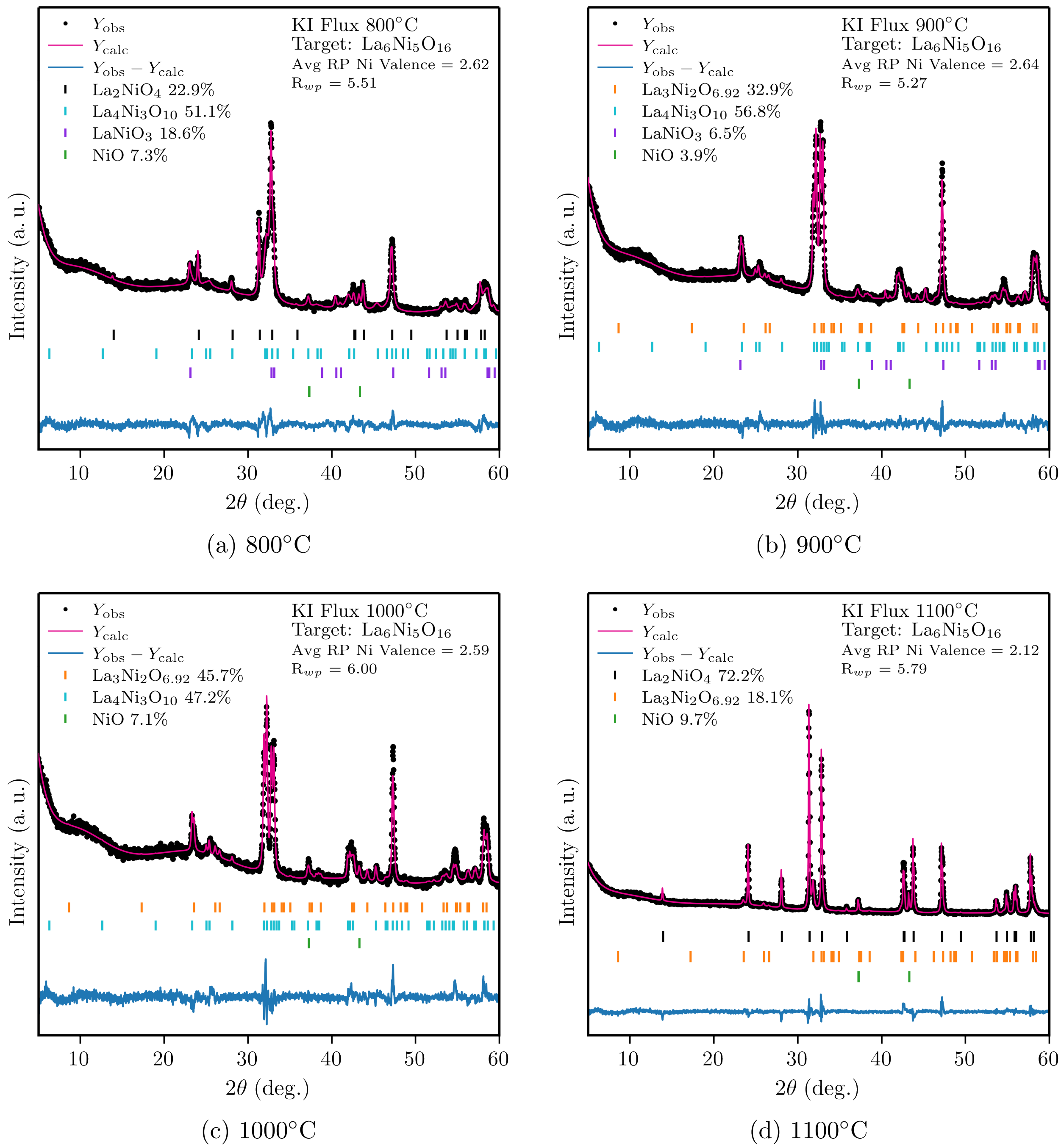

(a) 800°C (b) 900°C

(c) 1000°C (d) 1100°C

Figure 43: PXRD and Rietveld refinements of targeted $La_6Ni_5O_{16}$ where $\frac{Ni}{Ni+La} = 0.454$ in KI flux at (a) 800°C, (b) 900°C, (c) 1000°C, and (d) 1100°C.

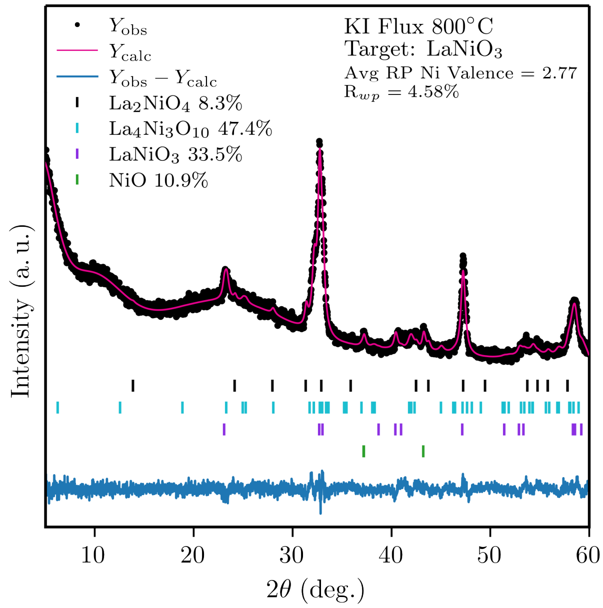

(a) 800°C

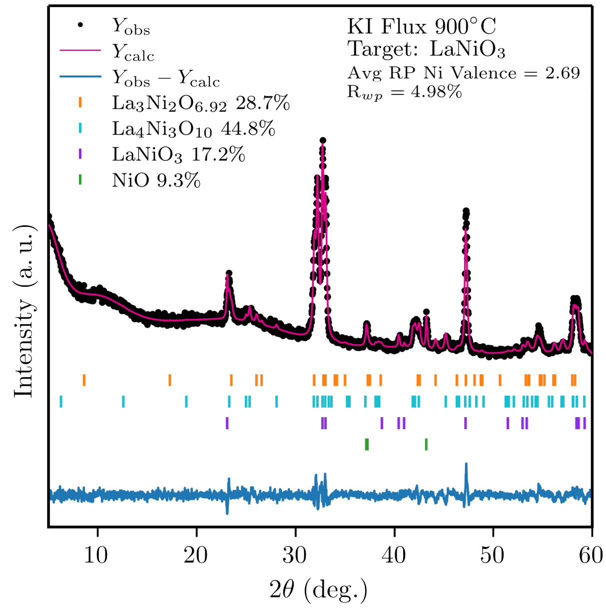

(b) 900°C

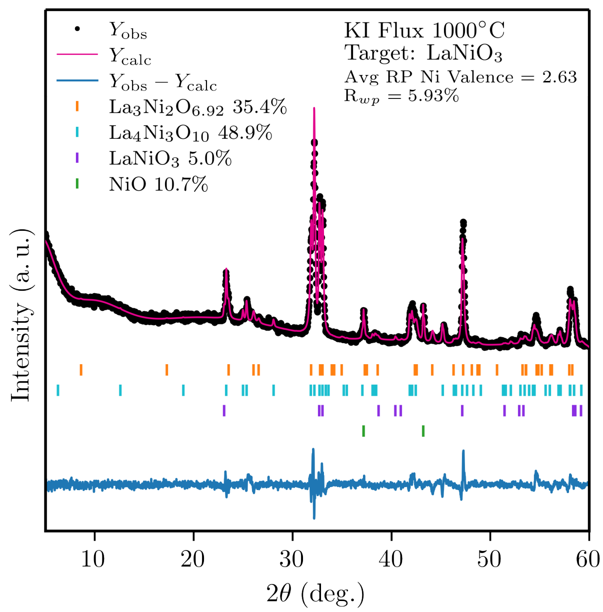

(c) 1000°C

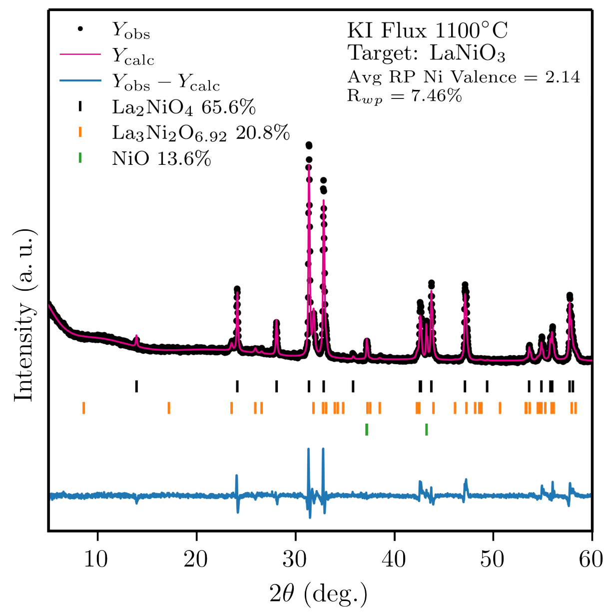

(d) 1100°C

Figure 44: PXRD and Rietveld refinements of targeted $LaNiO_3$ where $\frac{Ni}{Ni+La} = 0.5$ in KI flux at (a) 800°C, (b) 900°C, (c) 1000°C, and (d) 1100°C.

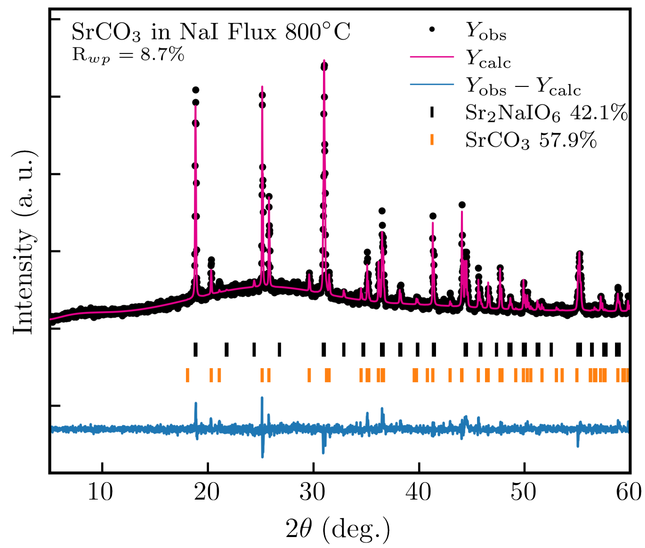

Figure 45: PXRD and Rietveld refinement of $SrCO_3$ in a NaI flux at 800°C forming Sr_2NaIO_6 to illustrate the oxidation of iodine to +7 in air.

0.1 Refinement Parameters, Results, and Thermodynamic Tables

Table 0.1: Fluxless: phase metrics vs targeted homology composition and temperature.

Target	T (°C)	La_2NiO_4 I4/mmm $\alpha = \beta = \gamma = 90°$ a, c	$La_3Ni_2O_{6.92}$ Fmmm $\alpha = \beta = \gamma = 90°$ a, b, c	$La_4Ni_3O_{10}$ Fmmm $\alpha = \beta = \gamma = 90°$ a, b, c	$LaNiO_3$ R$\bar{3}$c $\alpha = \beta = \gamma = 90°$ a, c	NiO R$\bar{3}$m $\alpha = \beta = \gamma = 90°$ a, c	Impurities	GOF	Rwp
La_2NiO_4	800	a=3.8613(8); c=12.725(6)	—	—	—	a=2.9550(6); c=7.249(3)	La_2O_3; $La(OH)_3$	1.47	5.20
	900	a=3.8576(4); c=12.687(3)	—	—	—	a=2.9547(3); c=7.2248(15)	$La(OH)_3$	1.53	5.42
	1000	a=3.85941(9); c=12.6840(6)	—	—	—	a=2.9538(3); c=7.2260(17)	$La(OH)_3$	1.45	5.18
	1100	a=3.86143(6); c=12.6829(3)	—	—	—	a=2.9547(3); c=7.2281(14)	La_2O_3; $La(OH)_3$	1.31	8.84
$La_3Ni_2O_7$	800	a=3.8567(17); c=12.608(12)	—	—	—	a=2.9537(3); c=7.2240(15)	La_2O_3; $La(OH)_3$	1.46	5.02
	900	a=3.8633(5); c=12.709(3)	—	—	—	a=2.9590(3); c=7.2342(13)	$La(OH)_3$	1.74	6.03
	1000	a=3.85938(15); c=12.6845(6)	a=5.397(3), b=5.460(3); c=20.492(12)	—	—	a=2.9536(2); c=7.2250(10)	$La(OH)_3$	1.42	4.91
	1100	a=3.86092(7); c=12.6830(3)	a=5.404(3), b=5.447(3); c=20.566(11)	—	—	a=2.9525(3); c=7.2391(16)	La_2O_3	1.56	10.84
$La_4Ni_3O_{10}$	800	a=3.8585(4); c=12.574(9)	—	—	—	a=2.9507(4); c=7.238(2)	$La(OH)_3$	1.73	12.43
	900	a=3.8595(5); c=12.639(6)	—	—	—	a=2.95(14); c=7.23(7)	$La(OH)_3$	2.08	15.72
	1000	a=3.85949(7); c=12.6908(4)	a=5.4069(8), b=5.4538(9); c=20.479(4)	—	—	a=2.9514(4); c=7.240(2)	$La(OH)_3$	1.52	5.58
	1100	a=3.86341(4); c=12.6928(2)	a=5.407(14), b=5.456(16); c=20.577(6)	—	—	a=2.9565(2); c=7.231(11)	La_2O_3	1.56	10.42
$La_6Ni_5O_{16}$	800	a=3.8643(5); c=12.632(8)	—	—	—	a=2.9545(5); c=7.250(3)	La_2O_3; $La(OH)_3$	1.47	5.09
	900	a=3.8612(3); c=12.684(5)	—	—	—	a=2.9583(5); c=7.231(3)	$La(OH)_3$	1.65	5.59
	1000	a=3.8623(14); c=12.7151(9)	a=5.4149(6), b=5.4598(7); c=20.469(3)	—	—	a=2.955(11); c=7.247(6)	—	1.60	5.89
	1100	a=3.86201(5); c=12.6900(3)	a=5.4098(7), b=5.4509(9); c=20.572(4)	—	—	a=2.9538(3); c=7.241(2)	—	1.68	12.47
$LaNiO_3$	800	a=3.864(3); c=12.51(15)	—	—	—	a=2.9558(2); c=7.250(12)	$La(OH)_3$	1.50	4.99
	900	a=3.858(2); c=12.71(13)	—	—	—	a=2.9548(2); c=7.248(11)	$La(OH)_3$	1.70	5.60
	1000	a=3.86305(9); c=12.7000(6)	a=5.402(14), b=5.465(16); c=20.532(6)	—	—	a=2.9542(3); c=7.244(15)	$La(OH)_3$	1.36	4.93
	1100	a=3.86162(7); c=12.6902(3)	a=5.4029(4), b=5.4500(5); c=20.537(19)	—	—	a=2.9527(14); c=7.2400(7)	La_2O_3; $La(OH)_3$	1.50	10.64

Table 0.2: NaCl flux: phase metrics vs targeted homology composition and temperature.

Target	T (°C)	La_2NiO_4 I4/mmm $\alpha=\beta=\gamma=90°$ a, c	$La_3Ni_2O_{6.92}$ Fmmm $\alpha=\beta=\gamma=90°$ a, b, c	$La_4Ni_3O_{10}$ Fmmm $\alpha=\beta=\gamma=90°$ a, b, c	$LaNiO_3$ R$\bar{3}$c $\alpha=\beta=\gamma=90°$ a, c	NiO R$\bar{3}$m $\alpha=\beta=\gamma=90°$ a, c	Impurities	GOF	Rwp
La_2NiO_4	830	a=3.86418(19); c=12.6424(9)	a=5.44(10), b=5.44(10); c=19.729	—	—	—	LaOCl; La_2O_3	1.41	5.48
	900	a=3.86181(5); c=12.6294(3)	—	—	—	—	La_2O_3	1.38	5.13
	1000	a=3.86703(5); c=12.6281(3)	a=5.3957(15), b=5.4480(18); c=20.506(6)	—	—	—	LaOCl	1.49	9.88
	1100	a=3.85979(7); c=12.6722(3)	—	—	—	—	—	1.57	5.86
$La_3Ni_2O_7$	830	a=3.86390(19); c=12.6346(8)	a=5.4(5), b=5.4(5); c=19.78(2)	—	—	a=2.9573(10); c=7.205(5)	—	1.39	5.06
	900	a=3.85885(8); c=12.6247(4)	a=5.422(7), b=5.473(8); c=20.39(2)	—	—	a=2.9526(16); c=7.226(8)	—	1.40	4.93
	1000	a=3.86476(14); c=12.6263(6)	a=5.4038(16), b=5.455(2); c=20.559(7)	—	—	a=2.952(6); c=7.23(3)	LaOCl	1.38	5.09
	1100	a=3.85528(8); c=12.6240(3)	a=5.4031(13), b=5.4551(17); c=20.622(6)	—	—	a=2.95(4); c=7.2(2)	—	1.57	5.66
$La_4Ni_3O_{10}$	830	a=3.8661(4); c=12.677(2)	—	a=5.418(3), b=5.467(3); c=28.12(14)	a=5.448(11); c=13.494(5)	a=2.952(15); c=7.283(8)	LaOCl	1.60	5.65
	900	a=3.8631(18); c=12.658(12)	a=5.4057(7), b=5.4616(8); c=20.522(3)	a=5.407(18), b=5.461(19); c=28.111(8)	—	a=2.9504(9); c=7.257(5)	—	1.66	5.98
	1000	a=3.8712(2); c=12.654(15)	a=5.4029(3), b=5.4582(3); c=20.560(16)	—	—	a=2.953(17); c=7.262(9)	LaOCl	1.76	6.42
	1100	a=3.86051(6); c=12.6405(4)	a=5.401(13), b=5.466(13); c=20.586(4)	—	—	a=2.954(11); c=7.246(5)	—	1.67	6.35
$La_6Ni_5O_{16}$	830	a=3.8564(6); c=12.633(2)	—	a=5.402(3), b=5.466(3); c=27.947(14)	a=5.4625(9); c=13.230(3)	a=2.952(6); c=7.22(3)	—	1.22	4.11
	900	—	a=5.4050(7), b=5.4563(7); c=20.446(3)	a=5.4039(9), b=5.4555(10); c=28.082(5)	a=5.4551(7); c=13.160(3)	a=2.9535(18); c=7.215(9)	—	1.64	5.72
	1000	—	a=5.3996(17), b=5.4527(7); c=20.439(3)	a=5.3989(10), b=5.4551(11); c=28.204(6)	—	a=2.955(2); c=7.224(11)	LaOCl	1.81	6.81
	1100	a=3.85648(9); c=12.6261(4)	a=5.4001(10), b=5.4523(13); c=20.569(4)	—	—	a=2.9544(4); c=7.2214(19)	—	1.57	5.52
$LaNiO_3$	830	—	—	a=5.422(3), b=5.457(3); c=27.83(13)	a=5.4724(7); c=13.260(3)	a=2.952(3); c=7.260(5)	—	1.75	6.02
	900	—	a=5.4050(7), b=5.4563(7); c=20.492(2)	a=5.4110(7), b=5.4635(7); c=28.121(4)	a=5.4647(5); c=13.181(2)	a=2.9587(9); c=7.224(4)	—	1.78	6.50
	1000	—	a=5.4048(4), b=5.4585(3); c=20.469(19)	a=5.4045(9), b=5.4605(9); c=28.244(5)	—	a=2.954(10); c=7.250(5)	LaOCl	1.99	7.14
	1100	a=3.86385(9); c=12.6857(5)	a=5.4013(4), b=5.4625(5); c=20.573(2)	—	—	a=2.9586(3); c=7.233(15)	—	2.13	7.06

Table 0.3: NaBr flux: phase metrics vs targeted homology composition and temperature.

Target	T (°C)	La_2NiO_4 I4/mmm $\alpha=\beta=\gamma=90°$ a, c	$La_3Ni_2O_{6.92}$ Fmmm $\alpha=\beta=\gamma=90°$ a, b, c	$La_4Ni_3O_{10}$ Fmmm $\alpha=\beta=\gamma=90°$ a, b, c	$LaNiO_3$ $R\bar{3}c$ $\alpha=\beta=\gamma=90°$ a, c	NiO $R\bar{3}m$ $\alpha=\beta=\gamma=90°$ a, c	Impurities	GOF	Rwp
La_2NiO_4	800	a=3.86523(16); c=12.6252(6)	—	—	—	a=2.954(2); c=7.222(11)	La_2O_3	1.34	5.14
	900	a=3.86038(8); c=12.6563(5)	—	—	—	—	La_2O_3	1.43	5.54
	1000	a=3.87100(7); c=12.6646(4)	—	—	—	—	La_2O_3	2.11	7.80
	1100	a=3.86678(6); c=12.6564(4)	—	—	—	—	La_2O_3	1.81	7.05
$La_3Ni_2O_7$	800	a=3.86515(12); c=12.6272(5)	—	—	—	a=2.953(13); c=7.23(7)	La_2O_3	1.33	4.81
	900	a=3.85300(8); c=12.6347(5)	a=5.3920(10), b=5.4496(12); c=20.515(4)	—	—	a=2.95(3); c=7.23(13)	—	1.38	5.02
	1000	a=3.86388(11); c=12.6334(5)	a=5.399(2), b=5.456(3); c=20.577(9)	—	—	a=2.9513(15); c=7.238(7)	—	1.19	4.28
	1100	a=3.85920(6); c=12.6259(4)	a=5.4032(14), b=5.4562(18); c=20.622(6)	—	—	a=2.9485(17); c=7.276(9)	—	1.34	5.18
$La_4Ni_3O_{10}$	800	a=3.8707(14); c=12.6724(9)	—	a=5.421(4), b=5.477(4); c=27.61(5)	—	a=2.960(16); c=7.249(8)	—	2.18	7.33
	900	a=3.8577(3); c=12.672(2)	a=5.4060(5), b=5.4624(6); c=20.529(2)	—	—	a=2.956(2); c=7.27(13)	—	2.24	7.52
	1000	a=3.8684(2); c=12.665(12)	a=5.4031(3), b=5.4568(4); c=20.529(12)	—	—	a=2.957(4); c=7.26(2)	—	1.52	5.58
	1100	a=3.86539(6); c=12.6464(6)	a=5.405(15), b=5.476(2); c=20.641(6)	—	—	a=2.955(2); c=7.25(11)	—	2.08	8.05
$La_6Ni_5O_{16}$	800	a=3.86676(14); c=12.6590(9)	—	a=5.425(4), b=5.475(4); c=27.45(2)	—	a=2.9601(10); c=7.227(5)	—	1.95	6.93
	900	a=3.8617(4); c=12.665(2)	a=5.4087(5), b=5.4587(5); c=20.4933(18)	—	—	a=2.9603(19); c=7.231(9)	—	1.85	6.31
	1000	a=3.8657(7); c=12.680(4)	a=5.4031(4), b=5.4561(4); c=20.4989(16)	—	—	a=2.9607(11); c=7.217(5)	—	2.06	7.42
	1100	a=3.86283(11); c=12.6522(7)	a=5.4130(8), b=5.4729(10); c=20.691(3)	—	—	a=2.958(16); c=7.25(8)	—	2.17	7.97
$LaNiO_3$	800	a=3.8669(17); c=12.662(10)	—	a=5.425(3), b=5.467(3); c=27.859(8)	—	a=2.9602(7); c=7.226(4)	—	1.58	5.34
	900	a=3.8599(2); c=12.657(13)	a=5.4067(4), b=5.4580(4); c=20.476(18)	—	—	a=2.9526(6); c=7.262(3)	—	1.70	6.04
	1000	a=3.8682(2); c=12.668(15)	a=5.4046(3), b=5.4579(3); c=20.489(16)	—	—	a=2.955(2); c=7.248(2)	—	1.89	6.53
	1100	a=3.86168(7); c=12.6441(4)	a=5.4105(6), b=5.4647(6); c=20.665(3)	—	—	a=2.9548(6); c=7.243(3)	—	1.86	6.51

Table 0.4: NaI flux: phase metrics vs targeted homology composition and temperature (part 1).

Target	T (°C)	La_2NiO_4 I4/mmm $\alpha=\beta=\gamma=90°$ a, c	$La_3Ni_2O_{6.92}$ Fmmm $\alpha=\beta=\gamma=90°$ a, b, c	$La_4Ni_3O_{10}$ Fmmm $\alpha=\beta=\gamma=90°$ a, b, c	$LaNiO_3$ R$\bar{3}$c $\alpha=\beta=\gamma=90°$ a, c	NiO R$\bar{3}$m $\alpha=\beta=\gamma=90°$ a, c	Impurities	GOF	Rwp
La_2NiO_4	700	a=3.8336(3); c=12.6670(15)	a=5.42(6), b=5.42(6); c=20.767(6)	—	a=5.4629(6); c=13.230(3)	—	La_2O_3; $La(OH)_3$	1.67	6.10
	750	a=3.8351(5); c=12.667(3)	a=5.46(5), b=5.46(5); c=20.195(14)	—	a=5.4714(4); c=13.214(3)	—	La_2O_3; $La(OH)_3$	1.57	5.84
	800	a=3.8301(3); c=12.687(2)	a=5.415(3), b=5.442(3); c=20.50(1)	—	a=5.4681(8); c=13.232(4)	—	La_2O_3; $La(OH)_3$	1.60	5.96
	850	a=3.83488(8); c=12.6682(5)	a=5.43(5), b=5.44(5); c=20.360(14)	—	—	—	La_2O_3; $La(OH)_3$	1.72	6.53
	900	a=3.83236(7); c=12.6842(4)	—	—	—	—	—	1.94	7.70
	950	a=3.83379(5); c=12.6825(3)	—	—	—	—	La_2O_3	1.83	6.70
	1000	a=3.82946(5); c=12.6494(3)	—	—	—	—	La_2O_3	1.83	15.58
	1100	a=3.83745(5); c=12.6631(3)	—	—	—	—	La_2O_3	1.88	7.56
$La_3Ni_2O_7$	700	a=3.8285(4); c=12.6650(18)	a=5.410(2), b=5.455(3); c=20.615(8)	—	a=5.4631(4); c=13.212(2)	a=2.963(2); c=7.187(11)	La_2O_3; $La(OH)_3$	1.68	5.98
	750	a=3.835(14); c=12.644(7)	a=5.395(3), b=5.459(3); c=20.46(10)	—	a=5.4654(4); c=13.204(2)	—	$La(OH)_3$	1.63	6.14
	800	a=3.8317(5); c=12.677(2)	a=5.402(3), b=5.445(3); c=20.181(7)	—	a=5.4639(6); c=13.202(3)	—	$La(OH)_3$	1.49	5.33
	850	a=3.8336(2); c=12.6604(9)	a=5.420(4), b=5.448(4); c=20.112(12)	—	a=5.4664(6); c=13.264(3)	—	La_2O_3	2.08	7.06
	900	a=3.8275(2); c=12.6524(8)	a=5.4(5), b=5.4(5); c=20.477(11)	a=5.4139(11), b=5.4551(11); c=27.965(5)	a=5.4532(6); c=13.184(3)	—	—	1.51	5.34
	950	a=3.83802(18); c=12.6821(10)	—	a=5.4271(4), b=5.4687(4); c=28.0503(19)	—	—	—	1.85	6.35
	1000	a=3.8288(11); c=12.6450(5)	—	a=5.4145(5), b=5.4566(5); c=27.993(2)	—	—	—	1.92	15.49
	1100	a=3.83091(8); c=12.6469(4)	—	—	—	a=2.9537(6); c=7.224(3)	—	1.53	5.96

Table 0.5: NaI flux: phase metrics vs targeted homology composition and temperature (part 2).

Target	T (°C)	La_2NiO_4 I4/mmm $\alpha=\beta=\gamma=90°$ a, c	$La_3Ni_2O_{6.92}$ Fmmm $\alpha=\beta=\gamma=90°$ a, b, c	$La_4Ni_3O_{10}$ Fmmm $\alpha=\beta=\gamma=90°$ a, b, c	$LaNiO_3$ R$\bar{3}$c $\alpha=\beta=\gamma=90°$ a, c	NiO R$\bar{3}$m $\alpha=\beta=\gamma=90°$ a, c	Impurities	GOF	Rwp
$La_4Ni_3O_{10}$	700	a=3.8319(6); c=12.644(3)	a=5.412(2), b=5.449(2); c=20.439(7)	—	a=5.4668(6); c=13.212(2)	a=2.951(3); c=7.24(2)	—	1.76	6.21
	750	a=3.843(15); c=12.645(8)	—	—	a=5.4727(3); c=13.218(13)	—	—	1.95	6.67
	800	a=3.8304(4); c=12.6810(19)	—	—	a=5.4637(3); c=13.194(2)	—	—	1.76	6.40
	850	a=3.8380(3); c=12.670(15)	—	a=5.418(15), b=5.466(16); c=28.039(7)	a=5.4665(5); c=13.220(2)	—	—	1.69	5.99
	900	a=3.8353(4); c=12.670(2)	—	a=5.4223(7), b=5.4623(7); c=28.053(3)	a=5.4659(4); c=13.212(16)	a=2.9594(7); c=7.210(3)	—	1.85	6.67
	950	a=3.870(12); c=12.547(7)	—	a=5.4222(3), b=5.4666(3); c=28.043(17)	—	—	—	2.24	8.16
	1000	a=3.8293(5); c=12.633(3)	—	a=5.4134(4), b=5.4567(4); c=27.986(2)	—	—	—	2.08	16.27
	1100	a=3.83664(7); c=12.6708(4)	—	—	—	a=2.9654(7); c=7.250(4)	—	2.18	8.13
$La_6Ni_5O_{16}$	700	a=3.8367(7); c=12.655(4)	a=5.419(3), b=5.461(3); c=20.450(9)	—	a=5.4683(3); c=13.209(14)	—	—	1.64	5.58
	750	a=3.833(12); c=12.675(5)	—	—	a=5.4657(2); c=13.187(12)	—	—	1.86	6.31
	800	a=3.8272(6); c=12.632(3)	—	a=5.42(4), b=5.44(5); c=27.80(14)	a=5.4490(6); c=13.1475(16)	—	—	1.28	4.36
	850	a=3.843(13); c=12.643(6)	—	a=5.415(12), b=5.468(12); c=28.047(5)	a=5.4667(7); c=13.199(13)	—	—	1.64	5.74
	900	a=3.8305(18); c=12.619(8)	—	a=5.4127(7), b=5.4540(8); c=27.961(4)	a=5.4543(7); c=13.165(2)	—	—	1.20	4.49
	950	—	—	a=5.4179(2), b=5.4653(2); c=28.025(15)	—	—	—	1.79	6.68
	1000	a=3.828(13); c=12.618(6)	—	a=5.4128(2), b=5.4588(2); c=27.978(12)	—	—	—	2.08	15.89
	1100	a=3.83048(10); c=12.6461(4)	—	a=5.405(3), b=5.447(3); c=28.147(12)	—	a=2.9536(6); c=7.223(3)	—	1.32	4.87

Table 0.6: NaI flux: phase metrics vs targeted homology composition and temperature (part 3).

Target	T (°C)	La_2NiO_4 I4/mmm $\alpha = \beta = \gamma = 90°$ a, c	$La_3Ni_2O_{6.92}$ Fmmm $\alpha = \beta = \gamma = 90°$ a, b, c	$La_4Ni_3O_{10}$ Fmmm $\alpha = \beta = \gamma = 90°$ a, b, c	$LaNiO_3$ R$\bar{3}$c $\alpha = \beta = \gamma = 90°$ a, c	NiO R$\bar{3}$m $\alpha = \beta = \gamma = 90°$ a, c	Impurities	GOF	Rwp
$La_{13}Ni_{12}O_{37}$	700	a=3.846(12); c=12.571(6)	a=5.404(3), b=5.464(3); c=20.446(9)	—	a=5.4724(4); c=13.236(16)	—	—	1.64	5.71
	750	—	—	—	a=5.4627(2); c=13.177(11)	—	—	1.59	5.62
	800	—	—	—	a=5.4665(2); c=13.183(10)	—	—	1.67	5.68
	850	—	—	a=5.403(2), b=5.468(2); c=27.993(7)	a=5.4706(2); c=13.198(13)	—	—	1.79	6.06
	900	—	—	a=5.4155(8), b=5.4636(8); c=28.047(3)	a=5.4705(6); c=13.203(2)	a=2.96(8); c=7.240(8)	—	1.68	6.06
	950	—	—	a=5.4207(4), b=5.4665(2); c=28.0902(13)	a=5.4761(9); c=13.190(3)	a=2.955(4); c=7.24(2)	—	1.78	6.61
	1000	a=3.829(2); c=12.614 (9)	—	a=5.4140(3), b=5.4600(3); c=27.976(15)	—	a=2.9504(5); c=7.254(3)	—	1.71	13.88
	1100	a=3.83672(7); c=12.6674(4)	—	a=5.437(4), b=5.445(3); c=28.09(13)	—	a=2.9560(6); c=7.247(3)	—	1.88	6.68
$LaNiO_3$	700	a=3.8378(6); c=12.626(3)	a=5.417(3), b=5.454(3); c=20.523(7)	—	a=5.4675(4); c=13.223(2)	—	—	1.70	5.68
	750	—	—	—	a=5.4662(3); c=13.198(11)	—	—	1.62	5.80
	800	—	—	—	a=5.4666(15); c=13.1837(9)	—	—	1.72	5.69
	850	—	—	a=5.431(5), b=5.452(5); c=27.87(13)	a=5.4610(2); c=13.168(10)	—	—	1.54	5.51
	900	—	—	a=5.4156(6), b=5.4612(6); c=28.000(3)	a=5.4626(2); c=13.18(10)	a=2.952(17); c=7.246(8)	—	1.40	4.91
	950	—	—	a=5.4197(3), b=5.4667(3); c=28.019(16)	a=5.467(12); c=13.207(4)	a=2.952(17); c=7.24(5)	—	2.01	6.97
	1000	a=3.8256(4); c=12.642(2)	—	a=5.4126(3), b=4.4583(3); c=27.951(13)	—	a=2.9549(8); c=7.222(4)	—	1.63	12.99
	1100	a=3.83538(5); c=12.6610(3)	—	a=5.425(12), b=5.459(11); c=28.031(5)	—	a=2.9542(3); c=7.247(16)	—	1.91	6.79
$LaNi_{1.2}O_3$	700	a=3.8394(18); c=12.625(9)	a=5.435(7), b=5.485(7); c=20.364(19)	—	a=5.4678(2); c=13.2068(14)	a=2.9575(7); c=7.224(4)	—	1.54	5.04
	750	—	—	—	a=5.4587(5); c=13.1716(13)	a=2.9538(7); c=7.225(3)	—	1.70	5.66
	800	—	—	—	a=5.4591(5); c=13.1693(13)	a=2.9551(10); c=7.219(5)	—	1.59	5.61
	850	—	—	—	a=5.45288(16); c=13.1437(8)	a=2.9515(10); c=7.218(5)	—	1.55	5.51
	900	—	—	a=5.4117(19), b=5.4588(6); c=27.968(7)	a=5.4626(3); c=13.1885(10)	a=2.9568(4); c=7.228(2)	—	1.49	4.93
	950	—	—	a=5.4185(5), b=5.4670(3); c=28.0086(19)	a=5.4661(4); c=13.1941(14)	a=2.9583(5); c=7.225(2)	—	1.72	5.68
	1000	a=3.8293(3); c=12.6566(9)	—	a=5.4150(5), b=5.4600(5); c=27.982(2)	—	a=2.9561(3); c=7.226(16)	—	1.60	11.87
	1100	a=3.8305(4); c=12.621(2)	—	a=5.4239(15), b=5.4495(17); c=27.881(6)	a=5.4515(3); c=13.1693(14)	a=2.9480(6); c=7.230(3)	—	1.82	5.81

Table 0.7: KCl flux: phase metrics vs targeted homology composition and temperature.

Target	T (°C)	La_2NiO_4 I4/mmm $\alpha=\beta=\gamma=90°$ a, c	$La_3Ni_2O_{6.92}$ Fmmm $\alpha=\beta=\gamma=90°$ a, b, c	$La_4Ni_3O_{10}$ Fmmm $\alpha=\beta=\gamma=90°$ a, b, c	$LaNiO_3$ R$\bar{3}$c $\alpha=\beta=\gamma=90°$ a, c	NiO R$\bar{3}$m $\alpha=\beta=\gamma=90°$ a, c	Impurities	GOF	Rwp
La_2NiO_4	800	a=3.8700(2); c=12.6425(13)	—	—	—	—	KCl	1.50	6.48
	900	a=3.86752(6); c=12.6476(4)	—	—	—	—	—	1.54	6.19
	1000	a=3.86761(6); c=12.6484(4)	—	—	—	—	—	1.56	5.95
	1100	a=3.86478(8); c=12.6397(3)	—	—	—	—	—	1.77	6.71
$La_3Ni_2O_7$	800	a=3.86920(16); c=12.6461(7)	—	—	—	a=2.9506(12); c=7.255(6)	LaOCl; KCl	1.37	5.81
	900	a=3.86967(11); c=12.6683(7)	a=5.4022(4), b=5.4546(4); c=20.5046(18)	a=5.4093(16), b=5.4661(17); c=28.149(7)	—	a=2.957(2); c=7.237(10)	LaOCl	1.53	5.64
	1000	a=3.8684(4); c=12.665(2)	a=5.3966(4), b=5.4565(4); c=20.562(16)	—	—	a=2.958(4); c=7.24(18)	LaOCl	1.99	7.62
	1100	a=3.86471(13); c=12.6390(6)	a=5.4049(7), b=5.4588(9); c=20.644(3)	—	—	a=2.943(2); c=7.364(12)	—	2.16	8.03
$La_4Ni_3O_{10}$	800	a=3.8709(18); c=12.674(11)	—	a=5.429(3), b=5.466(2); c=27.67(13)	—	a=2.954(11); c=7.23(2)	LaOCl; KCl	1.93	6.77
	900	a=3.8667(3); c=12.683(2)	a=5.4070(6), b=5.4574(7); c=20.447(2)	a=5.4105(6), b=5.4611(7); c=28.092(3)	—	a=2.955(4); c=7.260(6)	LaOCl	1.69	6.13
	1000	a=3.8663(3); c=12.680(2)	a=5.3986(4), b=5.4550(4); c=20.501(17)	—	—	a=2.954(10); c=7.246(5)	LaOCl	1.87	7.11
	1100	a=3.8693(10); c=12.6676(7)	a=5.4086(9), b=5.475(11); c=20.678(4)	—	—	a=2.9582(8); c=7.244(4)	—	2.36	8.93
$La_6Ni_5O_{16}$	800	a=3.8694(2); c=12.656(13)	—	a=5.427(6), b=5.453(6); c=27.39(13)	—	a=2.956(2); c=7.21(11)	—	1.17	3.96
	900	a=3.8676(4); c=12.675(2)	a=5.412(11), b=5.457(10); c=20.402(4)	a=5.4146(6), b=5.4645(6); c=28.024(3)	a=5.4669(8); c=13.177(3)	a=2.9503(6); c=7.257(3)	LaOCl	1.42	5.50
	1000	—	a=5.4008(5), b=5.4554(5); c=20.503(2)	—	a=5.643(7); c=13.165(2)	a=2.956(3); c=7.25(17)	LaOCl	2.27	8.55
	1100	a=3.86654(9); c=12.6605(6)	a=5.405(10), b=5.469(12); c=20.662(4)	—	—	a=2.9525(7); c=7.251(4)	—	2.08	7.32
$LaNiO_3$	800	a=3.8703(3); c=12.670(16)	—	a=5.417(4), b=5.461(4); c=27.75(16)	a=5.446(13); c=13.487(8)	a=2.9529(9); c=7.261(4)	LaOCl	1.55	5.26
	900	a=3.872(16); c=12.648(9)	a=5.405(2), b=5.463(2); c=20.518(8)	a=5.418(11), b=5.463(12); c=28.131(6)	a=5.470(11); c=13.194(4)	a=2.956(3); c=7.23(14)	LaOCl; KCl	2.24	7.73
	1000	—	a=5.4015(5), b=5.4578(5); c=20.481(2)	—	a=5.4609(4); c=13.162(14)	a=2.9580(6); c=7.229(3)	LaOCl	2.83	9.80
	1100	a=3.8660(16); c=12.6526(8)	a=5.4087(6), b=5.4614(7); c=20.667(3)	—	—	a=2.9544(3); c=7.237(17)	—	2.26	8.28

Table 0.8: KBr flux: phase metrics vs targeted homology composition and temperature (I).

Target	T (°C)	La_2NiO_4 I4/mmm $\alpha=\beta=\gamma=90°$ a, c	$La_3Ni_2O_{6.92}$ Fmmm $\alpha=\beta=\gamma=90°$ a, b, c	$La_4Ni_3O_{10}$ Fmmm $\alpha=\beta=\gamma=90°$ a, b, c	$LaNiO_3$ R$\bar{3}$c $\alpha=\beta=\gamma=90°$ a, c	NiO R$\bar{3}$m $\alpha=\beta=\gamma=90°$ a, c	Impurities	GOF	Rwp
La_2NiO_4	800	a=3.8706(3); c=12.6698(18)	a=5.427(8), b=5.481(8); c=20.20(2)	—	—	a=2.9586(6); c=7.232(3)	La_2O_3; $La(OH)_3$	1.49	5.41
	900	a=3.86954(8); c=12.6752(5)	a=5.404(2), b=5.484(3); c=20.441(9)	—	—	—	La_2O_3	1.70	6.51
	1000	a=3.86571(6); c=12.6949(4)	—	—	—	—	—	2.19	8.76
	1100	a=3.86890(6); c=12.6635(4)	—	—	—	—	La_2O_3	1.68	6.48
$La_3Ni_2O_7$	800	a=3.87023(14); c=12.6739(8)	a=5.425(6), b=5.475(6); c=20.204(16)	a=5.422(3), b=5.458(3); c=27.463(14)	—	a=2.9544(7); c=7.254(4)	La_2O_3; $La(OH)_3$	1.29	4.30
	900	a=3.86964(8); c=12.6812(6)	a=5.4059(6), b=5.4584(5); c=20.514(2)	—	—	a=2.956(2); c=7.246(10)	—	1.86	6.48
	1000	a=3.87267(9); c=12.6625(6)	a=5.40187(7), b=5.4656(8); c=20.572(3)	—	—	a=2.963(9); c=7.24(5)	—	1.96	6.62
	1100	a=3.87022(8); c=12.6617(5)	a=5.3995(3), b=5.4539(4); c=20.5612(14)	—	—	a=2.961(2); c=7.223(12)	—	1.48	5.73
$La_4Ni_3O_{10}$	800	a=3.8701(15); c=12.6795(9)	—	a=5.421(17), b=5.4883(2); c=27.965(8)	—	a=2.96(13); c=7.233(7)	La_2O_3	1.90	6.51
	900	a=3.8687(2); c=12.68(13)	a=5.4058(3), b=5.4571(3); c=20.54(13)	—	—	a=2.96(1); c=7.27(5)	—	1.64	5.91
	1000	a=3.8740(12); c=12.6660(8)	a=5.4021(3), b=5.4573(3); c=20.55(13)	—	—	a=2.96(12); c=7.23(6)	—	2.25	7.75
	1100	a=3.86940(9); c=12.6563(6)	a=5.3969(3), b=5.4519(4); c=20.553(14)	—	—	a=2.9528(5); c=7.245(3)	—	1.66	6.11
$La_6Ni_5O_{16}$	800	a=3.8725(2); c=12.6810(14)	—	a=5.4228(17), b=5.4798(19); c=28.077(8)	—	a=2.9620(14); c=7.231(7)	La_2O_3	2.11	7.18
	900	a=3.8675(7); c=12.697(4)	a=5.4100(4), b=5.4587(4); c=20.5211(14)	—	—	a=2.9614(15); c=7.223(8)	—	1.91	6.67
	1000	a=3.8681(2); c=12.6508(14)	a=5.3955(3), b=5.4507(3); c=20.5011(11)	—	—	a=2.9571(10); c=7.218(5)	—	1.86	6.87
	1100	a=3.87068(9); c=12.6680(6)	a=5.4017(4), b=5.4558(4); c=20.5674(15)	—	—	a=2.9586(9); c=7.234(5)	—	1.85	6.62
$LaNiO_3$	800	a=3.8695(13); c=12.6716(6)	—	a=5.417(3), b=5.482(4); c=28.08(14)	—	a=2.9562(3); c=7.242(14)	La_2O_3; $La(OH)_3$	1.51	5.24
	900	a=3.87235(8); c=12.6660(5)	a=5.4041(6), b=5.4575(6); c=20.568(2)	—	—	a=2.9563(8); c=7.251(4)	—	1.95	6.77
	1000	a=3.87109(7); c=12.6673(4)	a=5.3993(6), b=5.4617(7); c=20.568(2)	—	—	a=2.9548(8); c=7.249(4)	—	2.19	7.29
	1100	a=3.86428(7); c=12.6431(5)	a=5.3931(2), b=5.4471(3); c=20.523(11)	—	—	a=2.9507(6); c=7.239(3)	—	1.40	4.96

Table 0.9: KI flux: phase metrics vs targeted homology composition and temperature (I).

Target	T (°C)	La_2NiO_4 I4/mmm $\alpha=\beta=\gamma=90°$ *a, c*	$La_3Ni_2O_{6.92}$ Fmmm $\alpha=\beta=\gamma=90°$ *a, b, c*	$La_4Ni_3O_{10}$ Fmmm $\alpha=\beta=\gamma=90°$ *a, b, c*	$LaNiO_3$ R$\overline{3}$c $\alpha=\beta=\gamma=90°$ *a, c*	NiO R$\overline{3}$m $\alpha=\beta=\gamma=90°$ *a, c*	Impurities	GOF	Rwp
La_2NiO_4	800	a=3.8546(15); c=12.695(9)	a=5.46(3), b=5.45(3); c=20.327(13)	a=5.45(14), b=5.45(14); c=27.717(18)	—	a=2.9591(11); c=7.230(6)	$La(OH)_3$	1.70	6.30
	900	a=3.85086(8); c=12.6812(5)	a=5.412(4), b=5.456(4); c=20.305(12)	—	—	—	La_2O_3	1.53	6.09
	1000	a=3.85553(4); c=12.6680(2)	—	—	—	—	—	1.55	5.74
	1100	a=3.85311(4); c=12.6688(2)	—	—	—	—	—	1.38	5.45
$La_3Ni_2O_7$	800	a=3.8549(7); c=12.713(4)	a=5.424(6), b=5.471(6); c=20.261(14)	a=5.421(2), b=5.469(3); c=27.230(13)	—	a=2.9612(7); c=7.223(3)	$La(OH)_3$	1.55	5.69
	900	a=3.8417(2); c=12.6734(11)	a=5.4072(8), b=5.4489(9); c=20.407(4)	a=5.4081(9), b=5.4528(9); c=28.021(4)	—	—	—	1.57	5.60
	1000	a=3.8485(4); c=12.6811(18)	a=5.3990(5), b=5.4466(5); c=20.513(2)	a=5.4008(18), b=5.450(2); c=28.221(8)	—	—	—	1.73	6.34
	1100	a=3.84539(9); c=12.6862(4)	a=5.4037(14), b=5.4463(16); c=20.523(5)	—	—	a=2.952(5); c=7.23(3)	—	1.49	5.47
$La_4Ni_3O_{10}$	800	a=3.8604(3); c=12.700(18)	—	a=5.440(6), b=5.464(6); c=28.01(12)	a=5.4751(8); c=13.263(3)	a=2.953(2); c=7.26(1)	$La(OH)_3$	1.68	6.06
	900	a=3.8474(3); c=12.715(19)	a=5.45(3), b=5.45(2); c=20.398(6)	a=5.435(11), b=5.466(12); c=28.151(4)	a=5.4740(6); c=13.242(2)	a=2.903(7); c=7.276(3)	—	1.61	5.61
	1000	a=3.846(6); c=12.71(12)	a=5.4090(6), b=5.4546(6); c=20.523(2)	a=5.4124(7), b=5.4624(7); c=28.112(4)	—	a=2.96(18); c=7.25(9)	—	1.70	6.26
	1100	a=3.85130(6); c=12.7056(4)	a=5.410(14), b=5.456(16); c=20.559(5)	—	—	a=2.955(13); c=7.247(6)	—	1.91	7.00
$La_6Ni_5O_{16}$	800	a=3.8462(5); c=12.660(3)	—	a=5.4(2), b=5.4(2); c=27.891(10)	a=5.4534(10); c=13.162(3)	a=2.949(7); c=7.22(3)	—	1.61	5.51
	900	—	a=5.4039(10), b=5.4480(10); c=20.394(5)	a=5.4055(7), b=5.4526(7); c=27.975(4)	a=5.4499(7); c=13.160(3)	a=2.95(9); c=7.2(4)	—	1.51	5.27
	1000	—	a=5.4011(9), b=5.4480(8); c=20.448(4)	a=5.4071(7), b=5.4557(8); c=28.010(5)	—	a=2.95(4); c=7.23(19)	—	1.64	6.00
	1100	a=3.84642(10); c=12.6813(4)	a=5.4031(12), b=5.4457(14); c=20.548(5)	—	—	a=2.9515(13); c=7.233(7)	—	1.63	5.79
$LaNiO_3$	800	a=3.844(3); c=12.751(8)	—	a=5.422(3), b=5.463(2); c=28.18(12)	a=5.4740(7); c=13.21(10)	a=2.958(12); c=7.242(6)	—	1.24	4.58
	900	—	a=5.428(3), b=5.442(3); c=20.498(4)	a=5.4192(2), b=5.468(10); c=28.080(4)	a=5.4697(4); c=13.202(2)	a=2.9606(3); c=7.231(17)	—	1.46	4.98
	1000	—	a=5.4165(9), b=5.457(10); c=20.496(3)	a=5.4195(4), b=5.4687(4); c=28.079(2)	a=5.472(10); c=13.190(6)	a=2.9576(3); c=7.245(14)	—	1.74	5.93
	1100	a=3.85170(12); c=12.7025(8)	a=5.408(15), b=5.457(17); c=20.587(6)	—	—	a=2.9553(5); c=7.247(3)	—	2.09	7.46

Table 0.10: Fluxless flux: resulting weight percent (%) vs targeted homology composition, temperature, and dwell time, with average Ruddlesden–Popper nickel valence.

Target	T (°C)	Dwell (h)	La_2NiO_4 (%)	$La_3Ni_2O_{6.92}$ (%)	$La_4Ni_3O_{10}$ (%)	$LaNiO_3$ (%)	NiO (%)	LaOCl (%)	La_2O_3 (%)	$La(OH)_3$ (%)	Flux (%)	$\bar{v}_{Ni,RP}$
La_2NiO_4	800	12	12.2(6)	—	—	—	43.3(6)	—	9.33(17)	35.1(4)	—	2.00(10)
	900	9	28.9(6)	—	—	—	33.1(6)	—	—	38.1(4)	—	2.00(4)
	1000	6	65.2(4)	—	—	—	14.7(4)	—	—	20.14(18)	—	2.00(1)
	1100	6	84.5(2)	—	—	—	6.5(2)	—	5.04(6)	4.00(7)	—	2.00(0)
$La_3Ni_2O_7$	800	12	31.5(1)	—	—	—	34.8(7)	—	8.14(19)	25.5(4)	—	2.00(1)
	900	9	33.8(7)	—	—	—	35.6(7)	—	—	30.6(4)	—	2.00(4)
	1000	6	62.5(5)	9.8(5)	—	—	17.5(4)	—	—	10.13(13)	—	2.08(11)
	1100	6	82.8(4)	7.0(4)	—	—	8.3(3)	—	1.88(60)	—	—	2.05(12)
$La_4Ni_3O_{10}$	800	12	46.6(10)	—	—	—	27.9(8)	—	—	25.5(6)	—	2.00(4)
	900	9	51.2(11)	—	—	—	32.2(9)	—	—	16.6(4)	—	2.00(4)
	1000	6	58.8(4)	31.7(3)	—	—	8.6(3)	—	—	0.9(1)	—	2.20(3)
	1100	6	70.1(4)	15.8(3)	—	—	13.2(3)	—	0.90(4)	—	—	2.11(4)
$La_6Ni_5O_{16}$	800	12	55.6(8)	—	—	—	24.9(7)	—	4.4(2)	15.0(3)	—	2.00(3)
	900	9	69.2(5)	—	—	—	18.3(6)	—	—	12.5(2)	—	2.00(1)
	1000	6	33.7(4)	56.4(4)	—	—	9.9(4)	—	—	—	—	2.34(3)
	1100	6	60.6(5)	26.0(5)	—	—	13.4(3)	—	—	—	—	2.17(5)
$LaNiO_3$	800	12	14.4(6)	—	—	—	53.6(5)	—	—	30.9(3)	—	2.00(8)
	900	9	20.8(5)	—	—	—	53.2(6)	—	—	26.0(5)	—	2.00(5)
	1000	6	49.5(3)	16.7(3)	—	—	26.1(3)	—	—	7.7(1)	—	2.15(4)
	1100	6	42.70(24)	30.1(2)	—	—	24.4(3)	—	0.40(3)	2.40(4)	—	2.23(2)

Table 0.11: NaCl flux: resulting weight percent (%) vs targeted homology composition, temperature, and dwell time, with average Ruddlesden–Popper nickel valence.

Target	T (°C)	Dwell (h)	La_2NiO_4 (%)	$La_3Ni_2O_{6.92}$ (%)	$La_4Ni_3O_{10}$ (%)	$LaNiO_3$ (%)	NiO (%)	LaOCl (%)	La_2O_3 (%)	$La(OH)_3$ (%)	Flux (%)	$\bar{v}_{Ni,RP}$
La_2NiO_4	830	12	66.4(4)	24.6(5)	—	—	—	4.40(18)	4.69(8)	—	—	2.16(5)
	900	9	98.26(7)	—	—	—	—	—	1.74(7)	—	—	2.00(0)
	1000	6	84.9(3)	7.8(3)	—	—	—	7.3(2)	—	—	—	2.05(8)
	1100	6	100	—	—	—	—	—	—	—	—	2.00(0)
$La_3Ni_2O_7$	830	12	64.0(3)	33.3(3)	—	—	2.5(3)	—	—	—	—	2.20(2)
	900	9	89.8(5)	4.4(4)	—	—	5.8(4)	—	—	—	—	2.03(18)
	1000	6	76.5(6)	10.8(4)	—	—	8.8(5)	3.9(3)	—	—	—	2.07(8)
	1100	6	80.1(5)	12.8(4)	—	—	7.1(4)	—	—	—	—	2.08(7)
$La_4Ni_3O_{10}$	830	12	28.9(4)	—	37.9(5)	26.3(4)	5.7(4)	1.3(2)	—	—	—	2.63(5)
	900	9	21.1(3)	66.3(4)	7.2(3)	—	5.3(4)	—	—	—	—	2.42(11)
	1000	6	18.3(3)	71.7(4)	—	—	6.3(4)	3.7(2)	—	—	—	2.41(4)
	1100	6	72.0(4)	15.9(3)	—	—	12.1(3)	—	—	—	—	2.11(4)
$La_6Ni_5O_{16}$	830	12	21.4(4)	—	43.8(7)	29.9(6)	4.8(5)	—	—	—	—	2.68(7)
	900	9	—	51.6(7)	39.5(7)	3.3(4)	5.6(5)	—	—	—	—	2.59(10)
	1000	6	—	59.9(11)	30.9(11)	—	6.1(6)	3.1(4)	—	—	—	2.56(10)
	1100	6	70.2(4)	15.7(3)	—	—	14.1(4)	—	—	—	—	2.11(4)
$LaNiO_3$	830	12	—	—	61.7(6)	29.6(6)	8.8(4)	—	—	—	—	2.79(3)
	900	9	—	43.0(4)	38.5(4)	7.1(3)	11.3(4)	—	—	—	—	2.62(4)
	1000	6	—	56.1(5)	26.9(5)	—	13.5(5)	3.6(3)	—	—	—	2.56(5)
	1100	6	45.3(13)	36.3(13)	—	—	18.5(6)	—	—	—	—	2.25(10)

Table 0.12: NaBr flux: resulting weight percent (%) vs targeted homology composition, temperature, and dwell time, with average Ruddlesden–Popper nickel valence.

Target	T (°C)	Dwell (h)	La_2NiO_4 (%)	$La_3Ni_2O_{6.92}$ (%)	$La_4Ni_3O_{10}$ (%)	$LaNiO_3$ (%)	NiO (%)	LaOCl (%)	La_2O_3 (%)	$La(OH)_3$ (%)	Flux (%)	$\bar{v}_{Ni,RP}$
La_2NiO_4	800	12	89.0(3)	—	—	—	5.5(3)	—	5.42(7)	—	—	2.00(1)
	900	9	98.73(9)	—	—	—	—	—	1.27(9)	—	—	2.00(0)
	1000	6	99.21(12)	—	—	—	—	—	0.79(12)	—	—	2.00(0)
	1100	6	99.19(7)	—	—	—	—	—	0.81(7)	—	—	2.00(0)
$La_3Ni_2O_7$	800	12	90.8(5)	—	—	—	7.7(5)	—	1.46(60)	—	—	2.00(1)
	900	9	81.4(6)	13.5(4)	—	—	5.1(6)	—	—	—	—	2.09(6)
	1000	6	86.2(5)	7.8(4)	—	—	6.1(4)	—	—	—	—	2.05(11)
	1100	6	78.8(7)	12.9(4)	—	—	8.3(7)	—	—	—	—	2.08(7)
$La_4Ni_3O_{10}$	800	12	63.6(6)	—	31.3(6)	—	5.0(4)	—	—	—	—	2.27(5)
	900	9	51.4(4)	43.1(4)	—	—	5.5(5)	—	—	—	—	2.26(3)
	1000	6	28.1(3)	66.4(4)	—	—	5.5(4)	—	—	—	—	2.37(3)
	1100	6	79.6(4)	10.0(3)	—	—	10.4(4)	—	—	—	—	2.07(6)
$La_6Ni_5O_{16}$	800	12	81.6(5)	—	10.5(3)	—	7.9(4)	—	—	—	—	2.10(6)
	900	9	12.1(5)	82.6(7)	—	—	5.3(7)	—	—	—	—	2.45(10)
	1000	6	12.6(3)	81.4(5)	—	—	6.0(4)	—	—	—	—	2.44(6)
	1100	6	67.3(5)	17.7(3)	—	—	15.0(5)	—	—	—	—	2.12(4)
$LaNiO_3$	800	12	44.5(4)	—	42.9(5)	—	12.6(4)	—	—	—	—	2.38(3)
	900	9	21.0(3)	65.5(5)	—	—	13.5(6)	—	—	—	—	2.40(4)
	1000	6	15.9(3)	71.5(4)	—	—	12.6(4)	—	—	—	—	2.42(5)
	1100	6	56.2(4)	22.0(3)	—	—	21.8(5)	—	—	—	—	2.16(3)

Table 0.13: NaI flux: resulting weight percent (%) vs targeted homology composition, temperature, and dwell time, with average Ruddlesden–Popper nickel valence.

Target	T (°C)	Dwell (h)	La_2NiO_4 (%)	$La_3Ni_2O_{6.92}$ (%)	$La_4Ni_3O_{10}$ (%)	$LaNiO_3$ (%)	NiO (%)	LaOCl (%)	La_2O_3 (%)	$La(OH)_3$ (%)	Flux (%)	$\bar{v}_{Ni,RP}$
La_2NiO_4	700	48	33.1(4)	31.0(4)	—	27.8(4)	—	—	2.59(8)	5.46(10)	—	2.55(6)
	750	48	14.1(3)	36.1(5)	—	36.5(5)	—	—	5.9(3)	7.44(11)	—	2.69(8)
	800	12	31.5(5)	22.2(6)	—	39.8(5)	—	—	0.6(1)	5.9(1)	—	2.63(9)
	850	12	81.0(4)	14.3(4)	—	—	—	—	1.17(7)	3.55(8)	—	2.09(6)
	900	9	100	—	—	—	—	—	—	—	—	2.00(0)
	950	9	99.5(1)	—	—	—	—	—	0.5(1)	—	—	2.00(0)
	1000	6	98.40(8)	—	—	—	—	—	1.60(8)	—	—	2.00(0)
	1100	2	97.76(7)	—	—	—	—	—	2.24(7)	—	—	2.00(0)
$La_3Ni_2O_7$	700	48	18.4(5)	33.0(8)	—	40.0(7)	5.8(6)	—	0.79(10)	1.94(10)	—	2.69(11)
	750	48	15.4(4)	16.0(5)	—	65.3(6)	—	—	—	3.1(1)	—	2.82(12)
	800	12	26.5(4)	24.7(5)	—	47.6(5)	—	—	—	1.3(1)	—	2.69(7)
	850	12	44.2(6)	28.5(8)	—	26.8(6)	—	—	0.55(6)	—	—	2.50(10)
	900	9	41.2(1)	16.0(2)	27.5(8)	15.6(5)	—	—	—	—	—	2.49(8)
	950	9	36.338(4)	—	63.662(4)	—	—	—	—	—	—	2.47(0)
	1000	6	50.5(3)	—	49.5(3)	—	—	—	—	—	—	2.38(2)
	1100	2	95.2(3)	—	—	—	4.8(3)	—	—	—	—	2.00(1)
$La_4Ni_3O_{10}$	700	48	20.6(5)	26.9(9)	—	49.7(7)	2.8(4)	—	—	—	—	2.72(12)
	750	48	17.2(4)	—	—	82.8(4)	—	—	—	—	—	2.89(7)
	800	12	28.9(4)	—	—	71.1(4)	—	—	—	—	—	2.80(4)
	850	12	25.9(5)	—	38.6(8)	35.5(9)	—	—	—	—	—	2.68(10)
	900	9	18.4(3)	—	56.5(4)	21.0(3)	4.1(3)	—	—	—	—	2.66(5)
	950	9	2.2(3)	—	97.8(3)	—	—	—	—	—	—	2.66(36)
	1000	6	14.3(4)	—	85.7(4)	—	—	—	—	—	—	2.59(7)
	1100	2	90.2(5)	—	—	—	9.8(5)	—	—	—	—	2.00(1)
$La_6Ni_5O_{16}$	700	48	15.2(5)	25.2(7)	—	59.7(8)	—	—	—	—	—	2.79(13)
	750	48	8.5(3)	—	—	91.5(3)	—	—	—	—	—	2.95(10)
	800	12	13.0(3)	—	27.9(5)	59.1(5)	—	—	—	—	—	2.83(8)
	850	12	8.5(3)	—	38.7(7)	52.7(6)	—	—	—	—	—	2.82(11)
	900	9	7.3(5)	—	64.5(5)	28.3(4)	—	—	—	—	—	2.74(19)
	950	9	—	—	100	—	—	—	—	—	—	2.67(0)
	1000	6	6.7(4)	—	89.1(5)	—	4.2(3)	—	—	—	—	2.63(16)
	1100	2	78.0(5)	—	10.7(4)	—	11.3(4)	—	—	—	—	2.10(8)
$La_{13}Ni_{12}O_{37}$	700	48	6.4(3)	16.2(5)	—	77.4(5)	—	—	—	—	—	2.89(16)
	750	48	—	—	—	100	—	—	—	—	—	3.00(0)
	800	12	—	—	—	100	—	—	—	—	—	3.00(0)
	850	12	—	—	26.2(5)	73.8(5)	—	—	—	—	—	2.92(6)
	900	9	—	—	44.2(4)	51.2(4)	4.7(4)	—	—	—	—	2.86(3)
	950	9	—	—	89.4(3)	6.1(3)	4.5(2)	—	—	—	—	2.69(13)
	1000	6	2.4(2)	—	88.6(5)	—	9.0(4)	—	—	—	—	2.65(22)
	1100	2	80.3(5)	—	5.0(3)	—	14.7(4)	—	—	—	—	2.05(12)
$LaNiO_3$	700	48	11.9(3)	20.3(7)	—	58.4(7)	9.4(4)	—	—	—	—	2.81(12)
	750	48	—	—	—	100	—	—	—	—	—	3.00(0)
	800	12	—	—	—	100	—	—	—	—	—	3.00(0)
	850	12	—	—	21.1(4)	77.0(5)	1.9(4)	—	—	—	—	2.94(6)
	900	9	—	—	50.7(3)	44.4(3)	4.9(2)	—	—	—	—	2.84(3)
	950	9	—	—	78.8(5)	12.0(4)	9.2(4)	—	—	—	—	2.72(9)
	1000	6	13.0(2)	—	74.5(3)	—	12.5(3)	—	—	—	—	2.59(4)
	1100	2	78.4(4)	—	6.7(3)	—	14.9(3)	—	—	—	—	2.07(9)
$LaNi_{1.2}O_3$	700	48	3.1(4)	13.6(8)	—	71.7(8)	11.6(4)	—	—	—	—	2.92(41)
	750	48	—	—	—	92.1(3)	7.9(3)	—	—	—	—	3.00(1)
	800	12	—	—	—	92.2(4)	7.8(4)	—	—	—	—	3.00(1)
	850	12	—	—	—	92.3(4)	7.7(4)	—	—	—	—	3.00(1)
	900	9	—	—	33.6(4)	57.1(5)	9.3(3)	—	—	—	—	2.89(4)
	950	9	—	—	56.6(4)	32.8(4)	10.6(3)	—	—	—	—	2.80(4)
	1000	6	13.8(2)	—	67.1(3)	—	19.1(3)	—	—	—	—	2.58(4)
	1100	2	12.3(3)	—	37.2(6)	36.1(5)	14.4(4)	—	—	—	—	2.76(8)

Table 0.14: KCl flux: resulting weight percent (%) vs targeted homology composition, temperature, and dwell time, with average Ruddlesden–Popper nickel valence.

Target	T (°C)	Dwell (h)	La_2NiO_4 (%)	$La_3Ni_2O_{6.92}$ (%)	$La_4Ni_3O_{10}$ (%)	$LaNiO_3$ (%)	NiO (%)	LaOCl (%)	La_2O_3 (%)	$La(OH)_3$ (%)	Flux (%)	$\bar{v}_{Ni,RP}$
La_2NiO_4	800	12	50.66	—	—	—	—	—	—	—	49.34	2.00(0)
	900	9	100	—	—	—	—	—	—	—	—	2.00(0)
	1000	6	100	—	—	—	—	—	—	—	—	2.00(0)
	1100	6	100	—	—	—	—	—	—	—	—	2.00(0)
$La_3Ni_2O_7$	800	12	43.8(2)	—	—	—	3.1(3)	1.380(15)	—	—	51.7(3)	2.00(1)
	900	9	38.6(5)	39.4(5)	12.5(5)	—	5.9(4)	3.5(2)	—	—	—	2.34(10)
	1000	6	14.4(3)	75.5(5)	—	—	3.7(4)	6.4(3)	—	—	—	2.43(5)
	1100	6	59.7(7)	29.2(5)	—	—	11.1(9)	—	—	—	—	2.19(5)
$La_4Ni_3O_{10}$	800	12	47.6(4)	—	29.4(4)	—	3.4(3)	1.70(12)	—	—	17.9(3)	2.30(4)
	900	9	13.4(3)	42.5(5)	37.5(4)	—	5.5(5)	1.2(2)	—	—	—	2.51(7)
	1000	6	9.4(2)	85.2(4)	—	—	4.3(3)	1.10(16)	—	—	—	2.46(5)
	1100	6	61.3(5)	28.1(4)	—	—	10.6(5)	—	—	—	—	2.18(4)
$La_6Ni_5O_{16}$	800	12	49.2(6)	—	42.8(6)	—	8.0(6)	—	—	—	—	2.36(4)
	900	9	11.5(4)	23.9(7)	49.5(7)	5.1(4)	8.8(4)	1.2(5)	—	—	—	2.58(14)
	1000	6	—	79.5(6)	—	13.8(4)	5.8(4)	1.0(2)	—	—	—	2.59(8)
	1100	6	64.9(4)	20.7(3)	—	—	14.4(4)	—	—	—	—	2.14(3)
$LaNiO_3$	800	12	41.6(5)	—	21.9(6)	21.2(6)	13.5(3)	1.70(12)	—	—	—	2.51(10)
	900	9	3.2(2)	15.4(3)	40.2(5)	9.0(3)	11.3(5)	12.7(2)	—	—	8.2(4)	2.66(18)
	1000	6	—	72.8(6)	—	13.2(4)	12.1(5)	1.8(2)	—	—	—	2.60(8)
	1100	6	40.5(6)	37.2(5)	—	—	22.2(5)	—	—	—	—	2.27(5)

Table 0.15: KBr flux: resulting weight percent (%) vs targeted homology composition, temperature, and dwell time, with average Ruddlesden–Popper nickel valence.

Target	T (°C)	Dwell (h)	La_2NiO_4 (%)	$La_3Ni_2O_{6.92}$ (%)	$La_4Ni_3O_{10}$ (%)	$LaNiO_3$ (%)	NiO (%)	LaOCl (%)	La_2O_3 (%)	$La(OH)_3$ (%)	Flux (%)	$\bar{v}_{Ni,RP}$
La_2NiO_4	800	12	51.5(8)	21.50(11)	—	—	10.8(5)	—	10.79(19)	5.42(16)	—	2.17(4)
	900	9	82.7(5)	14.2(5)	—	—	—	—	3.17(2)	—	—	2.09(7)
	1000	6	100	—	—	—	—	—	—	—	—	2.00(0)
	1100	6	99.27(8)	—	—	—	—	—	0.73(8)	—	—	2.00(0)
$La_3Ni_2O_7$	800	12	44.8(9)	22.4(13)	9.5(8)	—	13.0(6)	—	6.29(16)	3.95(15)	—	2.26(24)
	900	9	54.0(4)	44.0(4)	—	—	2.1(3)	—	—	—	—	2.25(3)
	1000	6	67.6(7)	27.6(3)	—	—	4.9(9)	—	—	—	—	2.17(3)
	1100	6	59.6(4)	36.8(3)	—	—	3.6(5)	—	—	—	—	2.22(2)
$La_4Ni_3O_{10}$	800	12	58.4(7)	—	35.1(7)	—	6.5(5)	—	—	—	—	2.30(5)
	900	9	17.8(3)	78.1(4)	—	—	4.0(4)	—	—	—	—	2.42(4)
	1000	6	41.0(3)	52.9(3)	—	—	6.2(4)	—	—	—	—	2.31(2)
	1100	6	58.2(3)	36.6(3)	—	—	5.2(3)	—	—	—	—	2.22(2)
$La_6Ni_5O_{16}$	800	12	48.4(4)	—	44.9(5)	—	6.8(4)	—	—	—	—	2.37(3)
	900	9	13.8(3)	81.3(5)	—	—	4.9(4)	—	—	—	—	2.44(6)
	1000	6	24.6(3)	68.1(4)	—	—	7.2(3)	—	—	—	—	2.39(3)
	1100	6	52.7(3)	38.0(3)	—	—	9.3(3)	—	—	—	—	2.24(2)
$LaNiO_3$	800	12	46.2(6)	—	21.5(9)	—	23.8(5)	—	5.6(1)	2.8(1)	—	2.26(10)
	900	9	58.4(4)	27.3(3)	—	—	14.4(4)	—	—	—	—	2.18(3)
	1000	6	64.6(3)	20.7(3)	—	—	14.7(3)	—	—	—	—	2.14(3)
	1100	6	42.4(2)	39.4(2)	—	—	18.1(3)	—	—	—	—	2.27(2)

Table 0.16: KI flux: resulting weight percent (%) vs targeted homology composition, temperature, and dwell time, with average Ruddlesden–Popper nickel valence.

Target	T (°C)	Dwell (h)	La_2NiO_4 (%)	$La_3Ni_2O_{6.92}$ (%)	$La_4Ni_3O_{10}$ (%)	$LaNiO_3$ (%)	NiO (%)	LaOCl (%)	La_2O_3 (%)	$La(OH)_3$ (%)	Flux (%)	$\bar{v}_{Ni,RP}$
La_2NiO_4	800	12	30.9(60)	10.7(5)	38.2(7)	—	6.9(4)	—	—	13.2(2)	—	2.43(49)
	900	9	82.5(4)	16.8(4)	—	—	—	—	0.65(5)	—	—	2.10(5)
	1000	6	100	—	—	—	—	—	—	—	—	2.00(0)
	1100	2	100	—	—	—	—	—	—	—	—	2.00(0)
$La_3Ni_2O_7$	800	12	20.3(8)	39.40(14)	21.9(9)	—	10.5(6)	—	—	7.8(2)	—	2.45(14)
	900	9	33.1(4)	34.0(6)	32.9(6)	—	—	—	—	—	—	2.42(7)
	1000	6	18.3(4)	75.0(6)	6.7(5)	—	—	—	—	—	—	2.44(19)
	1100	2	78.3(5)	17.8(4)	—	—	4.0(3)	—	—	—	—	2.11(5)
$La_4Ni_3O_{10}$	800	12	26.9(5)	—	48.0(7)	18.3(4)	5.7(3)	—	—	1.10(5)	—	2.60(6)
	900	9	15.4(3)	23.4(5)	47.1(5)	8.9(3)	5.1(5)	—	—	—	—	2.58(8)
	1000	6	3.8(3)	60.8(5)	29.4(4)	—	6.1(5)	—	—	—	—	2.54(20)
	1100	2	76.5(4)	17.4(3)	—	—	6.1(3)	—	—	—	—	2.11(4)
$La_6Ni_5O_{16}$	800	12	22.9(9)	—	51.1(17)	18.6(9)	7.3(6)	—	—	—	—	2.62(14)
	900	9	—	32.9(9)	56.8(10)	6.5(5)	3.9(6)	—	—	—	—	2.64(10)
	1000	6	—	45.7(9)	47.2(9)	—	7.1(7)	—	—	—	—	2.59(7)
	1100	2	72.2(4)	18.1(4)	—	—	9.7(3)	—	—	—	—	2.12(5)
$LaNiO_3$	800	12	8.3(4)	—	47.4(7)	33.5(7)	10.9(5)	—	—	—	—	2.77(14)
	900	9	—	28.7(5)	44.8(7)	17.2(12)	9.3(3)	—	—	—	—	2.69(8)
	1000	6	—	35.4(4)	48.9(4)	5.0(3)	10.7(3)	—	—	—	—	2.63(5)
	1100	2	65.6(5)	20.8(5)	—	—	13.6(4)	—	—	—	—	2.14(5)

Table 0.17: Standard Gibbs free energies used to compute ΔG_r° for $AX \rightarrow AXO_4$ [19]

.

Reaction	ΔG_f° [$\mathbf{AXO_4}$] ($\mathbf{kJ \cdot mol^{-1}}$)	ΔG_f° [$\mathbf{AX}$] ($\mathbf{kJ \cdot mol^{-1}}$)	$\Delta G^\circ_{reaction}$ ($\mathbf{kJ \cdot mol^{-1}}$)
$NaCl \rightarrow NaClO_4$	−254.85	−384.14	129.29
$KCl \rightarrow KClO_4$	−303.09	−409.14	106.05
$NaBr \rightarrow NaBrO_4$	−143.86	−348.98	205.12
$KBr \rightarrow KBrO_4$	−174.41	−380.66	206.25
$NaI \rightarrow NaIO_4$	−323.02	−286.06	−36.96
$KI \rightarrow KIO_4$	−361.35	−324.89	−36.46

Bibliography

[1] Wanklyn, B. M. Flux Growth of Some Complex Oxide Materials. *J Mater Sci* **1972**, *7*, 813–821.

[2] Bugaris, H., D. E.and Zur-Loye Materials Discovery by Flux Crystal Growth: Quaternary and Higher Order Oxides. *Angew Chem Int Ed* **2012**, *51*, 3780–3811.

[3] Klepov, V. V.; Juillerat, C. A.; Pace, K. A.; Morrison, G.; Zur-Loye, H.-C. "Soft" Alkali Bromide and Iodide Fluxes for Crystal Growth. *Front. Chem.* **2020**, *8*.

[4] Bednorz, J. G.; Müller, K. A. Possible highT c Superconductivity in the Ba-La-Cu-O System. *Z. Physik B - Condensed Matter* **1986**, *64*, 189–193.

[5] Park, C.; Snyder, R. L. Structures of High-Temperature Cuprate Superconductors. *Journal of the American Ceramic Society* **1995**, *78*, 3171–3194.

[6] Li, D.; Lee, K.; Wang, B. Y.; Osada, M.; Crossley, S.; Lee, H. R.; Cui, Y.; Hikita, Y.; Hwang, H. Y. Superconductivity in an Infinite-Layer Nickelate. *Nature* **2019**, *572*, 624–627.

[7] Osada, M.; Wang, B. Y.; Goodge, B. H.; Lee, K.; Yoon, H.; Sakuma, K.; Li, D.; Miura, M.; Kourkoutis, L. F.; Hwang, H. Y. A Superconducting Praseodymium Nickelate with Infinite Layer Structure. *Nano Lett.* **2020**, *20*, 5735–5740.

[8] Osada, M.; Wang, B. Y.; Goodge, B. H.; Harvey, S. P.; Lee, K.; Li, D.; Kourkoutis, L. F.; Hwang, H. Y. Nickelate Superconductivity without Rare-Earth Magnetism: (La,Sr)NiO_2. *Advanced Materials* **2021**, *33*, 2104083.

[9] Zeng, S.; Li, C.; Chow, L. E.; Cao, Y.; Zhang, Z.; Tang, C. S.; Yin, X.; Lim, Z. S.; Hu, J.; Yang, P.; Ariando, A. Superconductivity in Infinite-Layer Nickelate $La_{1-x}Ca_xNiO_2$ Thin Films. *Sci. Adv.* **2022**, *8*, eabl9927.

[10] Pan, G. A. et al. Superconductivity in a Quintuple-Layer Square-Planar Nickelate. *Nat. Mater.* **2022**, *21*, 160–164.

[11] Sun, H.; Huo, M.; Hu, X.; Li, J.; Liu, Z.; Han, Y.; Tang, L.; Mao, Z.; Yang, P.; Wang, B.; Cheng, J.; Yao, D.-X.; Zhang, G.-M.; Wang, M. Signatures of Superconductivity near 80 K in a Nickelate under High Pressure. *Nature* **2023**, *621*, 493–498.

[12] Zhu, Y. et al. Superconductivity in Pressurized Trilayer $La_4Ni_3O_{10}$ Single Crystals. *Nature* **2024**, *631*, 531–536.

[13] Wold, A.; Post, B.; Banks, E. Rare Earth Nickel Oxides. *J. Am. Chem. Soc.* **1957**, *79*, 4911–4913.

[14] Shivakumara, C.; Hegde, M. S.; Prakash, A. S.; Khadar, A. M. A.; Subbanna, G. N.; Lalla, N. P. Low Temperature Synthesis, Structure and Properties of Alkali-Doped La_2NiO_4, $LaNiO_3$ and $LaNi_{0.85}Cu_{0.15}O_3$ from Alkali Hydroxide Fluxes. *Solid State Sciences* **2003**, *5*, 351–357.

[15] Klein, Y. M.; Kozłowski, M.; Linden, A.; Lacorre, M., P.; Medarde; Gawryluk, D. J. $RENiO_3$ Single Crystals (RE = Nd, Sm, Gd, Dy, Y, Ho, Er, Lu) Grown from Molten Salts under 2000 Bar of Oxygen Gas Pressure. *Crystal Growth Design* **2021**, *21*, 4230–4241.

[16] Zhang, J.; Zheng, H.; Ren, Y.; Mitchell, J. F. High-Pressure Floating-Zone Growth of Perovskite Nickelate LaNiO3 Single Crystals. *Crystal Growth Design* **2017**, *17*, 2730–2735.

[17] Zhang, J.; Zheng, H.; Chen, Y.-S.; Ren, Y.; Yonemura, M.; Huq, A.; Mitchell, J. F. High Oxygen Pressure Floating Zone Growth and Crystal Structure of the Metallic Nickelates $R_4Ni_3O_{10}$(R = La , Pr). *Phys. Rev. Materials* **2020**, *4*, 083402.

[18] Guo, H.; Li, Z. W.; Zhao, L.; Hu, Z.; Chang, C. F.; Kuo, C.-Y.; Schmidt, W.; Piovano, A.; Pi, T. W.; Sobolev, O.; Khomskii, D. I.; Tjeng, L. H.; Komarek, A. C. Antiferromagnetic Correlations in the Metallic Strongly Correlated Transition Metal Oxide $LaNiO_3$. *Nat Commun* **2018**, *9*, 43.

[19] Reed, J. J. The NBS Tables of Chemical Thermodynamic Properties: Selected Values for Inorganic and C1 and C2 Organic Substances in SI Units. 2020; `https://data.nist.gov/od/id/mds2-2124`.